SEASONAL AND SPATIAL VARIATIONS IN THE WATER MASS

CHARACTERISTICS OF MUIR INLET,

GLACIER BAY, ALASKA

APPROVED:

W. S. Ruff

Robert F. Carlson

Pat Kanary et Ten Brooke

Chairman

Department Head

APPROVED: _____ Date Aug 26, 1969

Dean of the College of
Mathematics, Physical Sciences
and Engineering

Vice President for Research and Advanced Study

SEASONAL AND SPATIAL VARIATIONS IN THE WATER MASS CHARACTERISTICS OF MUIR INLET, GLACIER BAY, ALASKA

A

THESIS

Presented to the Faculty of the
University of Alaska in Partial Fulfillment
of the Requirements
for the Degree of
MASTER OF SCIENCE

By

Alician Veronica Quinlan, B.S.

College, Alaska

May, 1970

ABSTRACT

Muir Inlet, a Southeast Alaska fjord with tidal glaciers, is investigated. Its water masses show definite seasonal and spatial responses in temperature, salinity, and dissolved oxygen distributions and in circulation patterns. Its basin water is continually renewed.

Two seasonal parameter structures are found. The winter--spring structure is characterized by the homogeneity of the water masses, with up to 84% of the fjord water having a temperature between 3.0--3.5°C.; and up to 55%, a salinity of 31.3--31.4‰. The summer--fall fjord water masses are heterogeneous, with temperatures ranging from 0.5--7.5°C., salinities from 13.0--32.0‰ and dissolved oxygen levels ranging from 1.8-- 0.5 milliliters per liter. The heterogeneous state develops gradually from April through November. The homogeneous state is regained abruptly in late fall. The salinity of water below the pycnocline continually increases from late fall through early summer. The salinity of the surface water decreases from mid-spring through early fall.

Several spatial parameter patterns are observed. Both salinities and temperatures decrease progressively from the Pacific Ocean to the head of the fjord. The tidal glaciers serve both as heat sinks and as freshwater sources, producing negative temperature and salinity gradients upfjord.

The data are consistent with a three-layer flow system: outflowing brackish surface layer, intermediate zone of net upward transport, and a higher salinity deep layer with an upfjord transport. Advective inflows and thermohaline convection may occur from late fall through early summer.

ACKNOWLEDGMENTS

This investigation was supported by the Office of Naval Research Contract NONR 3010 (05) and the National Science Foundation Grant GB 8204.

Dr. George L. Pickard, Director of the Institute of Oceanography of the University of British Columbia, kindly supplied Data Reports 24 and 25 from his institution. These reports contain the only June and August oceanographic data available for Muir Inlet.

The section of my thesis discussing climatic conditions in Glacier Bay National Monument is based on data compiled by the Institute of Polar Studies of the Ohio State University. George M. Haselton (now of Clemson University), Gary D. McKenzie, John F. Splettstoesser, and Lawrence D. Taylor (now of Albion College) supplied the climatic data which they and their colleagues had gathered.

I wish to thank the Institute of Marine Science of the University of Alaska for supplying the oceanographic data upon which my thesis is based and for assisting me throughout the course of my research. In particular, I wish to thank the gentlemen on my advisory committee for their help in editing my thesis and Mrs. John (Judith) Henshaw for her assistance in preparing my graphs for publication.

I especially wish to express my gratitude to Dr. William S. Reeburgh for his continuing interest and guidance during the course of my studies and research at the University of Alaska.

FOTABM
AUQ

TABLE OF CONTENTS

LIST OF TABLES

LIST OF FIGURES

Figure Page

Figure Page

CHAPTER I

INTRODUCTION

The coast of Southeastern Alaska and British Columbia has been carved by glaciers into a maze of islands and long, narrow and tortuous inlets and channels. This shoreline constitutes the famed Inland Passage, over 850 nautical miles of fjord coastline extending from Tacoma, Washington (latitude 47°17'N, longitude 122°25'W), on the south to Skagway, Alaska (latitude 59°27'N, longitude 135°20'W), on the north.

Geomorphologically, this coastline is a classic example of a glacially eroded fjord system (Peacock 1935); oceanographically, it constitutes a special class among the various coastal regimes (Tully 1949; Pickard 1961, 1967; Bowden 1967; Saelen 1967).

This thesis deals with the physical oceanography of one particular subsystem of interconnecting inlets and channels lying west and south of Skagway, Alaska. Attention is focused on the fjord system delineated by the boundaries of Glacier Bay National Monument (about 58°--59°N, 135°30'--136°30'W), and in particular on Muir Inlet and its direct connection to the Pacific Ocean (see Figure 1, p. 2).

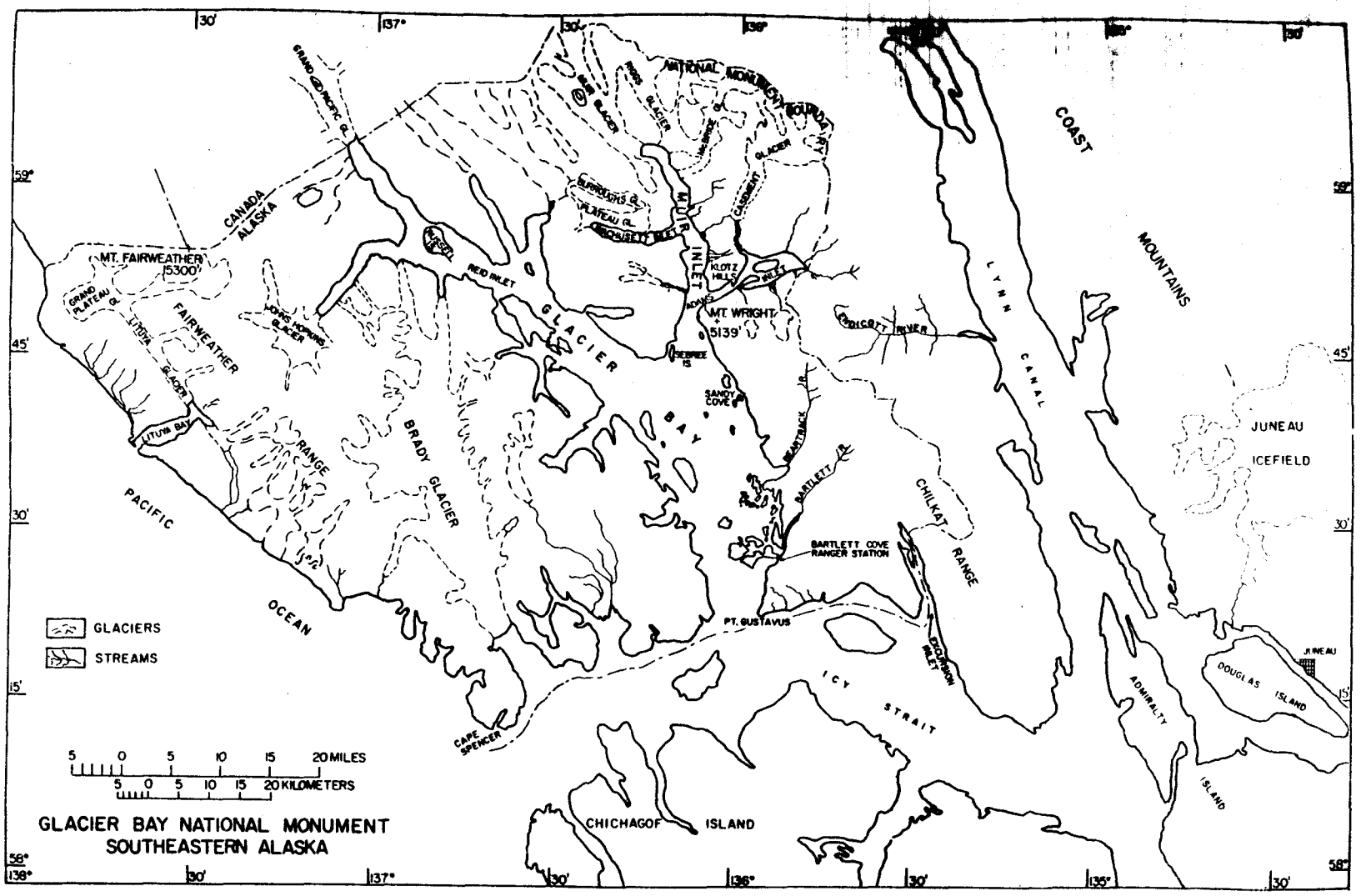

Figure 1. Glacier Bay National Monument, Southeastern Alaska (after Goldthwait et al. 1966)

Previous Work in Fjords

The bulk of the pioneering work in the physical oceanography of fjords has been done in Norway and British Columbia. Significant work has been done in Norway since 1900 (Gade 1963; Saelen 1967), and in British Columbia since the late 1940s (Tully 1949; Tabata and Pickard 1957; Gilmartin 1962; Waldichuk 1957; Pickard 1961).

Prior to the present study, Jones 1964, Powers 1962, Rosenberg 1966, Pickard 1967, McLain 1968, Matthews and Rosenberg 1968 and 1969, and Wallen and Hood 1968, have studied the physical oceanography of Alaskan fjords.

Only one of these studies (Pickard 1967) describes Glacier Bay and Muir Inlet, and it is limited to the results of two summertime cruises, one in June of 1964 and the other in August of 1965.

According to Pickard (1967), a characteristically small range of temperature, salinity, and density and a high dissolved oxygen content are found during June of 1964 and August of 1965 in the subsurface waters of fjords having icebergs. Also, surface salinities appear to be higher and surface temperatures lower in these "iceberg inlets" than in "non-iceberg inlets" during these same months. The small vertical density gradients in "iceberg inlets" are taken to be indicative of low stability and high eddy diffusivity throughout the water column. Turbulent mixing of highly

oxygenated meltwater, introduced by ice melting below the pycnocline, is assumed responsible for the high oxygen levels below the pycnocline.

Geographic and Historical Description of Glacier Bay and Muir Inlet

Glacier Bay National Monument (see Figure 2, p. 5) encompasses within its boundaries Glacier Bay and twelve major tributary inlets (Geike, Charpentier, Hugh Miller, Reid, Johns Hopkins, Tarr, Rendu, Queen, Tidal, Muir, Adams, Wachusetts). Six of these inlets possess one or more tidewater glaciers.

As a consequence of the calving of large chunks of ice from the termini of their tidewater glaciers, these six inlets contain a unique source of freshwater, meltwater from glaciers and icebergs. Within the Inland Passage, the presence of tidal glaciers and icebergs is restricted to Alaskan fjords, and thus introduces a new environmental variable not found in British Columbia inlets. Hence, ice as a year-around source of oxygenated freshwater and as a heat sink may be responsible for seasonal and spatial fjord water mass characteristics at variance with those reported for British Columbian inlets.

The possible importance of actively discharging tidewater glaciers to the dynamics and characteristics of

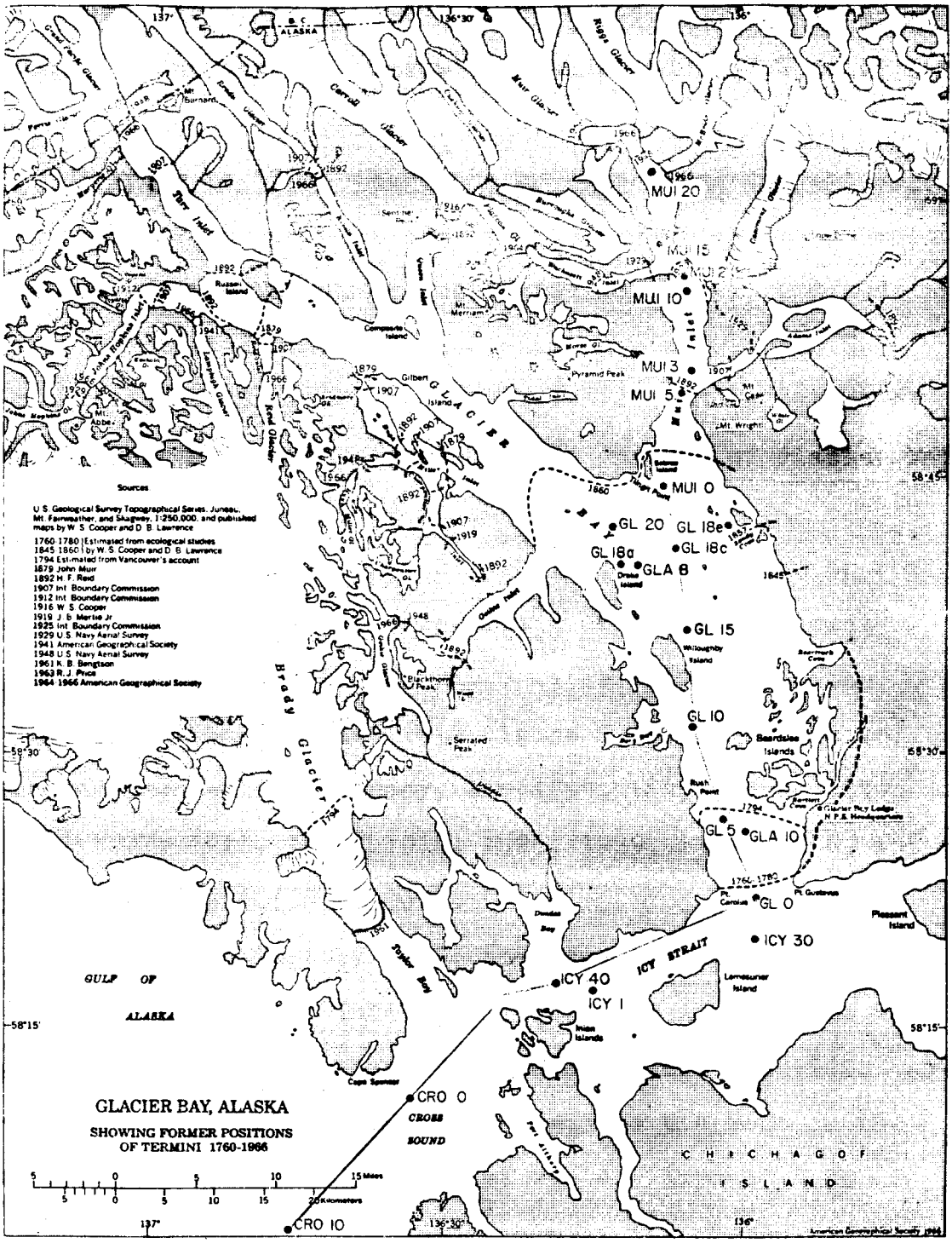

Figure 2. Glacier Bay National Monument, Southeastern Alaska: Former Positions of Termini, Station Loci, and Line of Communication Muir Inlet with the Pacific Ocean (after Bohn 1967)

the water masses in this estuarine system compels this study to consider the recent glacial history of Glacier Bay and its tributary inlets.

Prior to 1794, there are no reports of the actual locations of the termini of any glaciers within this region. In 1794, George Vancouver penetrated Icy Strait and made the first documented report on the existence of Glacier Bay. At that time, the ice field blanketed the whole extent of the present monument, excepting that portion of Glacier Bay south of Beardslee Island (Cooper 1956).

Ecological studies (Cooper 1937) provide an approximate date of 1760--1780 as the beginning of the most recent glacial retreat in Glacier Bay. Since 1760--1780, the positions of the termini (see Figure 2, p. 5) are known, to varying degrees of accuracy, for 1794, 1845--1860, 1879, 1892, 1907, 1912, 1916, 1919, 1925, 1929, 1941, 1948, 1961, 1963, 1964--1966 (Bohn 1967).

By approximately 1860, the edge of the ice field was at the mouth of Muir Inlet. The mouth of Adams Inlet was evident in 1907, and that of Wachusetts Inlet in 1929. As recently as 1948, the almost 90° bend to the west in the northernmost reach of Muir Inlet was not exposed. As of the mid-1960s, Muir Inlet had achieved its present form, possessing two major tributaries, Adams and Wachusetts Inlets, and at its head an arm toward the west.

For the purposes of this study, Muir Inlet is considered as that body of water extending northward from a line through MUI 0 (see Figure 2, p. 5, and Table 12, p. 140) connecting Tlingit Point to the east shore of Glacier Bay and terminating on the north at the line through MUI 20 (see Figure 2, p. 5, and Table 12, p. 140). The boundaries separating Adams and Wachusetts Inlets from Muir Inlet are taken to be the lines tangent to the points where the shores of Muir Inlet sharply curve into the tributary channels. See Figure 2, (p. 5) for the arbitrarily defined boundaries of Muir Inlet.

The line of communication of Muir Inlet with the Pacific Ocean is arbitrarily defined as that line joining the midpoints of the main channel of Glacier Bay south of the mouth of Muir Inlet to the mouth of Glacier Bay, which is set by the line connecting Point Carolus and Point Gustavus, and then westward through Icy Strait into Cross Sound, ending at CRO 10 (see Table 12, p. 140). Figure 2 (p. 5) shows this line drawn on a map of this region.

Data Available and Limitations of Data

As has been indicated above, this study attempts to analyze and explain the annual cycle of physical oceanographic parameters in a glaciated fjord. Unfortunately, several gaps exist in the monthly sequence of environmental data, thus

presenting many interpretive problems and leaving many questions unanswered.

It is not sufficient to assume that one year's worth of environmental data spaced at monthly intervals can adequately reflect the annual variations in water mass characteristics. The various oceanographic, meteorological, and hydrological parameters should, ideally, be monitored daily over at least a five-year span to enable a statistical representation of the data.

Gilmartin (1962) reports the results of an extensive study of Indian Arm, a British Columbia fjord, in which data from 35 approximately monthly cruises during a three-year period are examined. Using this data, he is only able to establish the gross trends in the annual cycle of fjord properties. Many of the fine details, such as responses to short-term, aperiodic, and diurnal climatic and tidal conditions are lost in the long intervals between samplings.

Hence, a program allowing for more frequent sampling over a longer period of time is desirable to assure a realistic portrayal of the cyclic and acyclic variations in fjord water mass properties and to ascertain the causative mechanisms accounting for such changes.

Climatic Conditions in Glacier Bay National Monument

Very little meteorological data have been gathered in this region. Extrapolations of meteorological data collected elsewhere in Southeastern Alaska are used to supplement climatic data recorded during the summer from 1960 to 1967 in the vicinity of Muir Inlet (Taylor 1962; Price 1964; Goldthwait et al. 1966; McKenzie 1968). However, because of the local effects of glaciers, mountains, and fjords, the actual values for the various meteorological parameters may be grossly different from those of the outlying stations.

The climate of Glacier Bay National Monument is best described as maritime. Characteristic of this type of climate are high humidity, heavy precipitation, few clear days, and low diurnal and annual temperature ranges. Close to the glaciers and near the heads of the inlets, the climate becomes more dependent on the presence of the glaciers.

Table 13 (p. 141) lists the meteorological stations consulted and shows their latitude, longitude, and elevation. The locations of most of these stations are shown in Figures 1 and 3 (pp. 2 and 10). The nearest outlying weather stations are at Gustavus near the mouth of Glacier Bay, at Haines 50 kilometers northeast, at Cape Spencer 65 kilometers southwest, and at Juneau 90 kilometers southeast.

Figure 3. Muir Inlet, Glacier Bay National Monument: Former Positions of Termini and Locations of Meteorological Stations (after Goldthwait et al. 1966)

Sunshine and cloudiness. No records of the solar and sky radiation flux (calories per square centimeter per day, cal./cm^2/day) incident to the water surface are available for Glacier Bay National Monument. The closest station monitoring this parameter is located at Annette Island. Data from Annette for 1958--1964 are shown in Table 1. The average maximum flux of solar radiation at the outer boundary of the earth's atmosphere occurs during June and equals 980 cal./cm^2/day. The average maximum flux of radiant energy incident to the earth's surface occurs during May and equals 460 cal./cm^2/day. The phase difference between these two maxima is a function of several other climatic variables, such as cloudiness and length of day (Goldthwait et al. 1966).

Based on Juneau records for 1958--1964, May is the clearest month and has the greatest number of hours of actual sunshine (see Table 2). Thus, in spite of May's not having the highest intensity of sun and sky radiation, the longer duration of sunshine during May more than compensates for its lower intensity (Goldthwait et al. 1966).

Examination of sunshine data (shown in Table 3) gathered in Adams Inlet from June 22 to August 25, 1967, shows ratios of actual to possible sunshine for these three months, which are in good agreement with those for Juneau (McKenzie 1968).

TABLE 1. SOLAR RADIATION AT ANNETTE ISLAND FOR 1958--1964 (Goldthwait et al. 1966)*

	Month (cal/cm^2-day)							
	Jan	Feb	Mar	Apr	May	Jun	Jul	Aug
Total incident to surface	55	95	210	325	460	445	445	320
Total available outside atmosphere	140	280	480	680	890	980	940	770
	Sep	Oct	Nov	Dec	Year ($Kcal/cm^2$-year)			
Total incident to surface	230	100	50	35	85			
Total available outside atmosphere	520	340	190	120	93			

*This table is to be read as follows: The first line shows the total sun and sky radiation incident to a horizontal earth surface. The second line gives the total radiation available outside the atmosphere. The monthly values are given in calories per square centimeter per day; the yearly values, in kilocalories per square centimeter per year.

TABLE 2. MEAN DURATION OF SUNSHINE IN HOURS PER MONTH AND FRACTION OF POSSIBLE SUNSHINE RECEIVED AT JUNEAU, ALASKA, 1958--1964 (Goldthwait et al. 1966)

	Month						
	Jan	Feb	Mar	Apr	May	Jun	Jul
Actual sunshine (hrs./mon.)	55	75	140	180	225	155	175
Ratio of actual to possible sunshine	.24	.28	.38	.41	.43	.29	.32
	Aug	Sep	Oct	Nov	Dec	Year	
Actual sunshine (hrs./mon.)	135	115	60	45	35	1400	
Ratio of actual to possible sunshine	.29	.30	.19	.18	.17	.32	

TABLE 3. SUNSHINE DATA FOR 1967 IN ADAMS INLET (McKenzie 1968)

Period	Total hours	Mean hours per day	Ratio actual to possible sunshine
June 22--30	34	4.3	.27
July 1--31	124	4.8	.31
August 1--17, 21--23	78	3.5	.26

Juneau averages annually only 50 clear days; Cape Spencer, 55. At the other extreme, Juneau averages 270 overcast days per year; Cape Spencer, 220 days. Nunatak Cove during July and August of 1963 and 1964 had an average cloudiness slightly less than Juneau's (Goldthwait et al. 1966).

Apparently, May is the month of maximum radiant energy input at the water surface in Glacier Bay National Monument.

Temperature. Characteristic of Southeastern Alaska is a small annual mean monthly temperature range. Of the stations examined, Haines exhibits the largest range, 19°C.; it is the station least exposed to maritime conditions. On the Pacific Ocean, Cape Spencer shows an 11°C. range (Goldthwait et al. 1966).

The maximum annual mean monthly temperature range in Muir Inlet is probably of the order of 20°C., since this fjord is relatively protected from maritime influences and is surrounded by large ice fields.

Loewe (Goldthwait et al. 1966) predicts a 3°C. difference between the average winter temperature at Gustavus and those occurring within the inlets.

Tables 4, 5, and 6 (pp. 15--17) show temperature data for the summer months at some stations in the vicinity of Muir Inlet and at some stations outside the Monument. The data from the Muir Inlet locale are consistently lower by

TABLE 4. MEAN TEMPERATURES FOR JUNE

Station name	Period	Mean maximum temperature	Mean minimum temperature	Mean temperature	Source
Adams Inlet	June 20--30, 1966	17.1°C.	5.8°C.		McKenzie 1968
	June 22--30, 1967	15.8	7.8		"
Cape Spencer				9.5°C.	Taylor 1962
Haines				12.8	"

TABLE 5. MEAN TEMPERATURES FOR JULY

Station name	Period	Mean maximum temperature	Mean minimum temperature	Mean temperature	Source
Adams Inlet	July 1--31, 1966	17.7°C.	7.5°C.		McKenzie 1968
	July 1--31, 1967	16.3	7.2		"
Cape Spencer				11.3°C.	Taylor 1962
Delta	June 18--July 31, 1965	14.0	4.0	10.6	Goldthwait et al. 1966; Price 1964
Gustavus	June 18--July 31, 1965	17.5	7.0	12.3	Goldthwait et al. 1966
Haines				14.2	Taylor 1962
Juneau	July 1963, 1964	16.5	9	12.7	Goldthwait et al. 1966
	July 1--31, 1966	18.9	8.3	13.4	McKenzie 1968
	July 1--31, 1967	17.2	7.2	12.1	"
Nunatak Cove	July 1963, 1964	15.0	5	10.0	Goldthwait et al. 1966
Terminus	June 18--July 31, 1965	14.0	4.5		"
Wachusetts Inlet	July 1--31, 1960			10.0	Taylor 1962

TABLE 6. MEAN TEMPERATURES FOR AUGUST

Station name	Period	Mean maximum temperature	Mean minimum temperature	Mean temperature	Source
Adams Inlet	August 1--31, 1966	13.8°C.	5.6°C.		McKenzie 1968
	August 1--25, 1967	15.5	7.3		"
Cape Spencer				11.5°C.	Taylor 1962
Delta				10.1	Price 1964
Haines				13.3	Taylor 1962
Juneau	August 1963, 1964	18	8.5	12.9	Goldthwait et al. 1966
	August 1--31, 1966	15.6	7.2	11.3	McKenzie 1968
	August 1--31, 1967	17.2	8.9	12.8	"
Nunatak Cove	August 1963, 1964	15	5.0		Goldthwait et al. 1966
Wachusetts Inlet	August 1--31, 1960			9.7	Taylor 1962

about 3°C. than the corresponding data from Juneau and Gustavus. McKenzie (1968) observes that in 1966 Adams Inlet was warmer than other parts of Glacier Bay in previous years.

The first frost is likely to occur around mid-December at Cape Spencer, mid-November at Gustavus, and late October at Haines. The last frost generally occurs near mid-March at Cape Spencer, late March at Gustavus, and mid-April at Haines. Cape Spencer is completely free of frost from May through October; Gustavus, only during June and July (Goldthwait et al. 1966).

Skim ice has been observed in Muir Inlet as early as October and November (J. B. Matthews, personal communication 1968).

Precipitation. Loewe (Goldthwait et al. 1966) predicts that over 125 centimeters water equivalent of precipitation falls annually throughout Glacier Bay National Monument. McKenzie (1968) reports 223.0 centimeters water equivalent of precipitation in Adams Inlet from August 1, 1966, to August 1, 1967. Consult Table 7 for seasonal amounts of precipitation at stations outside of Glacier Bay.

Over one-third of this total annual precipitation falls from August to October in Adams Inlet. October is the wettest month, with rain almost three out of four days (McKenzie 1968). The timing of this precipitation maximum compares favorably with the peak shown in Figure 4 (p. 19).

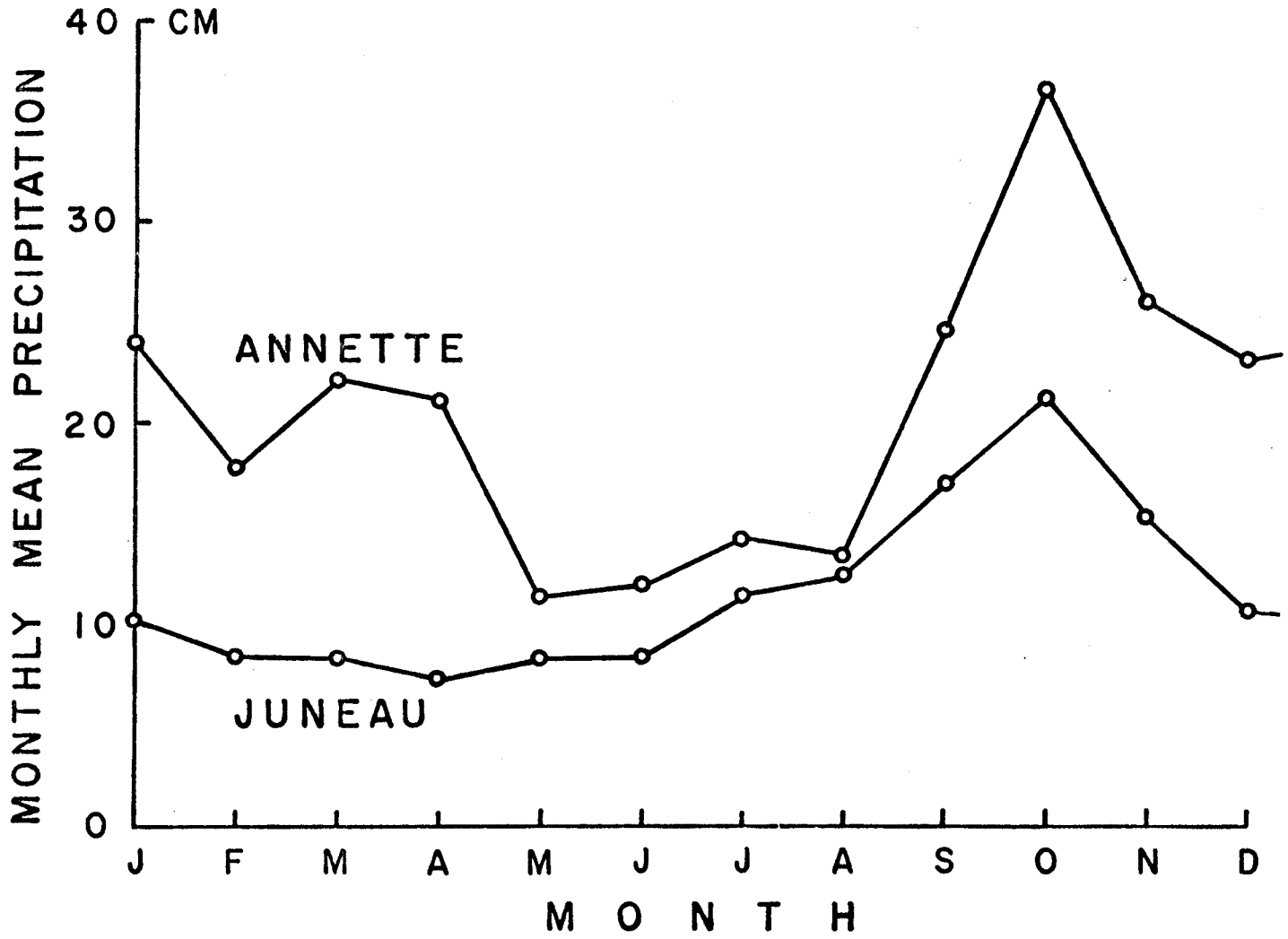

Figure 4. Monthly Mean Precipitation Patterns for Annette and Juneau, Alaska (after Pickard 1967)

TABLE 7. MEAN SEASONAL PRECIPITATION IN CENTIMETERS (Goldthwait et al. 1966)

Station	Season				Year
	Spring	Summer	Autumn	Winter	
Cape Spencer	47	61	112	58	278
Gustavus	24	26	52	34	136
Haines	26	15	61	43	145
Juneau	40	39	75	50	205
Little Port Walter	103	87	240	157	586
Yakutat	65	60	125	83	333

At elevations within the Monument, as much as six meters of water equivalent may accumulate annually from fall freeze-up to spring melt. Some of this precipitation falls as snow; some accumulates as rime deposition from water in the air (Goldthwait et al. 1966).

Table 8 shows that snowfall in Juneau begins during October and continues through April (Goldthwait et al. 1966).

The first snowfall in Muir Inlet usually comes in late August, but melts. New snow accumulation is evident by October (G. M. Haselton, personal communication 1969).

Storage and runoff. None of the streams in Muir Inlet has been gauged.

TABLE 8. RATIO OF SNOWFALL DAYS TO TOTAL NUMBER OF DAYS WITH PRECIPITATION AT JUNEAU, ALASKA (Goldthwait et al. 1966)

	Monthly												Yearly
	Jan	Feb	Mar	Apr	May	Jun	Jul	Aug	Sep	Oct	Nov	Dec	
Ratio	.85	.85	.85	.45	--	--	--	--	--	.15	.40	.85	.40

No numerical values can be assigned to the amounts and distribution of either direct or stored runoff.

The temperature and precipitation information suggest that the winter freeze-up of freshwater sources begins in October. At this time, the seasonal trend toward homogeneity of fjord water characteristics commences.

The spring melt, and the return to a stratified estuarine regime, must begin in April as a direct result of increasing amounts of sunshine and daytime warming of the air. On May 5, 1969, however, snow was observed three to five feet deep at the high tide line in Reid Inlet, and air temperatures hovered around 0°C. at sea level on that day.

The beginning of the winter freeze-up in late October and the beginning of the spring melt in late April bracket a six-month period of low runoff, during which the stability of the fjord is minimal.

Humidity and evaporation. Juneau has a mean relative humidity of 79%. The Muir Inlet and Juneau stations show similarly high values during the summer (Goldthwait et al. 1966; McKenzie 1968).

High relative humidity inhibits evaporation from surface water and ice.

Wind. Very scanty data exist with regard to winds throughout the Monument. The winds probably are under local control by glaciers, mountains, and fjords; recourse to data from outside stations, then, is useless.

Within Muir Inlet itself, the direction of the winds is probably controlled by the direction of the steep-walled fjord and the down flow of chilled air off the glaciers onto the inlet. Loewe (Goldthwait et al. 1966) reports that the only wind direction observed at the 300-meter elevation Casement station during the summer of 1965 was northeast by east. He interprets this consistent direction as a compromise between the prevailing maritime wind, from the southeast, and the "glacier wind," which would be north by east. Muir Inlet runs north, and slightly west in the upper reaches.

Tidal Effects

Strong tidal currents, up to six knots, occur in the vicinity of the mouth of Glacier Bay and up into the neighborhood of Willoughby Island. These currents combined with a 40-meter sill depth and numerous shoals and islands produce a thoroughly mixed water mass in Icy Strait and in Glacier Bay near its mouth (United States Coastal Pilot 8, 1962).

The tide in Glacier Bay National Monument is of the mixed type. The mean tidal range for Muir Inlet is about 4.25 meters. The diurnal range is about 5.02 meters (Tide Tables West Coast North and South America, 1967).

Physiography and Bathymetry

North of a line connecting Francis Island and Tlingit Point, Glacier Bay National Monument is not fully charted. The United States Coast and Geodetic Survey (U.S.C. & G.S.) Chart 8202 shows only the results of a preliminary survey and a few soundings made in 1892, with subsequent minor revisions, the most recent in 1965.

Glacier Bay is an unwieldy body of water, containing a number of inlets, shoals, basins, islands, tidal glaciers, and streams. Its irregular physiography and the lack of sufficient and accurate detail in chart soundings and shoreline boundaries make it difficult to study.

For several reasons, then, only Muir Inlet and its seaward connections are considered in this thesis. Because of its more regular plan form and smaller size, Muir Inlet is far easier to handle conceptually. It is also a classic example of a particular fjord type, having a sill at its mouth, a U-shaped profile, tidewater glaciers, icebergs, a long and narrow plan form, and several interior sills and basins. Furthermore, the scarcity of bathymetric information, which hinders an overall analysis of Glacier Bay data, is overcome through the application of longitudinal and transverse precision depth recorder traces taken in Muir Inlet on May 5, 1969.

Starting at MUI 0, the trace runs north along the axis of Muir Inlet and through all the Muir Inlet station loci, which are plotted in Figure 5 (p. 26), and listed in Table 12 (p. 140). Because of the danger presented by floating icebergs, the trace ends north of MUI 20 in the western arm of the fjord, 2.6 nautical miles from Muir Glacier and 0.9 nautical miles from Riggs Glacier. This is the first reported precision depth recorder trace of Muir Inlet and is shown in Figure 6 (p. 27).

In addition to the longitudinal profile, four transverse profiles, which are shown in Figure 7 (p. 28), were obtained at MUI 20, just north of MUI 15, at MUI 10, and at MUI 5. Figure 8 (p. 29) shows the cruise track and locations of the transverse runs.

Used in conjunction with the U.S.C. & G.S. Chart 8202, these traces provide sufficient bathymetric detail to allow a reasonably accurate estimation of the volumes of Muir Inlet, both <u>in toto</u> and in appropriately defined sub-volumes, as are required for the quantitative analysis to be outlined later. Moreover, the longitudinal profile can be used to demonstrate the temperature, salinity, and dissolved oxygen values along the inlet in relation to the sills and basins.

Muir Inlet extends 43.7 kilometers north from MUI 0. It has a sill depth of 58 meters, a mean width of 3.5 kilometers, a maximum depth of 300 meters, a mean mid-inlet

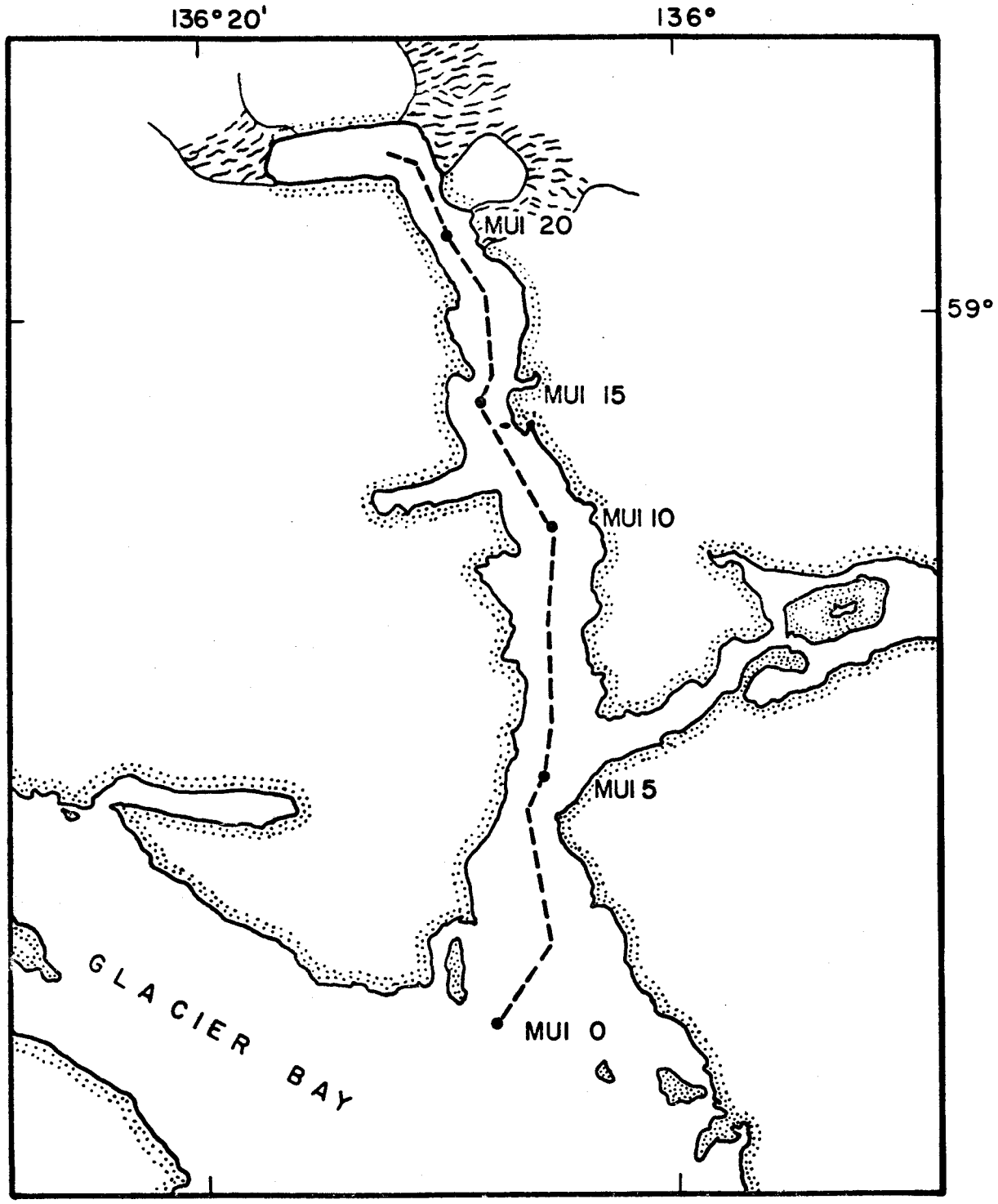

Figure 5. Cruise Track for Longitudinal Precision Depth Recorder Trace of Muir Inlet

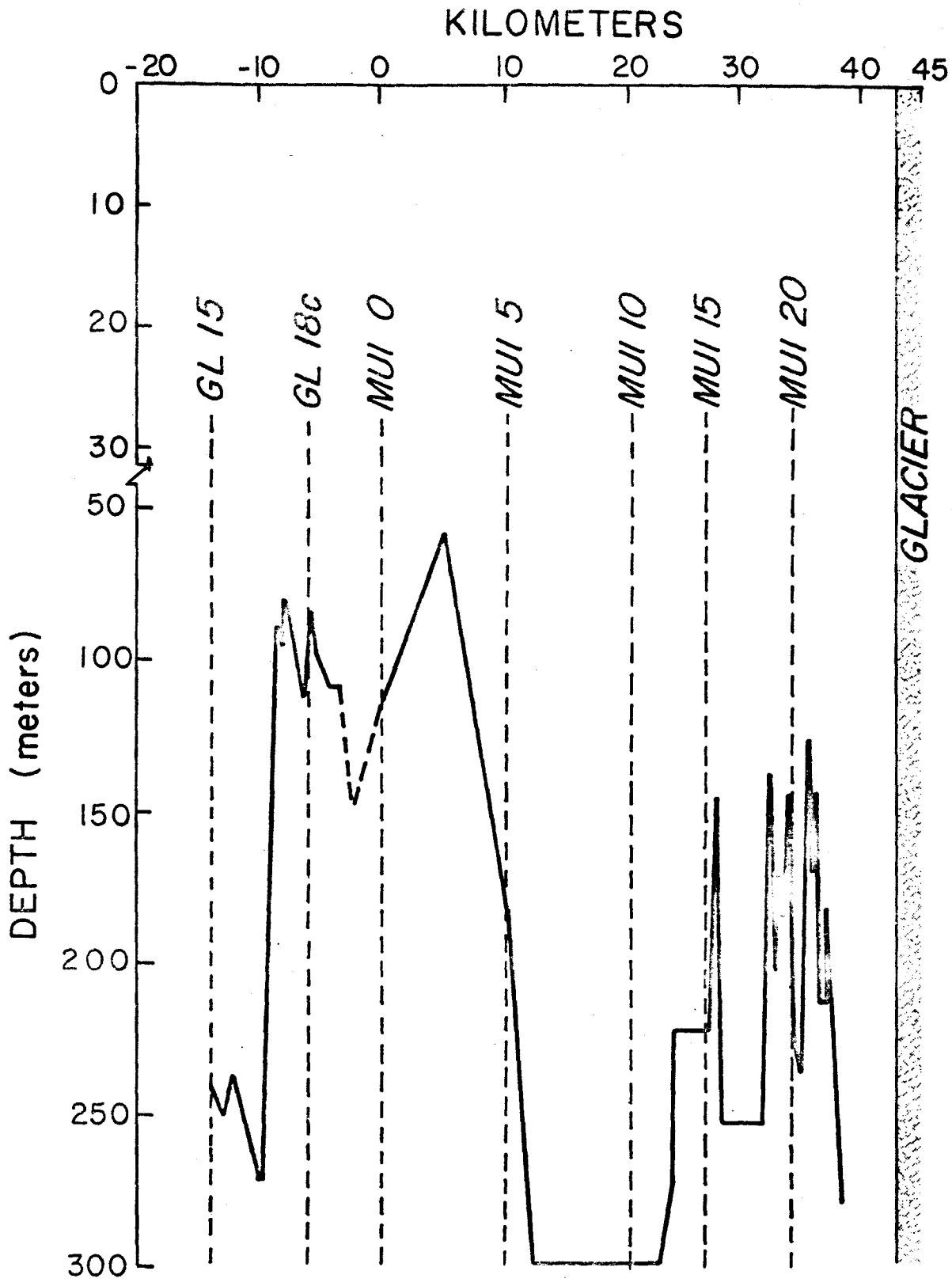

Figure 6. Longitudinal Bottom Profile of Muir Inlet

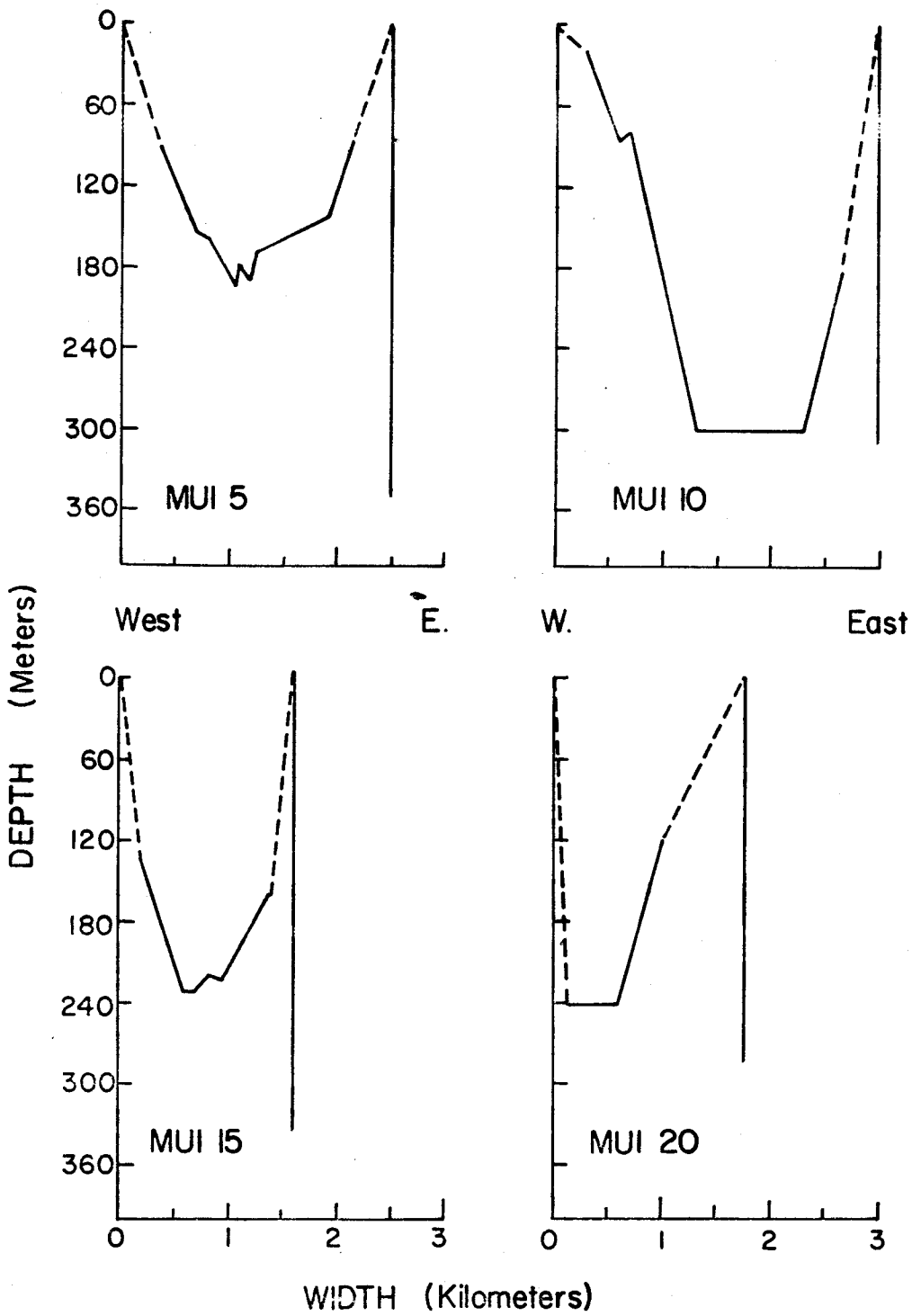

Figure 7. Transverse Bottom Profiles for Muir Inlet

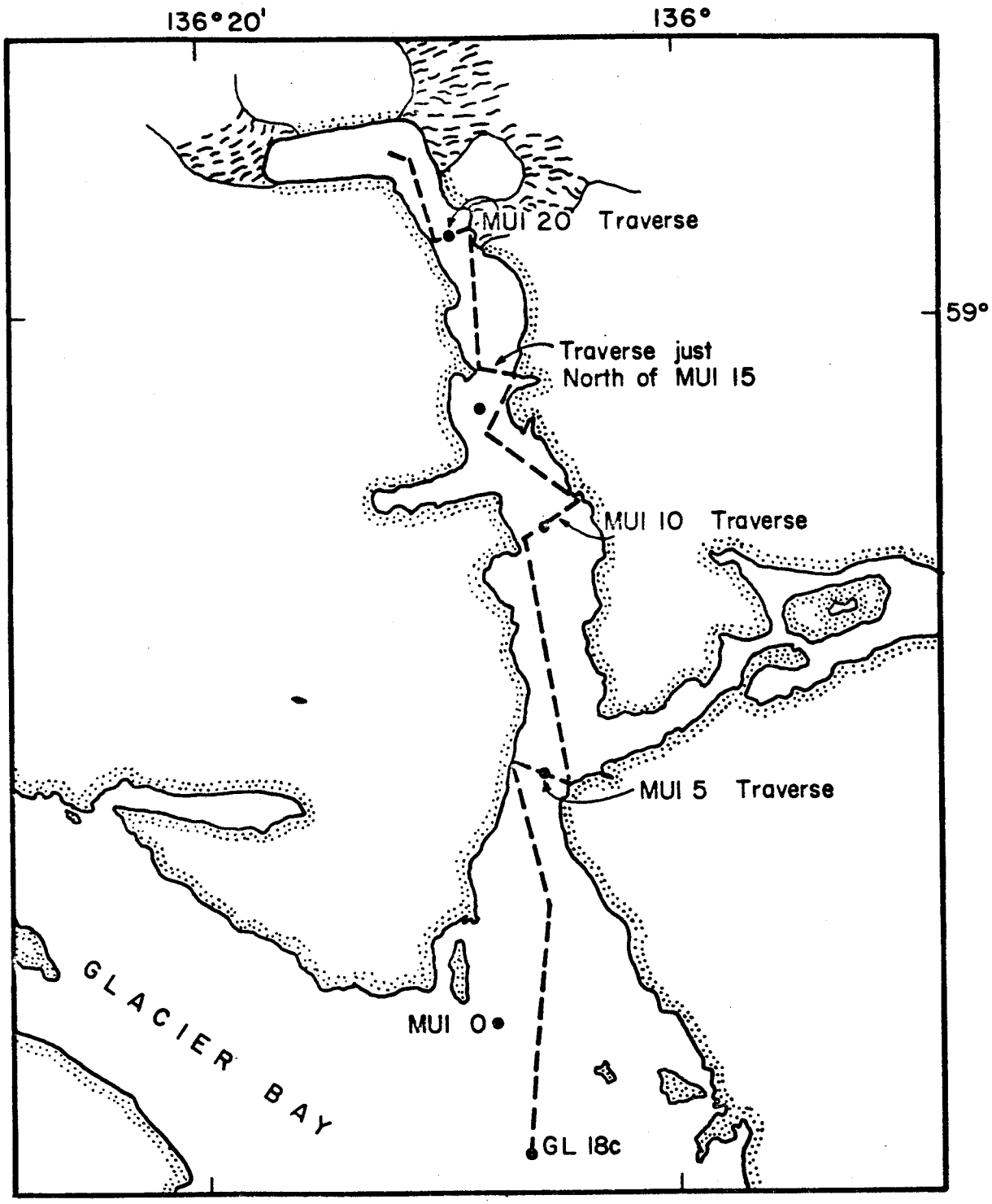

Figure 8. Cruise Track for Transverse Precision Depth Recorder Traces of Muir Inlet

depth of about 238 meters, a surface area of 129 square kilometers, and a volume of 16.55 cubic kilometers. There are at least four basins and four sills.

Pickard (1967) bases his bathymetric profile of Muir Inlet on the incomplete soundings of the U.S.C. & G.S. Chart 8202. Because of his reliance upon the incomplete sounding data, he limits himself to one major sill (58 meters), and one major basin (maximum depth of 300 meters), followed by an abrupt, and premature, rise to the inlet surface.

The precision depth recorder trace shows, in addition to the major sill and the major basin, at least three more minor basins, each bounded by a sill of 150 meters depth. Each basin is progressively more shallow, with maximum depths (as one moves toward the head of the fjord) of 256, 238, and 220 meters.

Such a sequence of sills and basins indicates a history of glacial retreat and stagnation. All the sills correspond to the locations of the glacier face during periods of stagnation (Goldthwait et al. 1966). Thus, the sills probably represent terminal moraine deposits.

Oceanographic Parameters

The hydrographic data upon which this investigation is based was collected from June of 1964 until September of

1967, at the stations listed in Table 12 (p.140). Starting at the head of Muir Inlet and moving south and west, the stations are MUI 20, MUI 15, MUI 2, MUI 10, MUI 3, MUI 5, MUI 0, GL 18C, GLA 8, GL 15, GL 10, GL 5, GLA 10, GL 0, ICY 30, ICY 1, ICY 40, CRO 0, and CRO 10. MUI 3, MUI 2, GLA 8, GLA 10, and ICY 1 are University of British Columbia stations (Anonymous 1965, 1966); those remaining are University of Alaska stations (Rosenberg 1966; Matthews and Rosenberg 1968; Wallen and Hood 1968). Table 12 (p.140) gives the station name and its latitude, longitude, and mean sonic depth.

Outstanding among the limitations of this thesis are those imposed by the poor time distribution of hydrographic data. No data exist for the months of December and January. The data for the remaining 10 months are scattered among the results of 13 cruises spanning a 3-year interval from June of 1964 to September of 1967. Tables 14 and 15 (p.142--145) list these 13 cruises in chronological order and indicate which stations were sampled and which parameters were measured at each station.

The standard depths sampled are 0, 2, 5, 10, 20, 30, 50, 75, 100, 150, 200, 250, and 300 meters.

The methods used to measure and process the data are described in Rosenberg (1966), Matthews and Rosenberg (1968), Wallen and Hood (1968), Anonymous (1965), and Anonymous (1966).

Objectives of Thesis

This thesis attempts a year-around analysis of fjord water masses and involves both a qualitative and a quantitative description of the water masses in a fjord with actively discharging glaciers at its head.

The qualitative aspects of this thesis consist of an analysis of Muir Inlet water masses with respect to seasonal and spatial variations in the hydrographic parameters of salinity, temperature, density, and dissolved oxygen. Conventional temperature-salinity, salinity-oxygen, and temperature-oxygen diagrams are constructed according to two forms: the first type shows data from each station for months typical of each season; the second type is restricted to MUI 10 data, and each diagram focuses on a particular depth, displaying data from all cruises. Lastly, the salinity, temperature, and oxygen depth profiles for representative months are drawn, and from them the longitudinal profiles of salinity and temperature are constructed.

The quantitative analysis involves the determination of the seasonal variations in the prevalence (frequency of occurrence by volume weighting) of characteristic salinity-temperature water types according to the method developed by Cochrane (1956, 1958), Montgomery (1955, 1958), and Pollak (1958). Quantitative salinity-temperature diagrams

are prepared, and from these the univariate distributions of temperature and salinity are determined.

CHAPTER II

QUALITATIVE ANALYSIS OF THE SEASONAL AND SPATIAL DISTRIBUTIONS OF TEMPERATURE, SALINITY, AND DISSOLVED OXYGEN

The temperature, salinity, and dissolved oxygen data from the thirteen cruises into Muir Inlet are presented in graphical form. Several methods of representation are employed.

Although the data were collected sporadically over three years, the results are presented in a seasonal sequence regardless of the year of the survey, since it is assumed that the data represent the major seasonal trends that occur in any year.

Depth Profiles

The temperature, salinity, and dissolved oxygen data from the cruises of November 1966, February 1967, July 1967, and September 1967, are plotted against depth for each station. These graphs are presented in Figures 9--13 (pp. 35--39). The data from these months represent the major seasonal trends expressed at each station.

Salinity Versus Depth

For all Muir Inlet stations and throughout all the seasons, the surface salinity is less than that at depth.

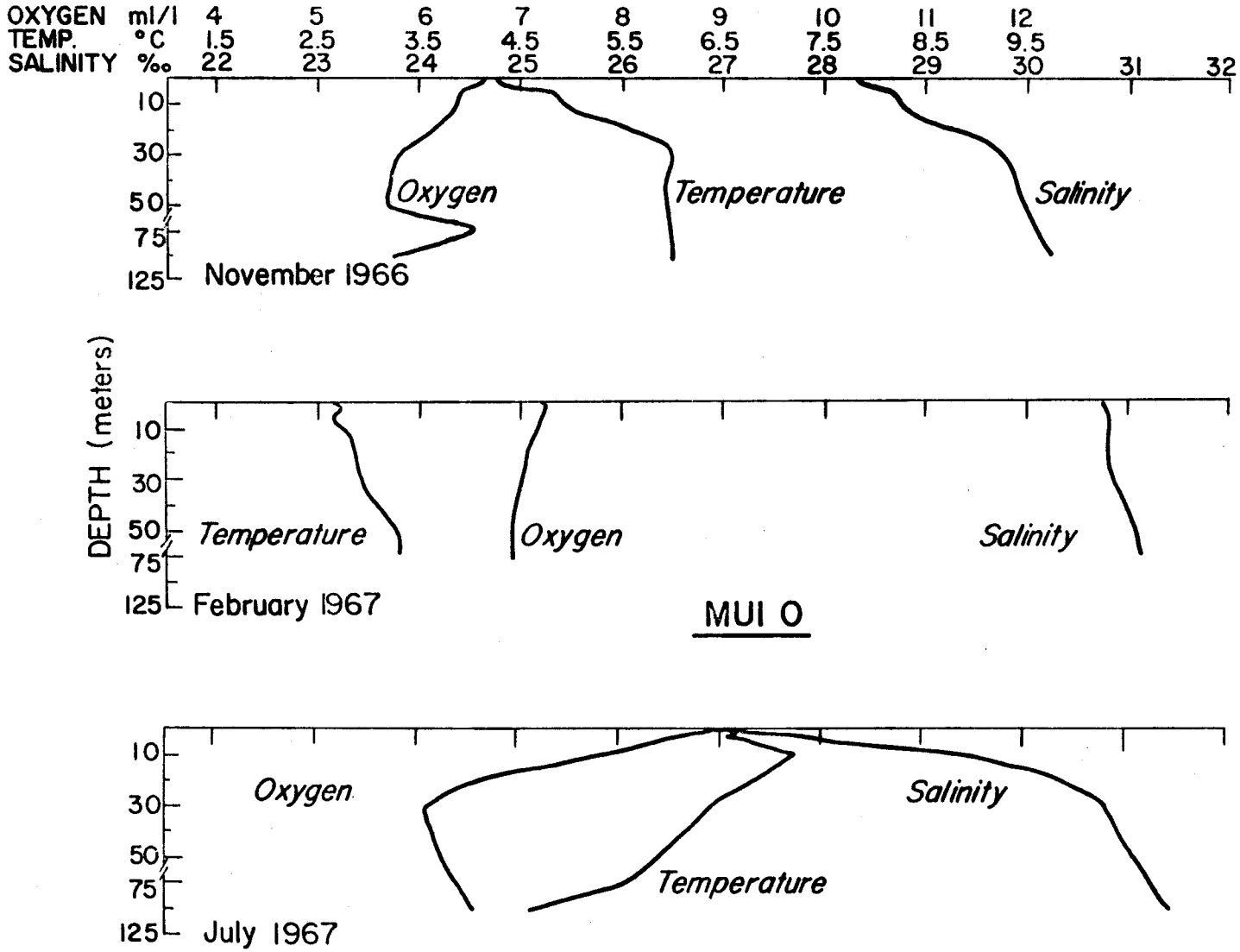

Figure 9. Temperature, Salinity, and Dissolved Oxygen Data from MUI 0 for November 1966, February 1967, and July 1967 Plotted Against Depth

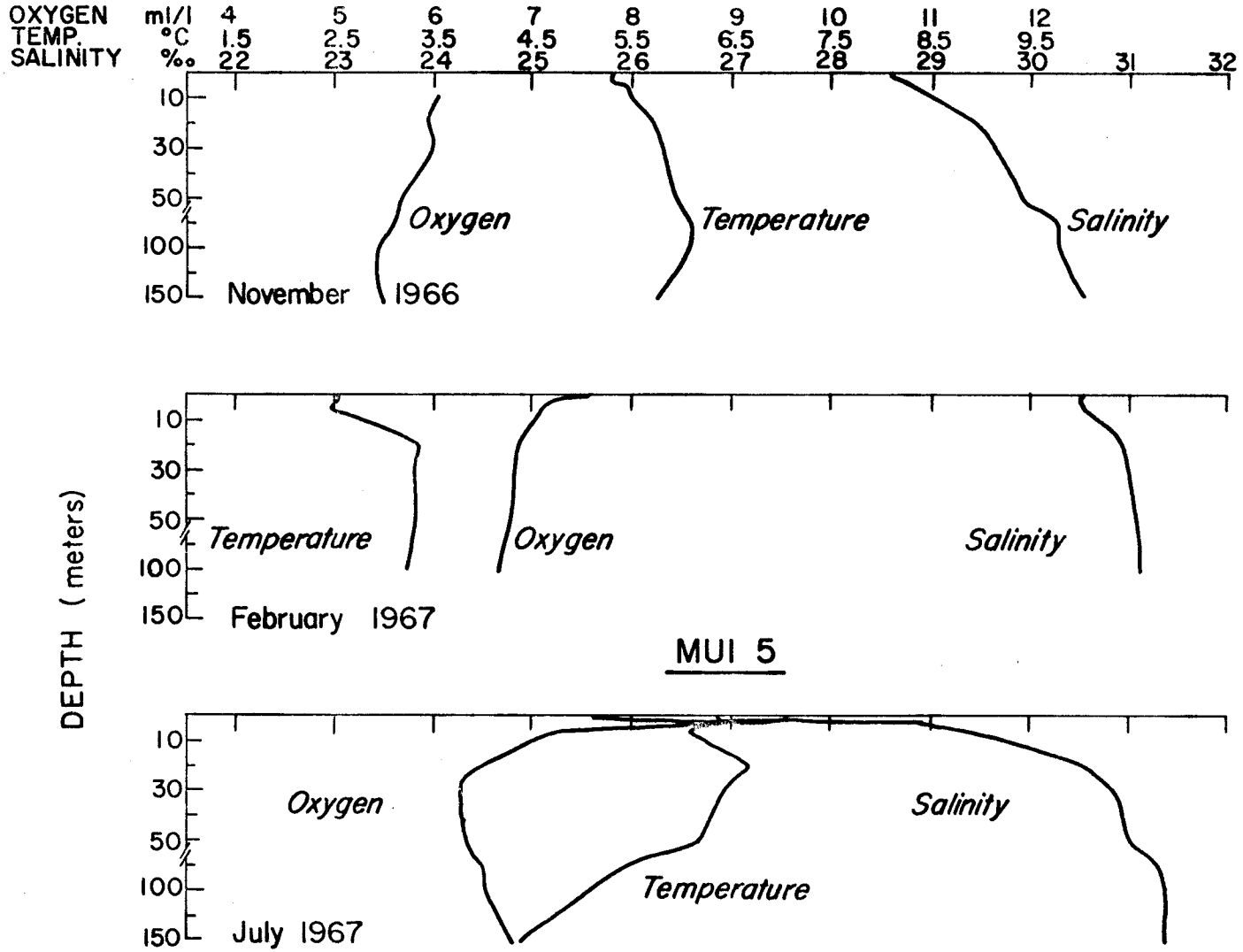

Figure 10. Temperature, Salinity, and Dissolved Oxygen Data from MUI 5 for November 1966, February 1967, and July 1967 Plotted Against Depth

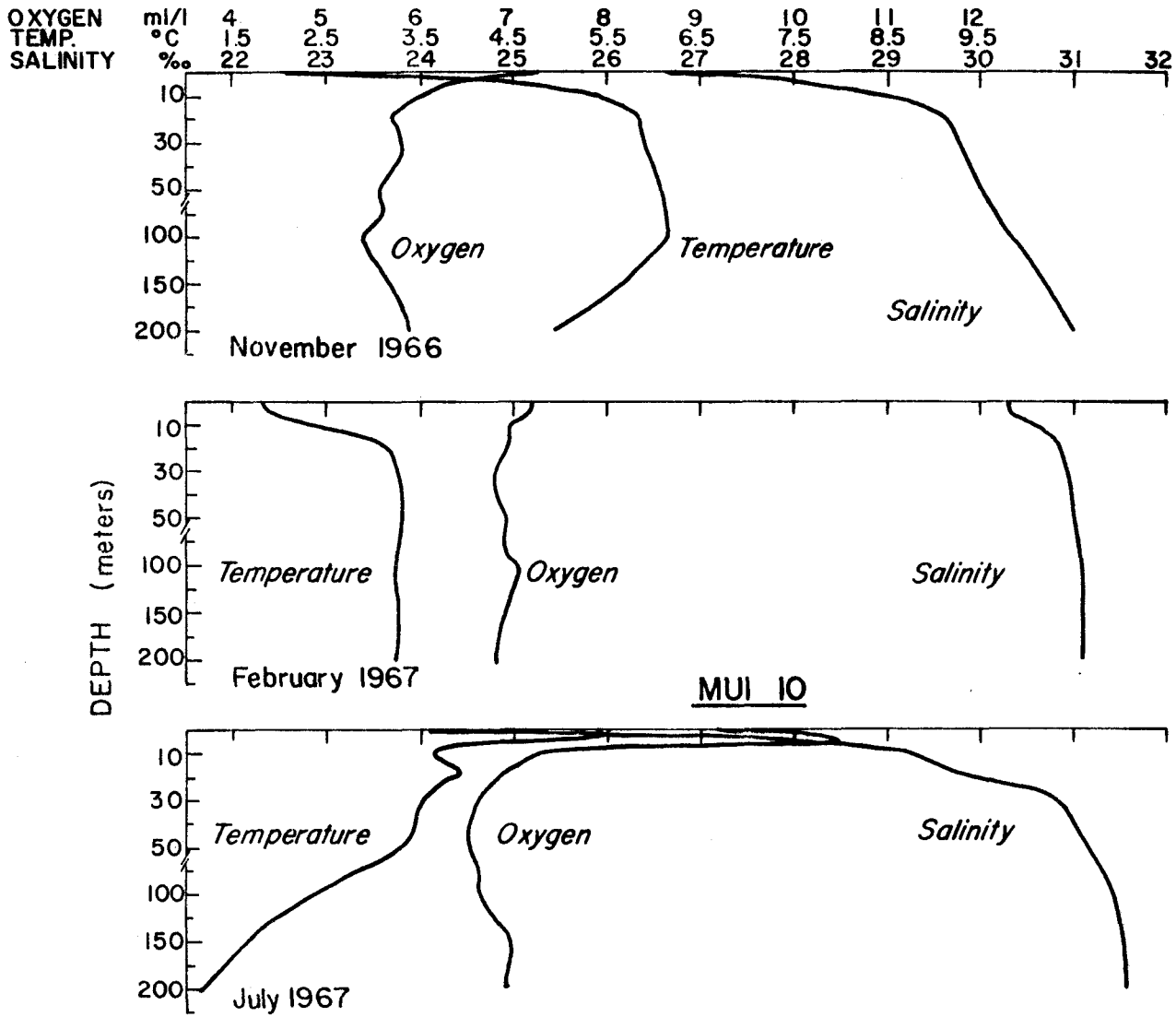

Figure 11. Temperature, Salinity, and Dissolved Oxygen Data from MUI 10 for November 1966, February 1967, and July 1967 Plotted Against Depth

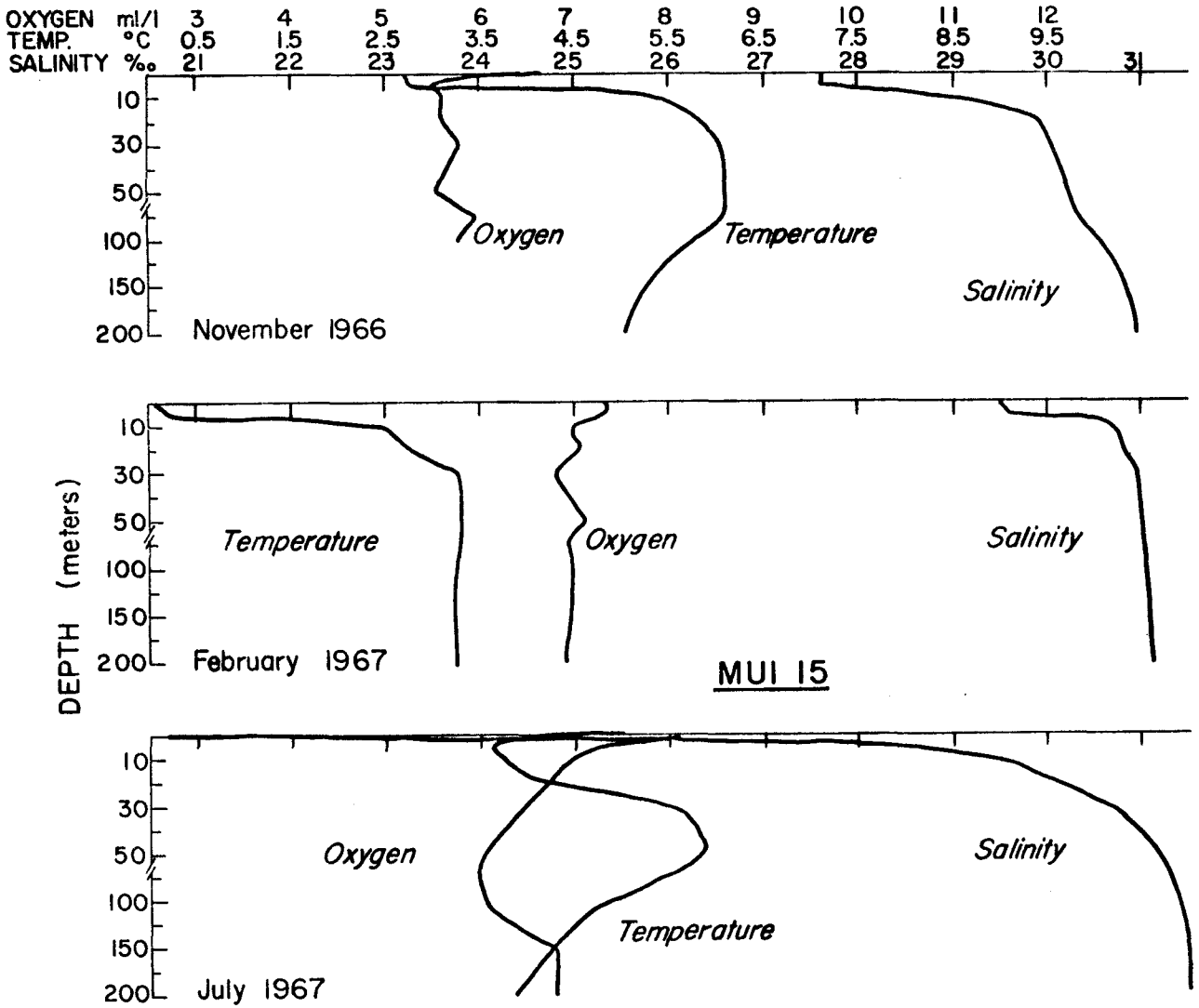

Figure 12. Temperature, Salinity, and Dissolved Oxygen Data from MUI 15 for November 1966, February 1967, and July 1967 Plotted Against Depth

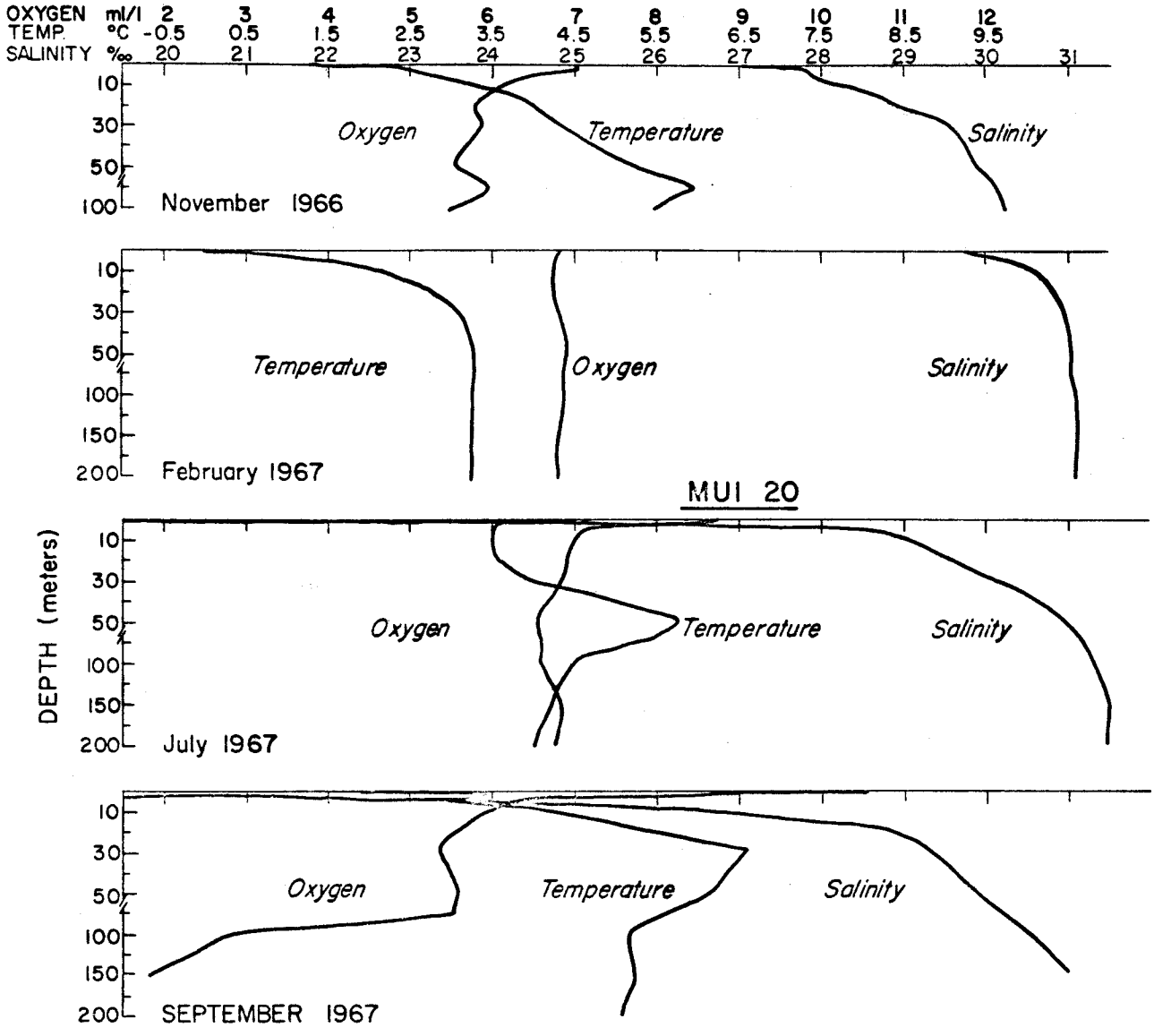

Figure 13. Temperature, Salinity, and Dissolved Oxygen Data from MUI 20 for November 1966, February 1967, July 1967, and September 1967 Plotted Against Depth

This trend is very pronounced from late spring through early fall, during which time occur high levels of freshwater runoff from meltwater and rainfall.

The lowest surface salinities are found at the head of Muir Inlet. Surface salinities increase toward the mouth, with the exception of a slight freshening at MUI 10. This local decrease in salinity is probably caused by the brackish surface outflow from Wachusetts Inlet. A similar effect is not detected near the mouth of Adams Inlet.

For February 1967, the surface salinities increase from 29.55‰ at MUI 20 to 30.75‰ at MUI 0. All the salinity values increase with depth to values of about 31.10‰ below the halocline, which terminates at 20--30 meters.

For July 1967, the lowest observed salinity values are found at the surface at MUI 20. The surface salinities increase from 13.95‰ at MUI 20 to 27.05‰ at MUI 0. The halocline penetrates to 100--200 meters, showing the vertical extent of surface mixing. Below the halocline, the salinity becomes uniform at 31.50‰, a 0.40‰ increase with respect to February's values. Thus, while there is a marked surface freshening extending below 50 meters, where the 31.10‰ value typical of February's deep water is encountered, the water below 50 meters has increased in salinity since February. Two separate and opposing sources or mechanisms of water exchange appear to exist in the spring and early [illegible] the salinity of the deep

water, and the other tends to decrease the salinity of the surface waters.

For September 1967, only data from MUI 20 exist. The surface salinity of 13.08‰ increases to 30.98‰ at 150 meters, which is 0.52‰ less than the 150-meter value observed at this station in July. Hence, fresher water has been introduced to a depth of at least 150 meters between July and September. The salinity profile shows that the salinity increases continually from the surface down to the deepest observations at 150 meters.

For November 1966, as in September 1967, salinity increases continually with depth from the surface to the deepest level sampled. Surface salinities are considerably higher, though. The increases in surface salinity reflect the decrease in freshwater runoff from precipitation and melting at the outset of the winter freeze-up. Surface salinities range from 26.95‰ at MUI 20 to 27.30‰ at MUI 0. The salinity increases downward to 31.00‰ at 200 meters.

Temperature Versus Depth

The lowest temperatures are associated with the tidewater glaciers at the head of the fjord. Surface temperatures progressively increase mouthward as a result of a longer exposure to solar and sky radiation and warm air. The [illegible] depends on the intensity

and duration of the radiant energy reaching the water surface and the downward rate of turbulent mixing.

The vertical temperature structure is frequently complex, showing maxima or minima and a thermocline. The degree to which these characteristics are developed depends upon the severity of the surface climatic and runoff conditions and the vertical stability of the water column. Heating at the surface promotes stability; cooling decreases stability. Thus, surface cooling effects penetrate the water column more rapidly than heating effects.

For February 1967, the graphs show a marked thermocline at all stations from MUI 20 to MUI 0. The temperature gradient is steepest at MUI 20, where it penetrates to about 40 meters. Beneath the thermocline, isothermal conditions prevail, with the temperature hovering around 3.25°C. Surface temperatures range from 0°C. at MUI 20 to 2.7°C. at MUI 0.

For July 1967, the data show prominent temperature maxima below the surface layers. With the exception of MUI 10, the surface layer is warmer than the deep water, but not as warm as the intermediate water. Surface temperatures are warmer than the 2-meter samples, probably because of solar heating and positive stability at the surface. MUI 10 has only a weakly developed maximum of 6.4°C. at 20 meters. The remaining stations have maxima ranging between 5.75°C. at 30 meters for MUI 20 to 7.3°C.

at 10 meters for MUI 0. The subsurface temperature maxima have higher temperatures and are shallower at the mouth than near the tidal glaciers at the head of the fjord. Surface temperatures vary from 3.75°C. at MUI 20 to 6.7°C. at MUI 0. Below the maxima, the temperatures rapidly fall off with depth. At the 200-meter level, MUI 20 and MUI 15 are warmer (4°C.) than MUI 10 (1.2°C.).

For November 1966, examination of the data shows temperature maxima which are deeper and less prominent than the ones found in July. Again, the strongest thermocline is found at MUI 20. The values of the maxima are all in the vicinity of 6.1°C., and the maxima occur at 30--75 meters. The surface temperatures rise from 1.25°C. at MUI 20 to 4.25°C. at MUI 0 and 5.0°C. at GL 18C. All the stations in Muir Inlet show rapidly decreasing temperatures below the thermocline. GL 18C, in contrast, is isothermal at 5.85°C. below 20 meters.

The schedule the water masses follow in re-acquiring the high salinity and low temperature characteristic of February water at all depths is not known because of the lack of any December or January data. The effects of the precipitation and runoff decreases during fall and winter are probably more immediately effective in changing the density structure of the water column than is the solar and sky radiation mechanism. The path the water mass

characteristics follow in returning to February values is probably via a continued reduction in salinity followed by a decrease in temperature. This path would retrace that followed during the spring and summer except that the processes governing the fall--winter changes bring them about more abruptly. The combined effects of an increased surface salinity and a decreased surface temperature in the late fall create an unstable vertical density structure with the surface water heavier than the immediately underlying layers. Such a vertical density structure initiates convective thermohaline mixing, culminating in the fall overturn.

Dissolved Oxygen Versus Depth

For February 1967, the oxygen values are fairly constant at all stations and at all depths, falling between 6.5--7.5 milliliters per liter.

For July 1967, higher oxygen values (8.5--10.5 milliliters per liter) are recorded near the surface at all stations. These high oxygen levels are related to the high rates of photosynthesis in the euphotic zone. Noticeable oxygen minima (6.1--6.5 milliliters per liter) are found between 30--100 meters.

For September 1967, one station, MUI 20, was sampled. Here, the lowest observed oxygen levels occur, 2.69

milliliters per liter at 100 meters and 1.82 milliliters per liter at 150 meters. Whether these values are the result of an error in the field determination of the dissolved oxygen content of the samples or whether they are the result of a seasonal phenomenon which produces near-anoxic conditions near the fjord bottom is unknown.

For November 1966, the water at all stations has moderately high surface oxygen concentrations (6.0--7.2 milliliters per liter) decreasing to lower values (5.5 milliliters per liter) at depth.

Longitudinal Profiles

Figures 14--19 (pp. 46--51) show the results of plotting the longitudinal profiles of temperature and salinity. The horizontal axis represents the positions of the stations GL 15, GL 18C, MUI 0, MUI 5, MUI 10, MUI 15, and MUI 20 and the terminus of the Muir Glacier. All distances are referenced to MUI 0, which is assigned the value of zero kilometers. Stations north of MUI 0 are measured in the positive direction; stations south, in the negative direction. The vertical axis shows depth in meters. The longitudinal bottom depth profile is included on the diagrams to facilitate interpretation of the data.

Upon this framework, the temperature and salinity data from these representative cruises (November 1966,

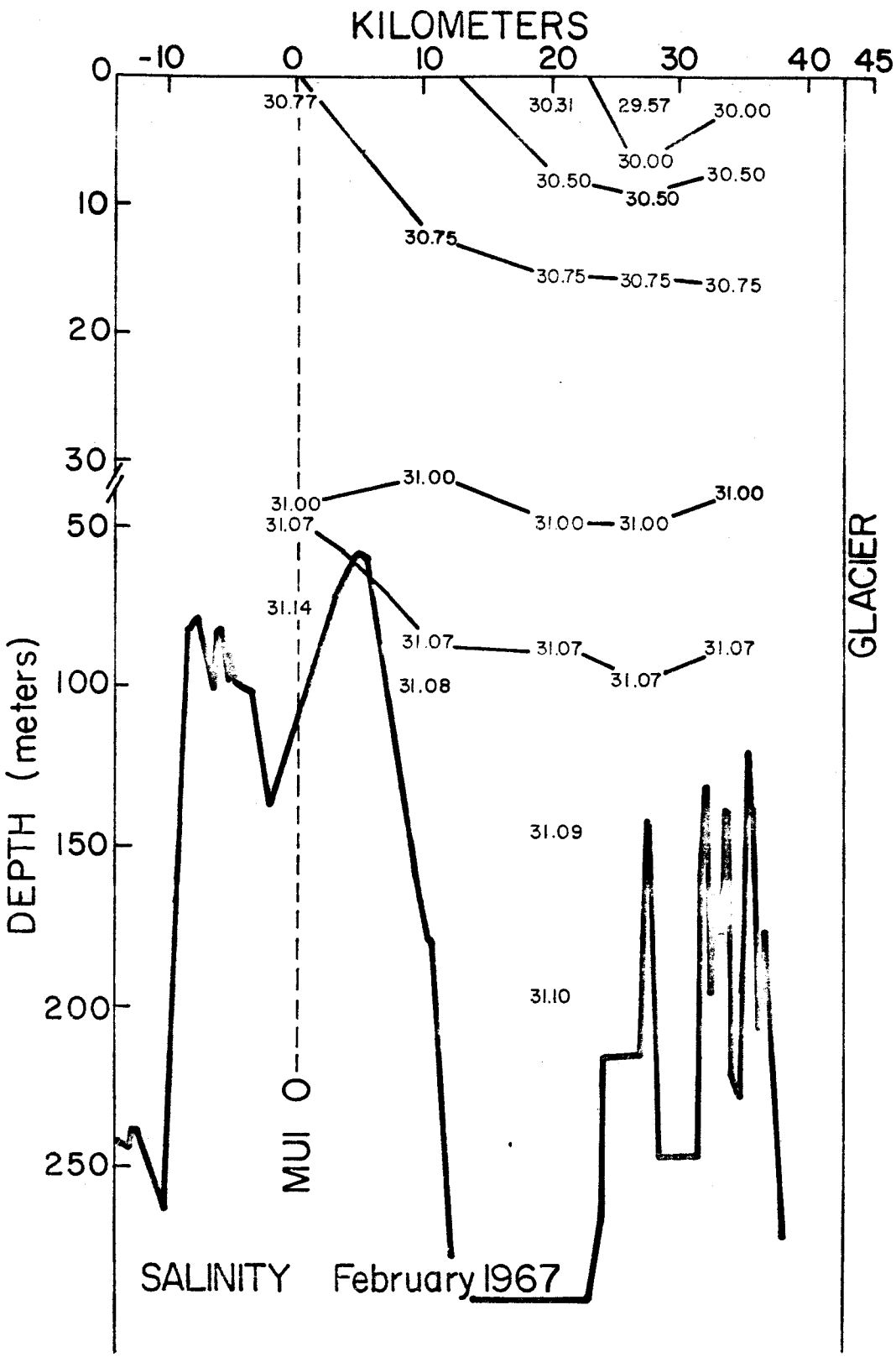

Figure 14. Longitudinal Salinity Profile for February 1967

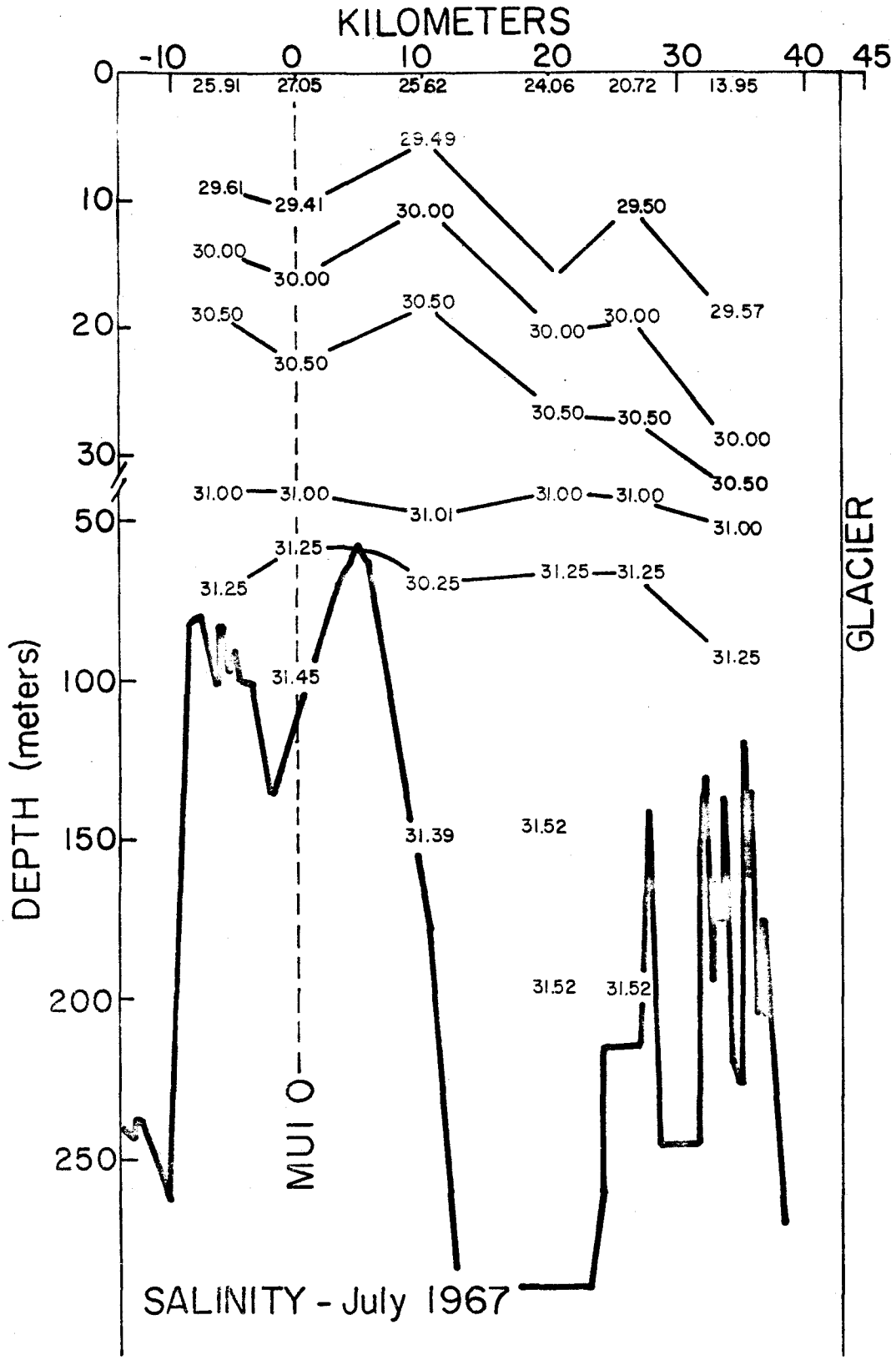

Figure 15. Longitudinal Salinity Profile for July 1967

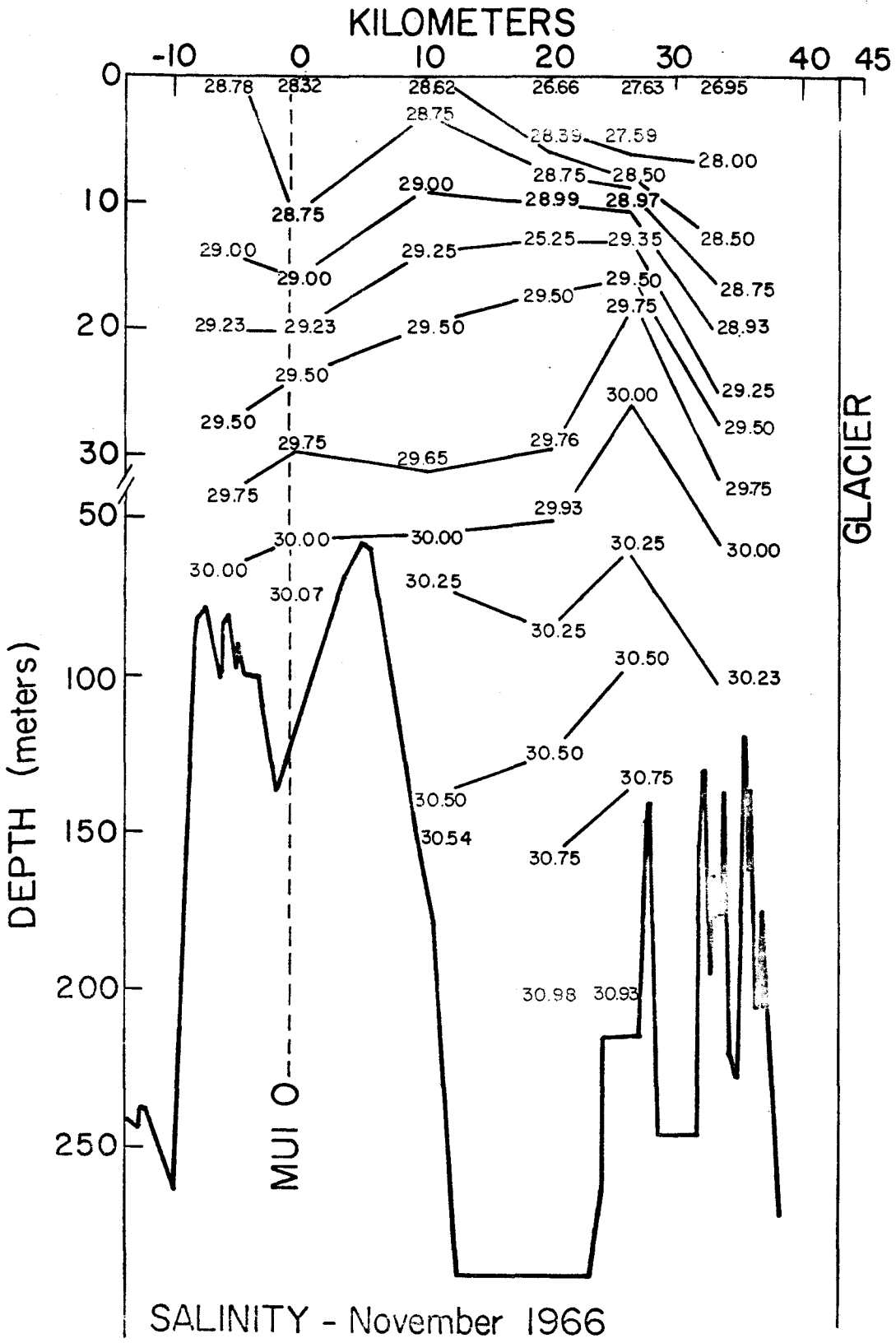

Figure 16. Longitudinal Salinity Profile for November 1966

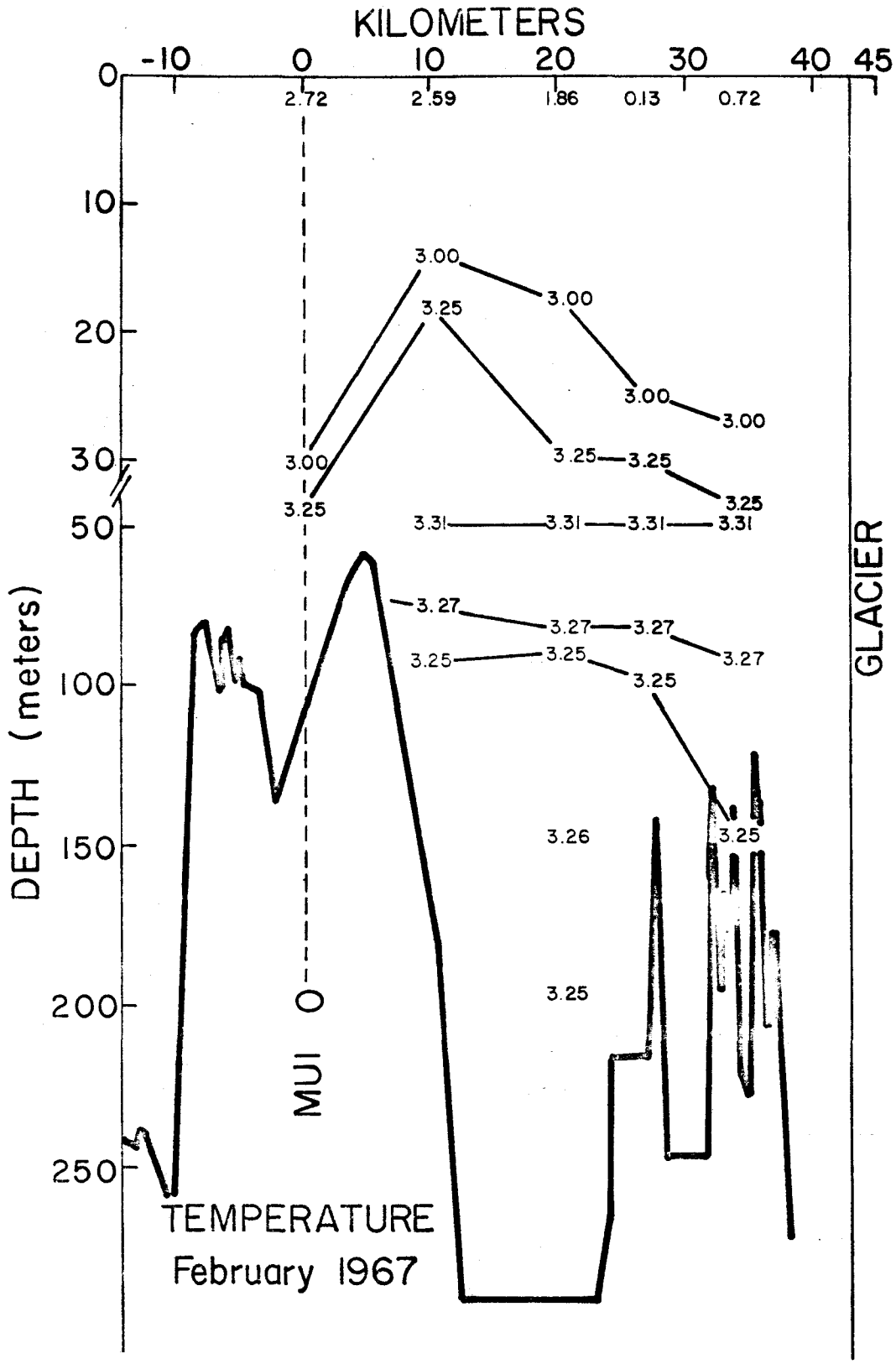

Figure 17. Longitudinal Temperature Profile for February 1967

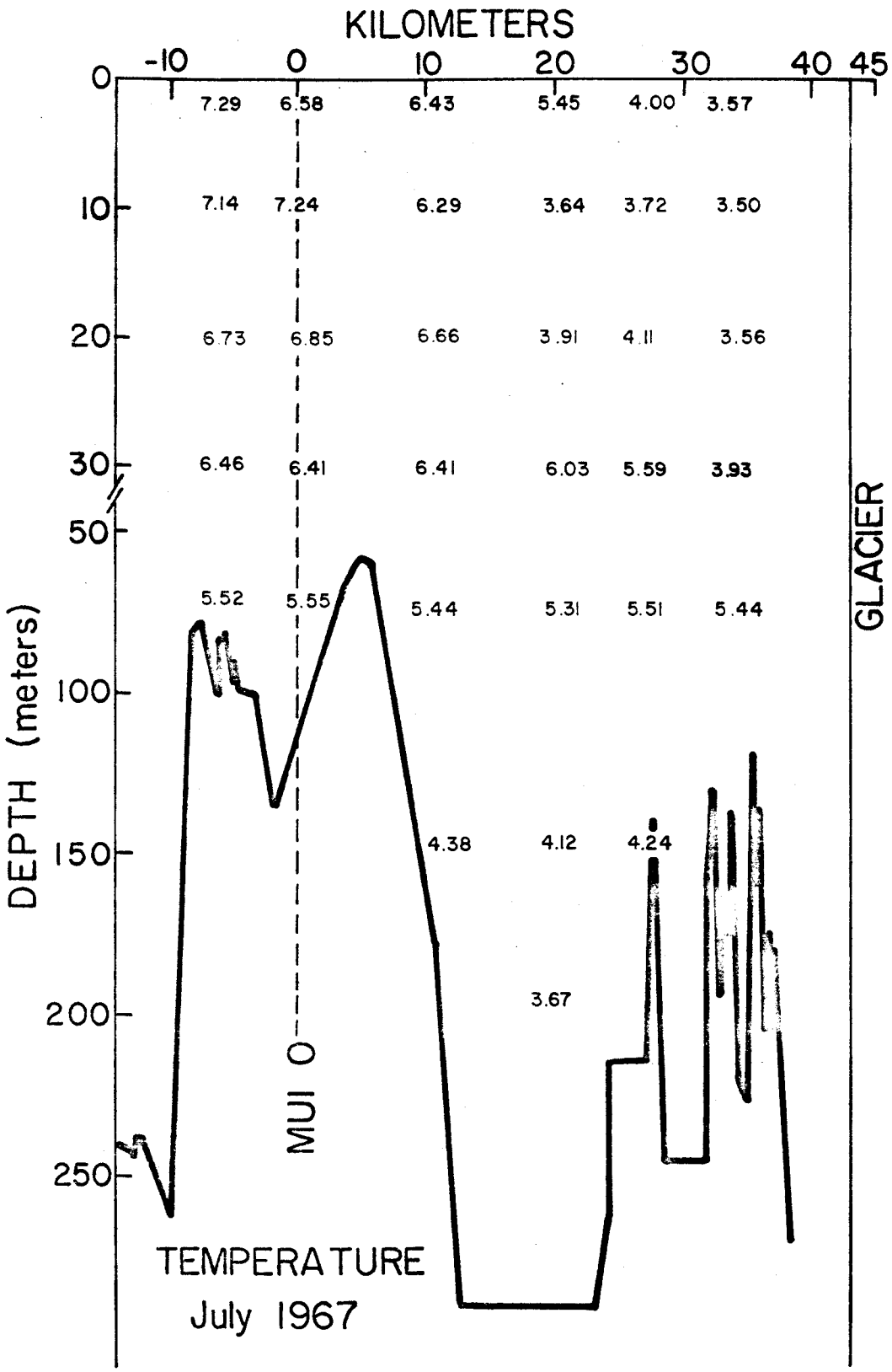

Figure 18. Longitudinal Temperature Profile for July 1967

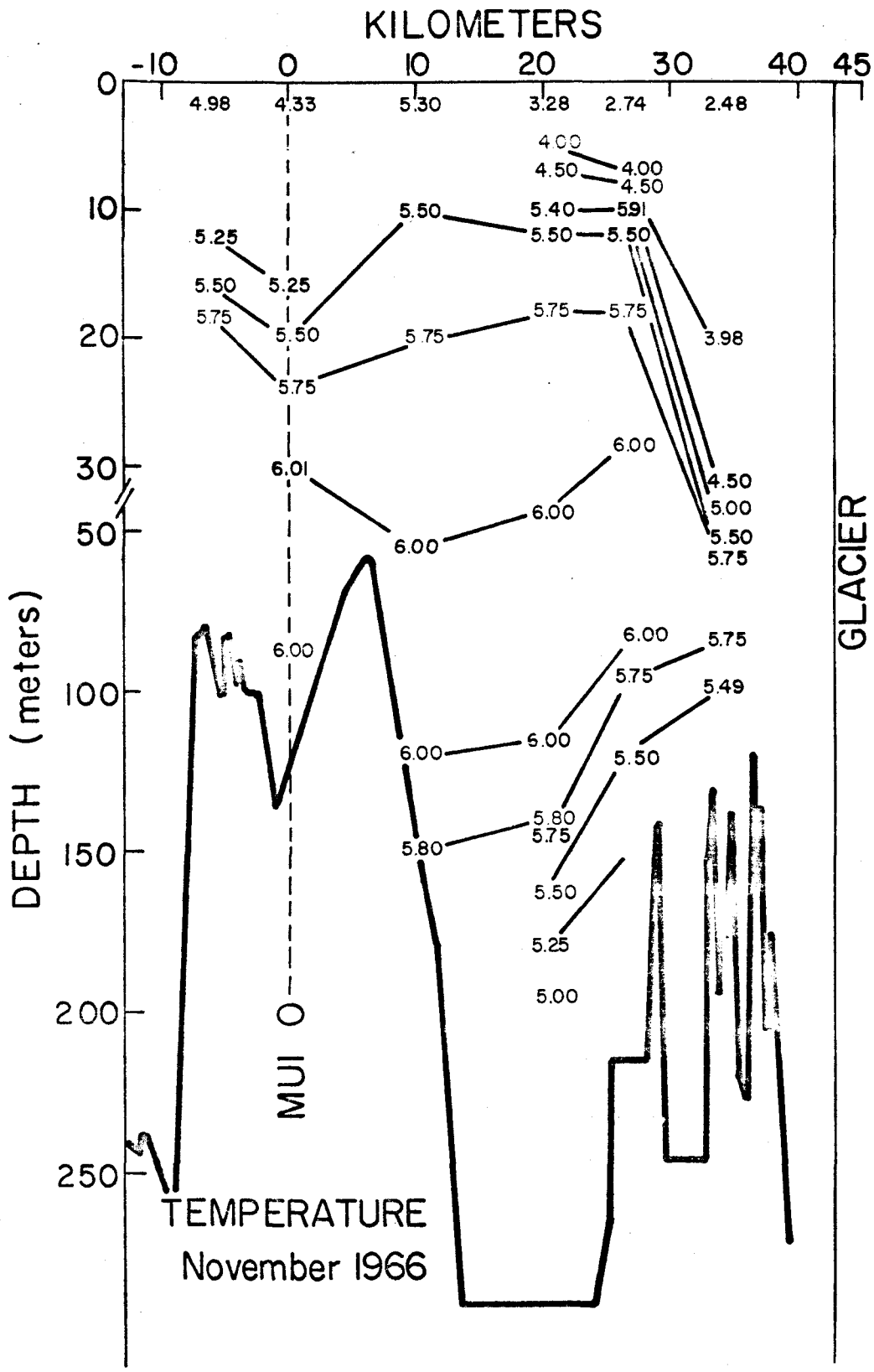

Figure 19. Longitudinal Temperature Profile for November 1966

February 1967, and July 1967) are displayed. Isohalines are drawn to emphasize trends. Linear interpolation is used to estimate the depths of arbitrarily chosen values of temperature and salinity.

Salinity

For February 1967, the salinity contours rise from MUI 20 to MUI 0 at all depths from 0--75 meters. Below 75 meters, the basin water is nearly homogeneous at 31.10‰. The steep downslope of the 31.07‰ isohaline from MUI 0 to MUI 5 may indicate a density flow over the sill from Glacier Bay into Muir Inlet. Such a density inflow of more saline water during the winter--spring runoff minimum would account for the observed increase in salinity in the deep basin water during this period. The sill is an effective barrier in holding the 31.14‰ 75-meter water outside the basin. Within the basin, the maximum salinity value found down to 200 meters is 31.12‰. In the surface layer, a well-defined tongue of brackish water emanates from the terminal of the tidal glaciers near MUI 10. By 20 meters depth, the boundaries of the tongue are not well-defined. The influence of glacial meltwater seems to extend only to 20--30 meters, where the isohalines remain fairly horizontal from MUI 20 to MUI 0.

By July 1967, the surface brackish layer is 40--50 meters thick. A peak and trough pattern for the isohalines is superimposed on a gradual trend toward higher salinities downfjord. This pattern in the surface layers may be related to several factors, such as runoff sources, entrainment, continuity of flow, and internal waves. Actual in situ vertical and horizontal current measurements and observations of the internal wave phenomena may solve this problem.

The trough at MUI 20 may result from the proximity of that station to the tidal glaciers. The combined effects of glacial meltwater, a relatively small cross sectional flow area, and the short duration of entrainment processes may be expressed in the depression of the isohalines.

At MUI 15, the isohalines form a peak. The fjord width is greater at MUI 15 than at MUI 20; thus, for a unit reach, the surface thickness necessary to contain the brackish water may be decreased. The combination of a decreased thickness of the brackish layer and the prolongation of the entrainment processes is probably sufficient to explain the rise in the isohalines at MUI 15.

At MUI 10, the inflow of brackish water from Wachusetts Inlet depresses the ischalines.

The downslope of the isohalines over the sill and their leveling off from MUI 0 to GL 180 shows the moderating and freshening influence of Glacier Bay surface water.

Within the main basin in July, the low salinity values from sill depth to 150 meters at MUI 5 may be caused by tidal mixing across the sill. At MUI 20, some freshening effects are evident at all depths. At the 150-meter level in the basin, the water mass appears to be unstable, because at MUI 5 the salinity is 31.39‰ and upfjord increases to 31.52‰, with no intervening barrier to separate the water masses of different densities.

Between July and November, the most striking change is the decrease in salinity values at all depths down to at least 200 meters. The lowest basin salinity values are observed in November. The increase in surface values in November reflects the beginning of the winter freeze-up and runoff minimum. The same general trend of increasing surface salinity downfjord is observed in the upper 25 meters. Between 25--70 meters, the salinities for corresponding depths at MUI 20 and GL 180 are equal; while the in-between stations all have higher values. In this layer, MUI 15 possesses up to a 1.00‰ higher salinity than its neighboring stations have at the same depth. The MUI 15 maxima in the isohalines are found down to the bottom. The mechanism responsible for maintaining the higher salinities at MUI 15 is not known.

Temperature

In February 1967, the entire water mass below sill depth is isothermal, with the temperature around 3.25°C. The temperatures on either side of the sill at the 75-meter level are the same. The vertical and horizontal homogeneity in the deep water is maintained upward to 50 meters. Above 50 meters, the coldest temperatures are found near the glaciers. The water becomes warmer from 50 meters to the surface and from MUI 20 to MUI 5. The temperatures drop off at MUI 0. The steady rise in surface temperatures from -0.01°C. at MUI 20 to 2.68°C. at MUI 0 results from solar warming of the outflowing surface water. Turbulent mixing causes the warming effects to reach the subsurface layers. The falling off of the temperature between 10 and 50 meters from MUI 5 to MUI 0 may result from an intrusion of cold Glacier Bay water, which is also suggested from the pattern of the isohalines.

Come July 1967, the warming effects of the sun have influenced all the water mass. Again, the water becomes warmer from MUI 20 to GL 18C. Vertically, however, temperature maxima exist: near 10 meters at GL 18C and MUI 0, near 20 meters at MUI 5, near 30 meters at MUI 10, and near 50 meters at MUI 15 and MUI 20. Both the depth and the temperature of the maxima sink upfjord. The temperatures of the maxima decrease upfjord from 7.24°C.

at MUI 0 to 5.75°C. at MUI 20. The relatively high 100-meter and 150-meter temperatures at MUI 5 reinforce the likelihood of a water mass instability, as postulated in the preceding salinity section, in the basin between MUI 5 and MUI 15. The water on either side of the sill, at MUI 0 and at MUI 5, differs by about 0.11°C. at 75 meters and by 0.38°C. at 100 meters, with MUI 5 possessing the warmer water. Thus, the sill is an effective barrier in isolating water masses of different characteristics below 75 meters, and perhaps even shallower depths too.

In November 1966, surface cooling is obvious. The temperature rises from a minimum at the surface to a maximum near 75 meters at all stations. Below 75 meters, the temperature falls to values which remain warmer than surface values. From MUI 15 to MUI 20, all the isothermals above 75 meters slope down from the surface; below 75 meters, they rise up from the bottom of the main basin. At sill depth, the water outside the main sill is colder than that inside the sill.

Characteristic Diagrams According to Depth

The temperature-salinity, salinity-oxygen, and temperature-oxygen data pairs obtained at MUI 10 over the three years' duration of the sampling program, supplemented by data from MUI 5 and MUI 20 data to fill in monthly gaps, are

displayed on characteristic diagrams. The data are organized according to depth. Each diagram shows the temperature-salinity, salinity-oxygen, or temperature-oxygen data from all the surveys at a particular depth. The graphs presented in Figures 20--33 (pp. 58--73) portray 10-, 30-, 100-, 150-, and 200-meter data.

Temperature Versus Salinity

Figures 20--23 (pp. 58--61) show seasonal variations in temperature and in salinity exist at all depths, including 200 meters. The range of the seasonal variations decreases with depth. The 10-meter diagram shows far more scatter among the data points than does the 200-meter diagram. At all depths, the winter--spring water characteristics are very homogeneous. The data points representing February through May are all clustered at the low temperature--high salinity end of the spectrum. The winter--spring water type, essentially homogeneous from 10--200 meters, is characterized by a 1.25‰ salinity range from 30.25--31.50‰ and a 1.25°C. temperature range from 2.15--3.40°C.

This type of diagram can also portray the sequence of the annual variations at each depth, if the samplings are frequent and the data points are connected in chronological order. Annual cycles need not overlap, reflecting annual

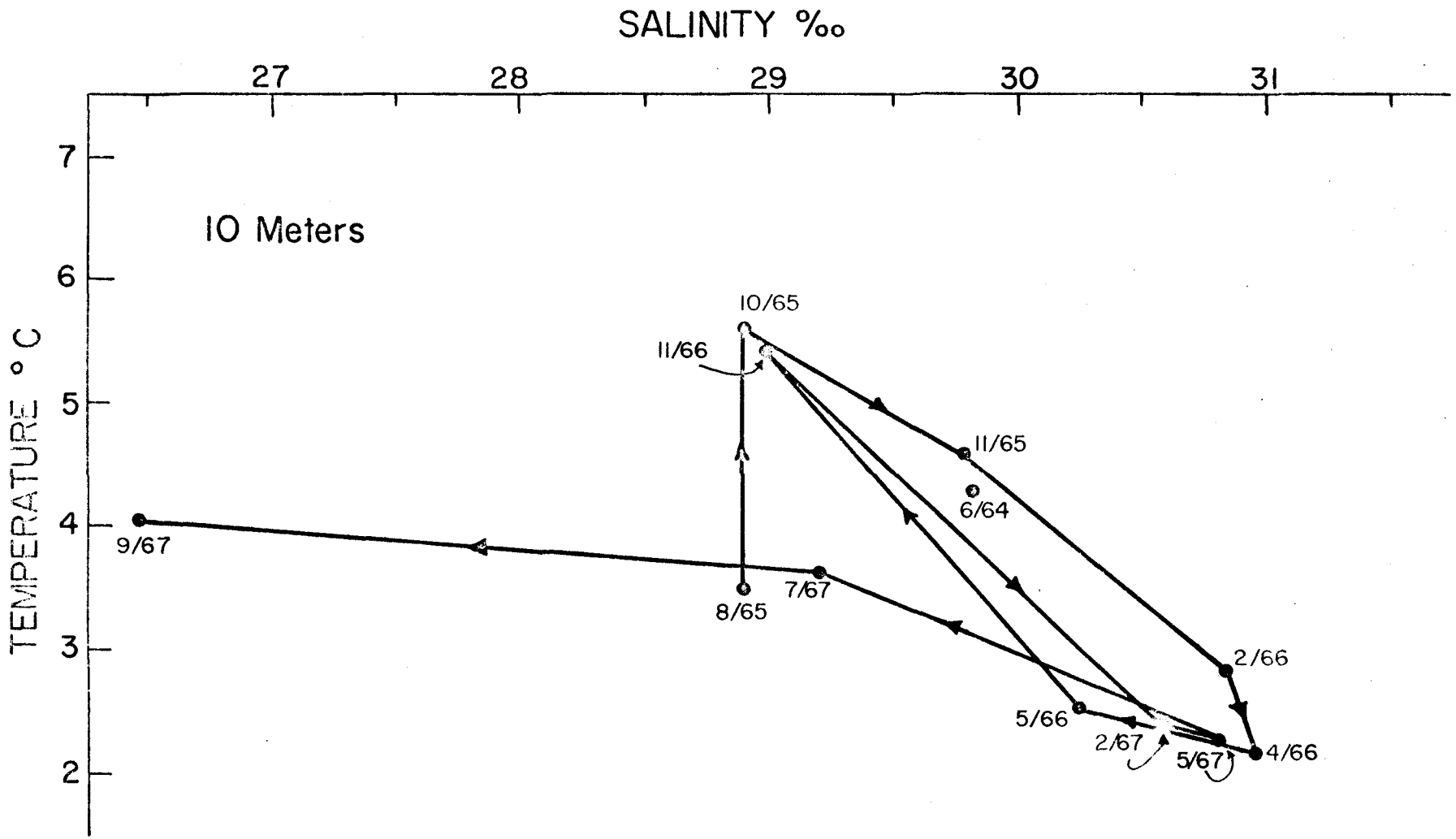

Figure 20. Temperature Versus Salinity Diagram Showing Data Collected at the 10-Meter Level During All Seasons. The data points are connected in chronological order.

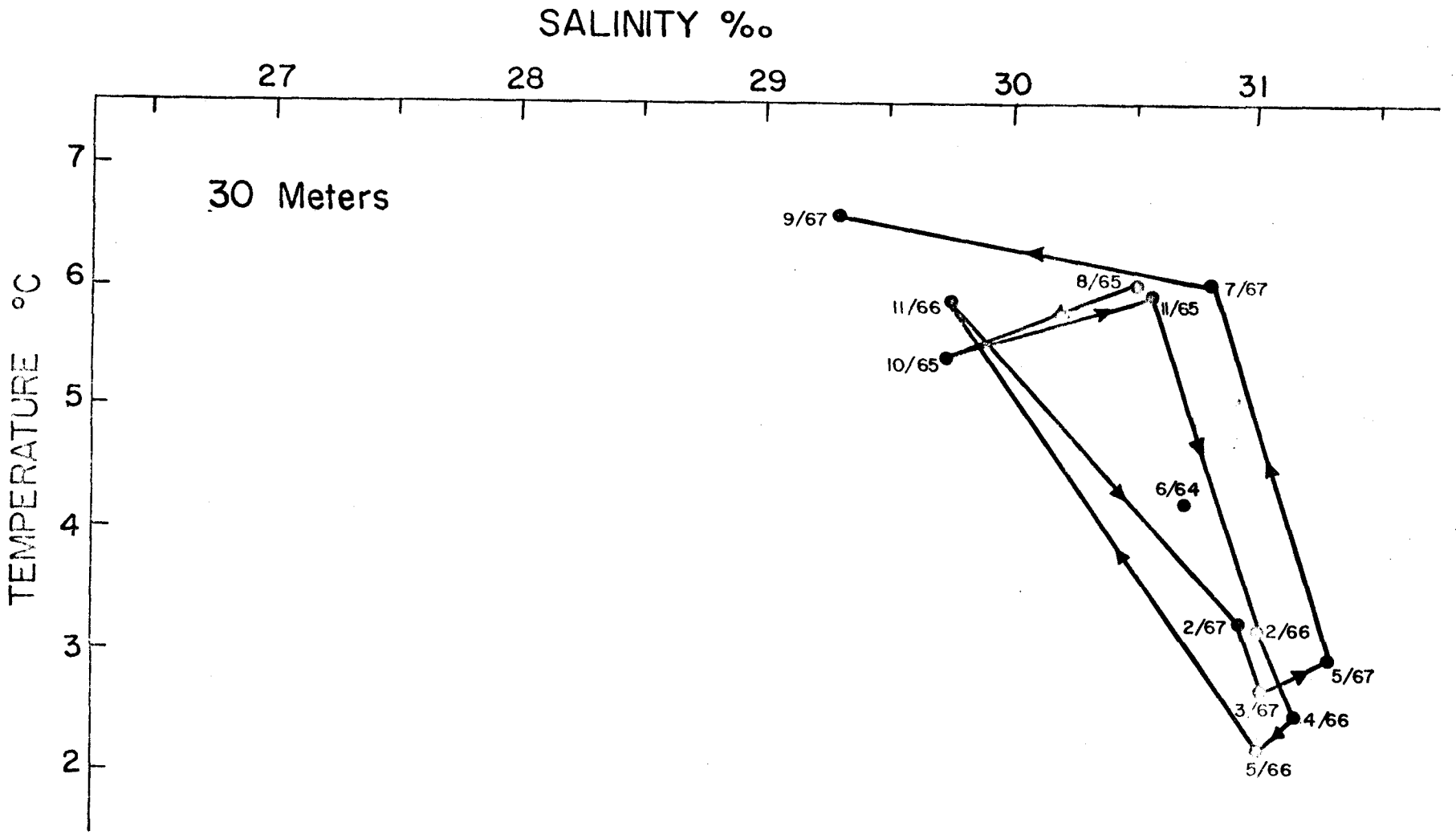

Figure 21. Temperature Versus Salinity Diagram Showing Data Collected at the 30-Meter Level During All Seasons. The data points are connected in chronological order.

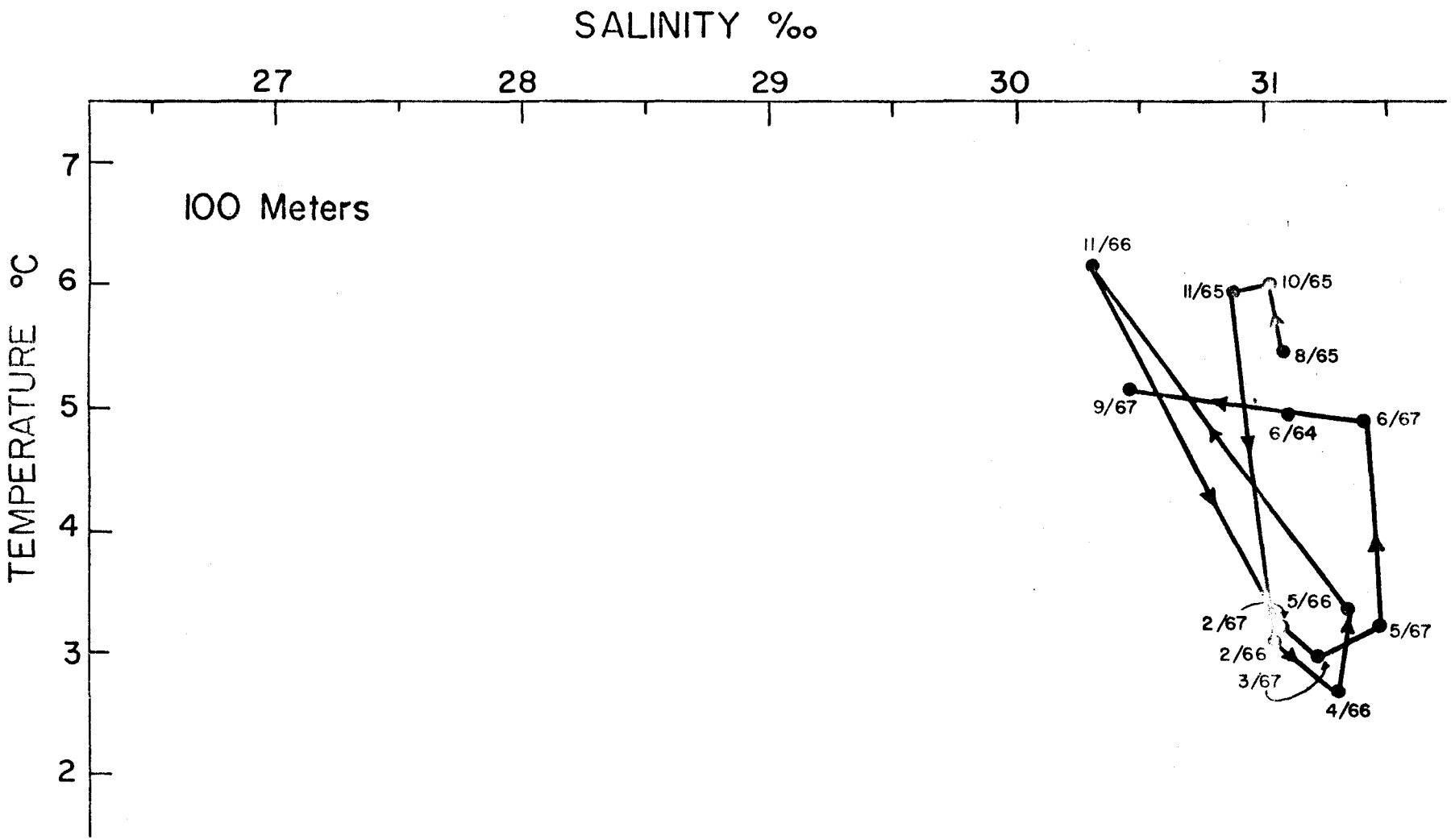

Figure 22. **Temperature Versus Salinity Diagram Showing Data Collected at the 100-Meter Level During All Seasons. The data points are connected in chronological order.**

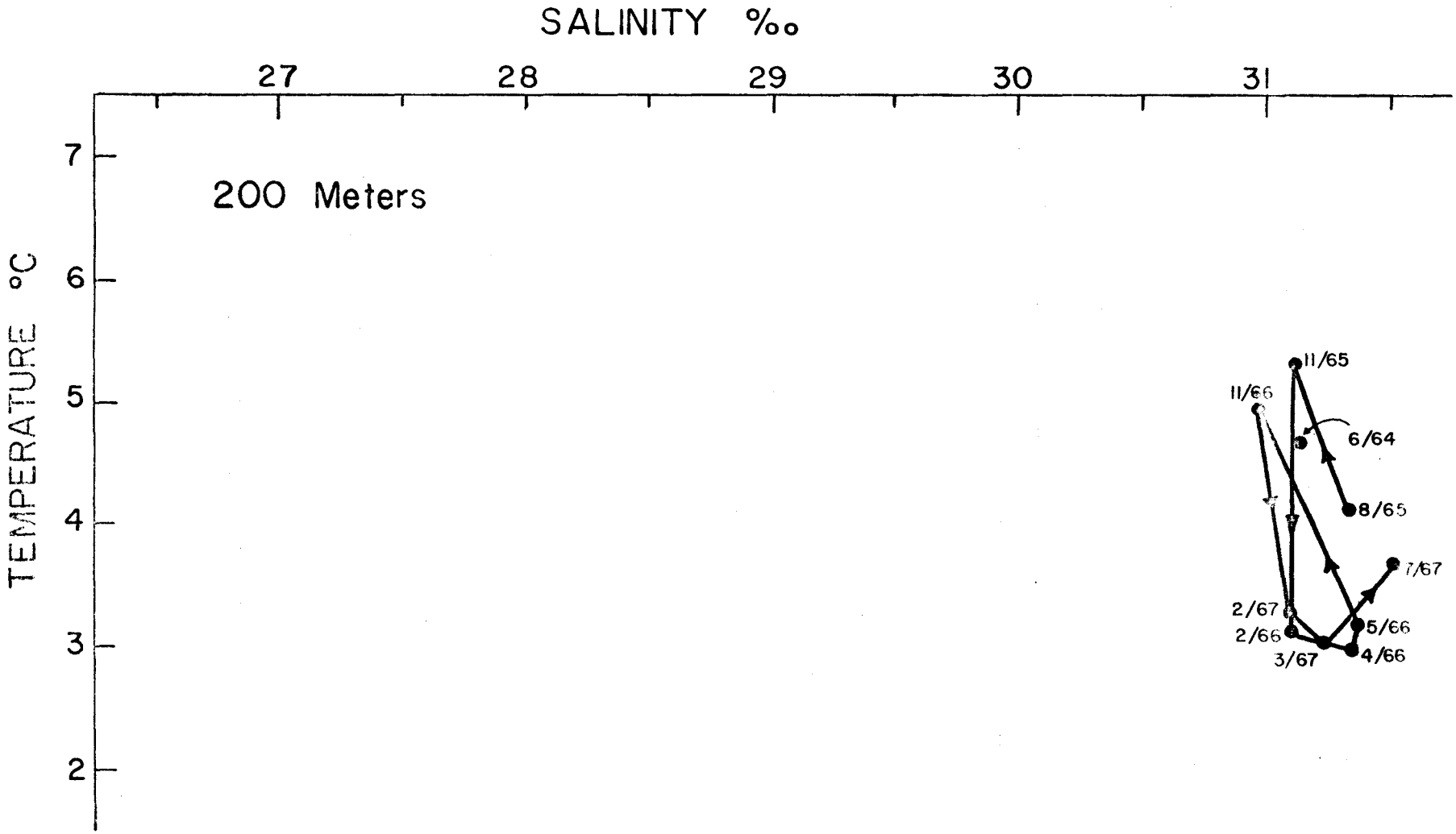

Figure 23. Temperature Versus Salinity Diagram Showing Data Collected at the 200-Meter Level During All Seasons. The data points are connected in chronological order.

climatological differences, such as in air temperatures, sun and sky radiation, runoff, and precipitation.

At 10 meters, the trend is clockwise. From February to April, the salinity increases, and the temperature decreases. From April to May, the salinity decreases, and the temperature increases; thus, at 10 meters the effects of the increased surface input of radiant energy and the spring melt are felt no earlier than April. Through spring and summer and into fall, the salinity continues to decrease and the temperature to increase. Then, some time between November and February, the trends reverse and winter characteristics are re-established.

Below 30 meters, the trend is counterclockwise, because spring warming occurs before spring dilution. Warming is noticeable even at 200 meters by May. At 30 meters, the salinity continues to increase through May; at 200 meters, through July.

Salinity Versus Dissolved Oxygen

Figures 24--28 (pp. 63--67) show the salinity-oxygen diagrams for 10, 30, 100, 150, and 200 meters.

Here, too, the cycle for 10-meter water is clockwise, while that for deeper water is counterclockwise.

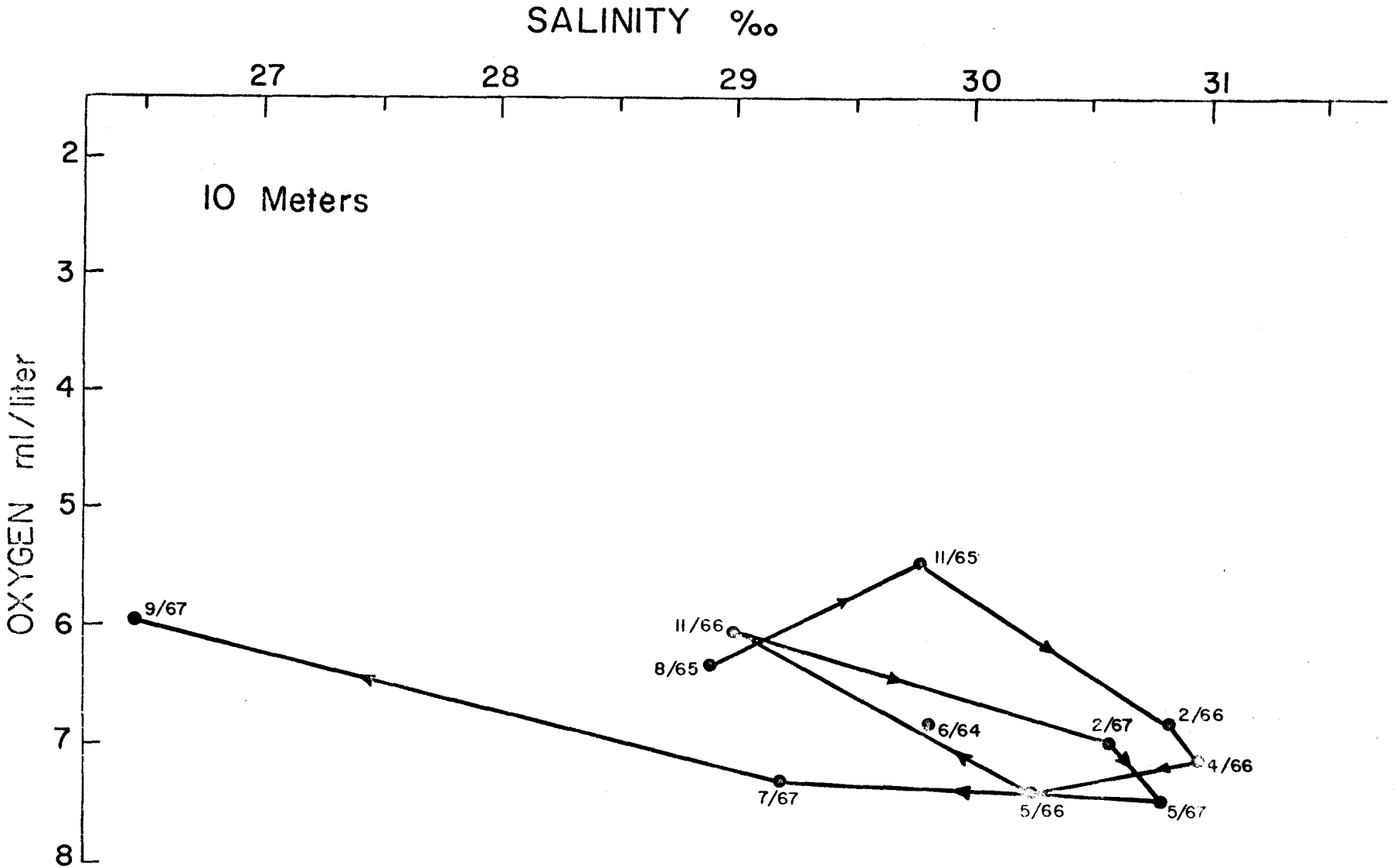

Figure 24. Salinity Versus Dissolved Oxygen Diagram Showing Data Collected at the 10-Meter Level During All Seasons. The data points are connected in chronological order.

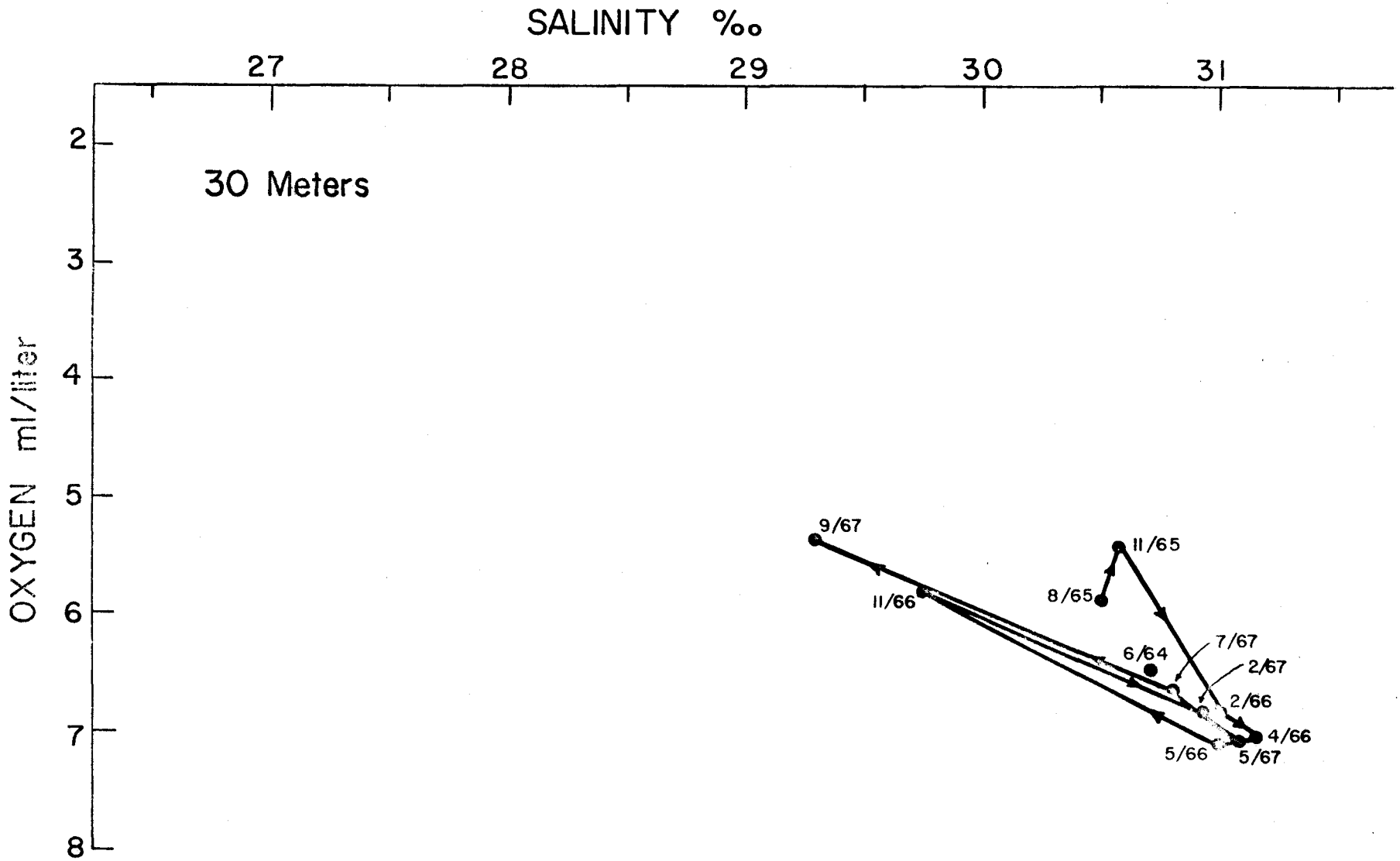

Figure 25. Salinity Versus Dissolved Oxygen Diagram Showing Data Collected at the 30-Meter Level During All Seasons. The data points are connected in chronological order.

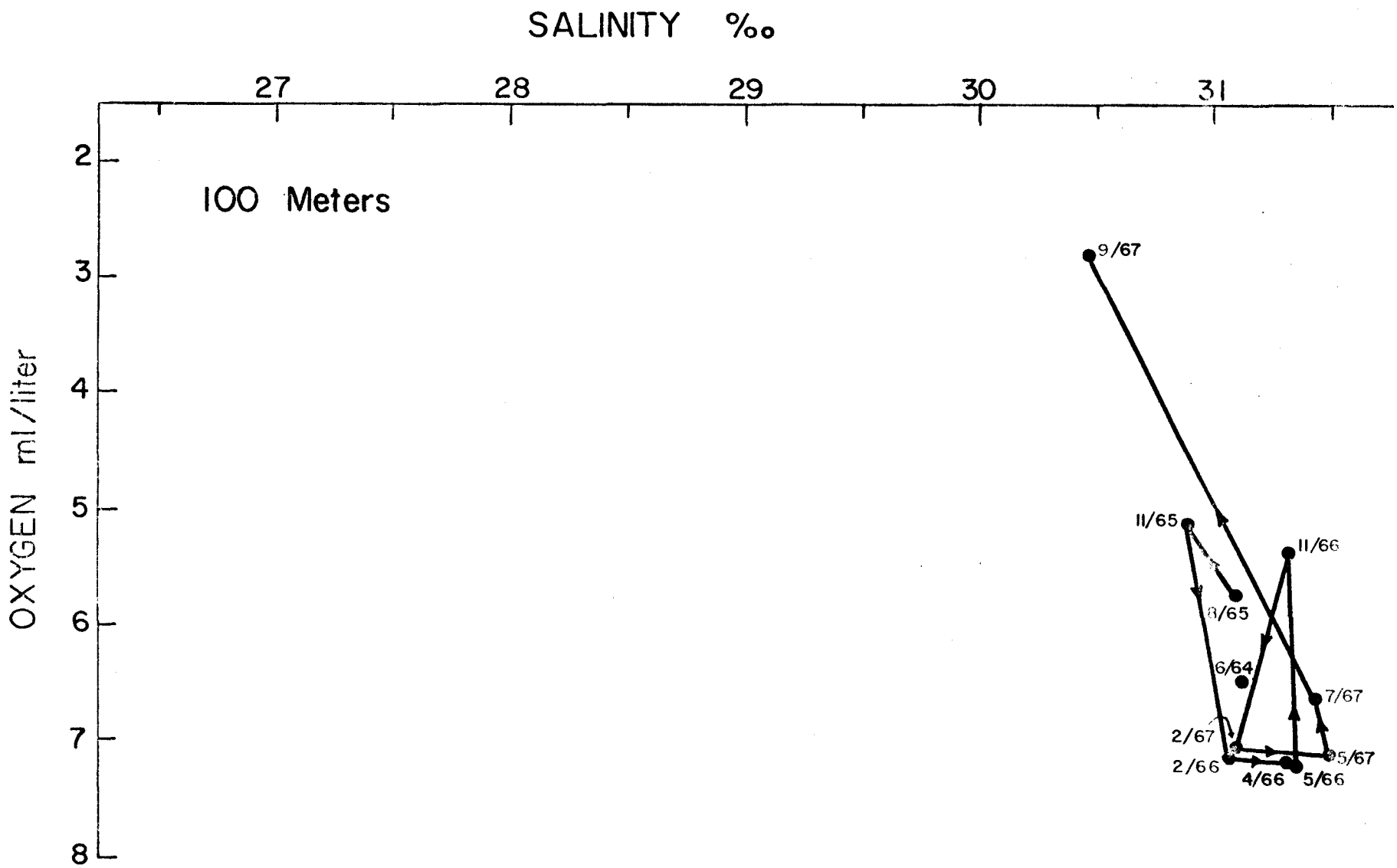

Figure 26. Salinity Versus Dissolved Oxygen Diagram Showing Data Collected at the 100-Meter Level During All Seasons. The data points are connected in chronological order.

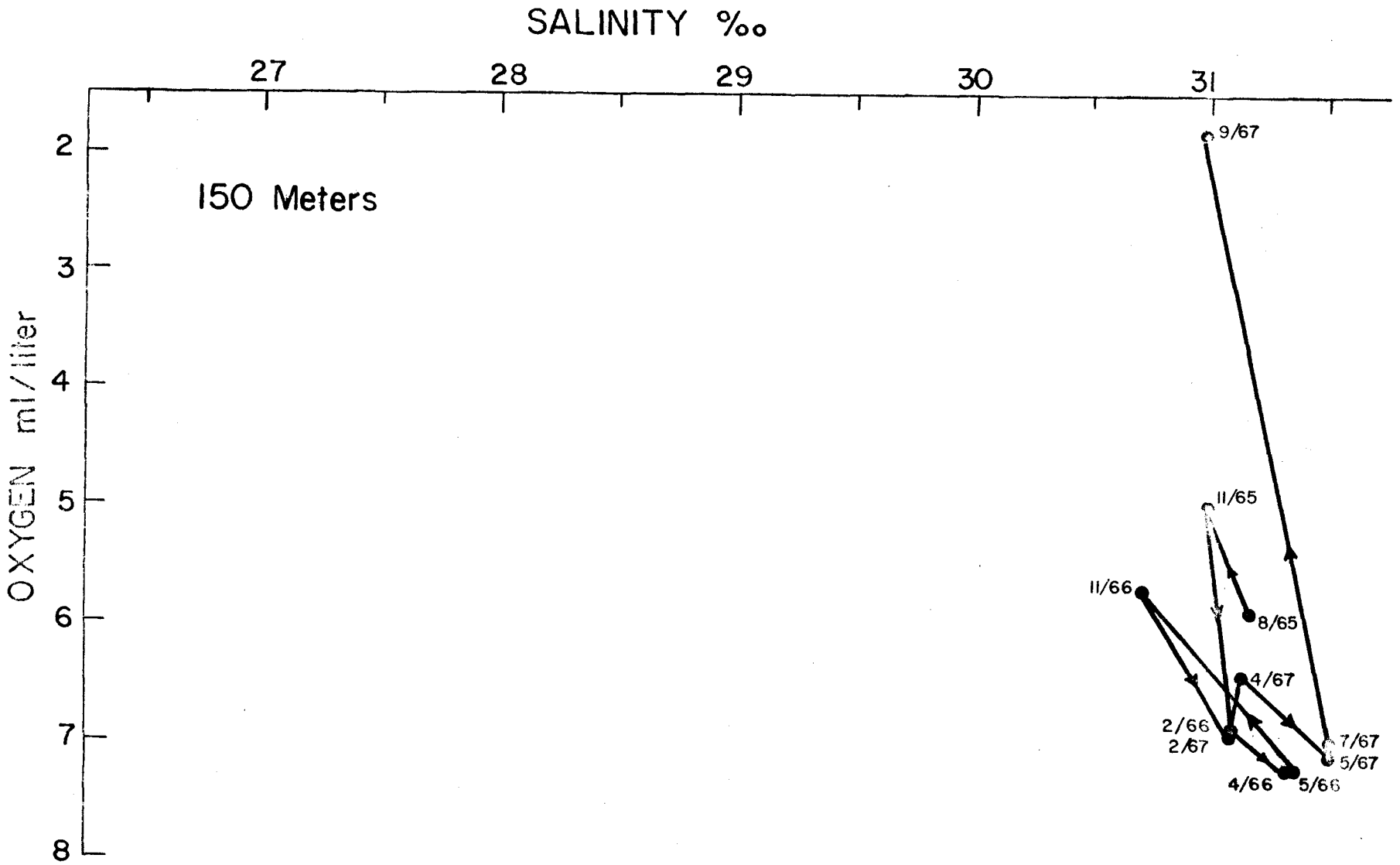

Figure 27. Salinity Versus Dissolved Oxygen Diagram Showing Data Collected at the 150-Meter Level During All Seasons. The data points are connected in chronological order.

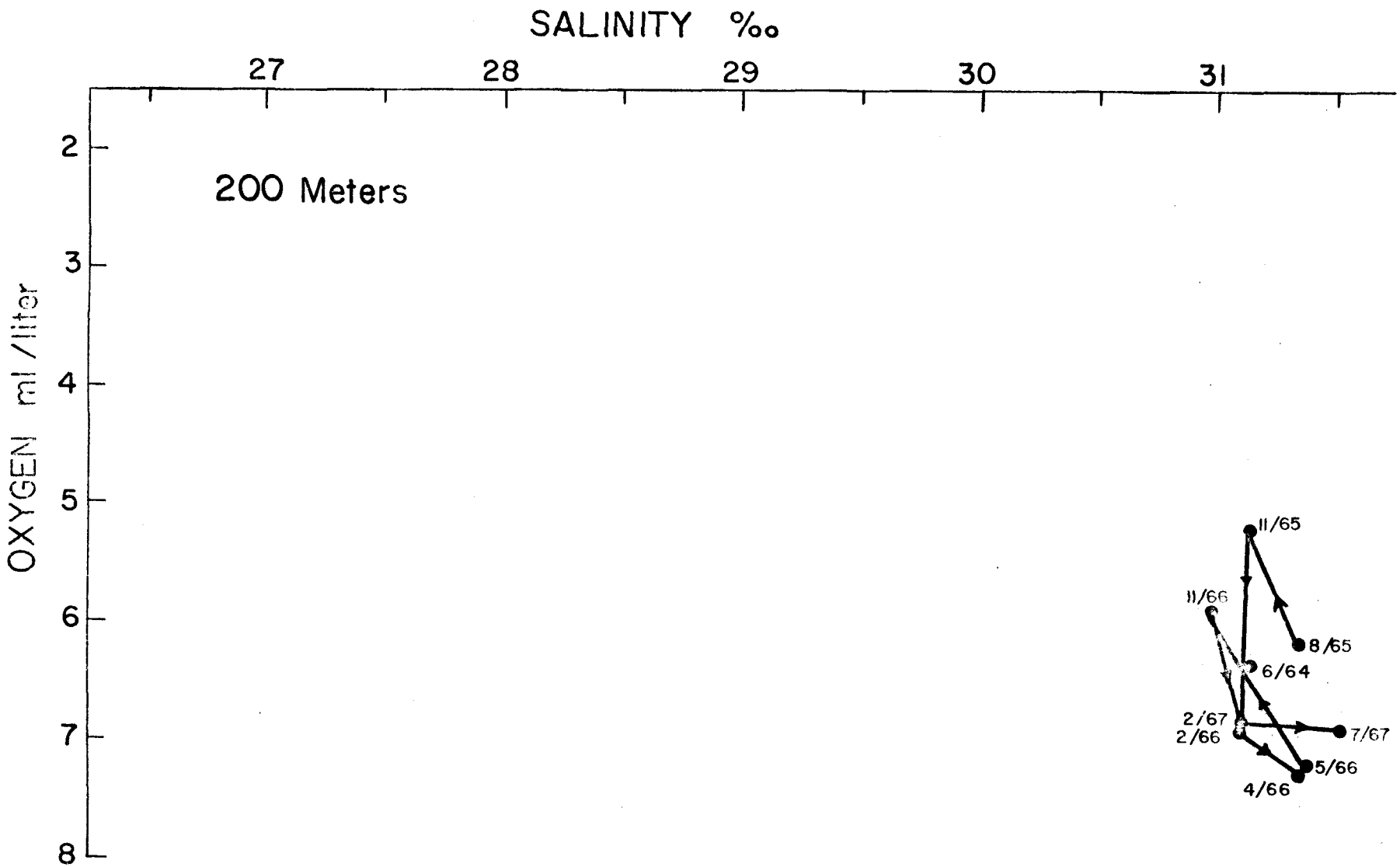

Figure 28. Salinity Versus Dissolved Oxygen Diagram Showing Data Collected at the 200-Meter Level During All Seasons. The data points are connected in chronological order.

At all depths below 10 meters, the minimum dissolved oxygen concentrations occur during late summer and early fall; the maximum, during winter and spring.

The scatter of the data points decreases with depth, with the exception of the deviation of the relatively depleted dissolved oxygen levels in September 1967 at MUI 20.

Temperature Versus Dissolved Oxygen

Figures 29--33 (pp. 69--73) show the temperature-dissolved oxygen data for 10, 30, 100, 150, and 200 meters.

Dissolved oxygen saturation in seawater is a function of temperature, salinity, and pressure. High dissolved oxygen concentrations should correspond to low temperatures; hence, the winter--spring cluster of points is observed at the low temperature and high oxygen end of the spectrum.

In contrast to the temperature-salinity and salinity-oxygen diagrams, the data points representative of particular months and seasons show much more scatter with increasing depth. This scatter occurs because the variations in the rates of oxygen utilization and supply in the deeper water are not well-correlated with temperature and depth, since the changes in dissolved oxygen levels are more a function of photosynthesis, respiration, and turbulence in the water column. These [illegible] determine the availability of

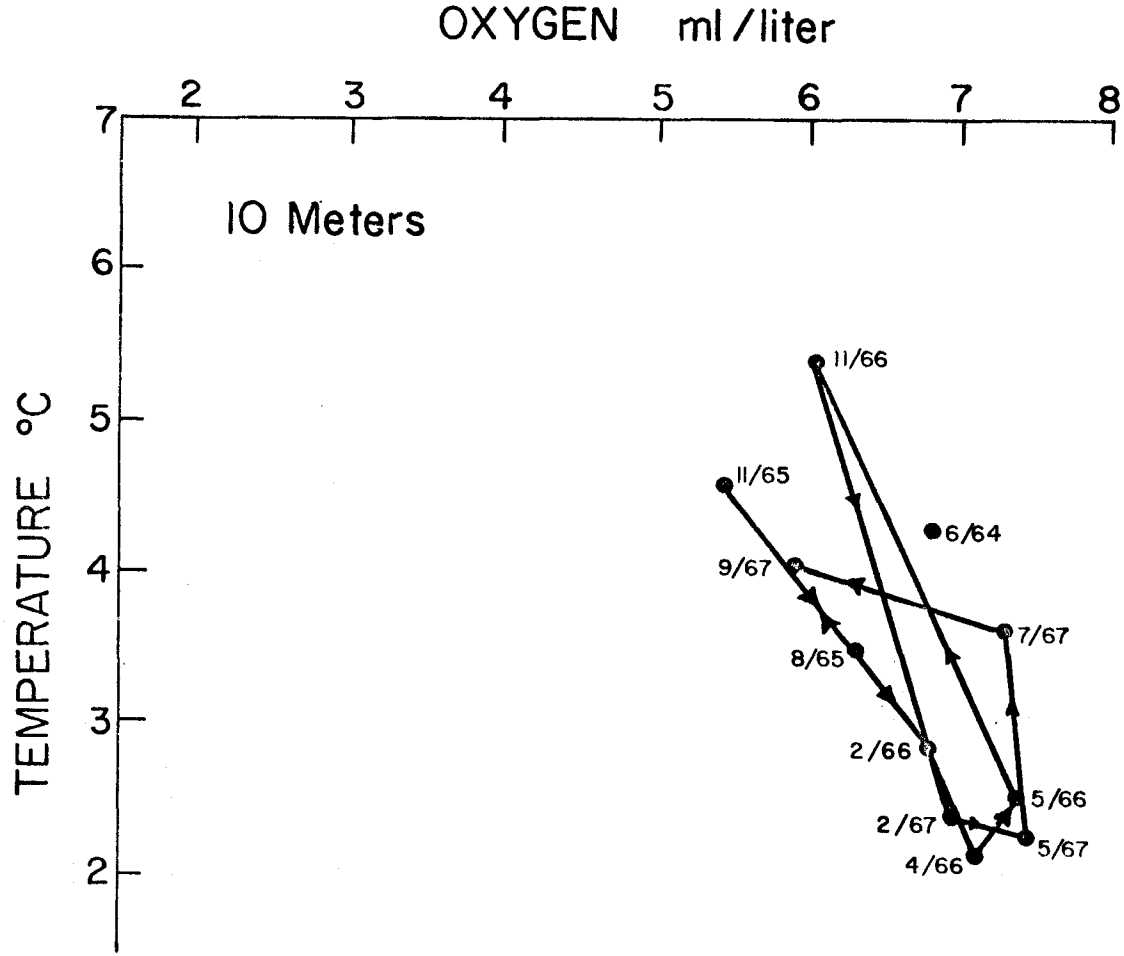

Figure 29. Temperature Versus Dissolved Oxygen Diagram Showing Data Collected at the 10-Meter Level During All Seasons. The data points are connected in chronological order.

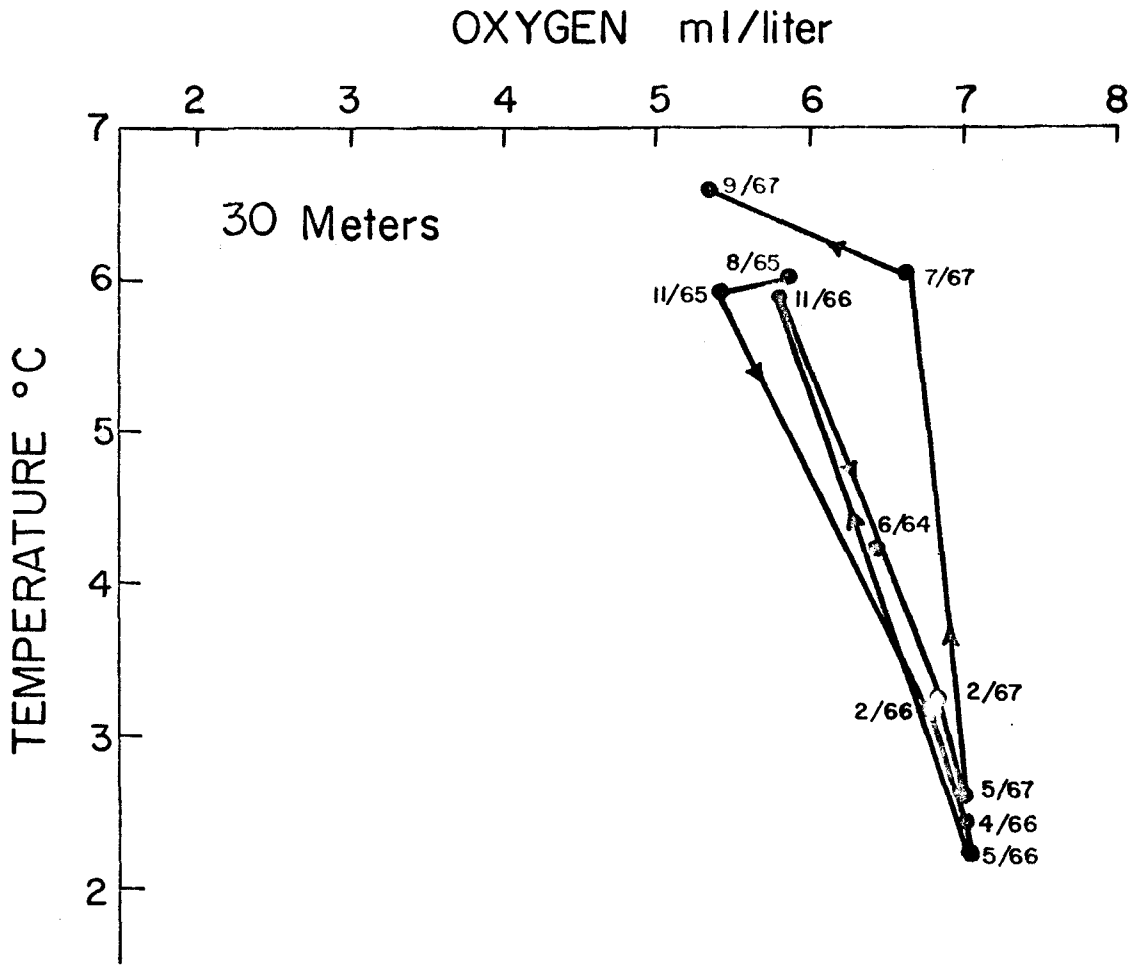

Figure 30. Temperature Versus Dissolved Oxygen Diagram Showing Data Collected at the 30-Meter Level During All Seasons. The data points are connected in chronological order.

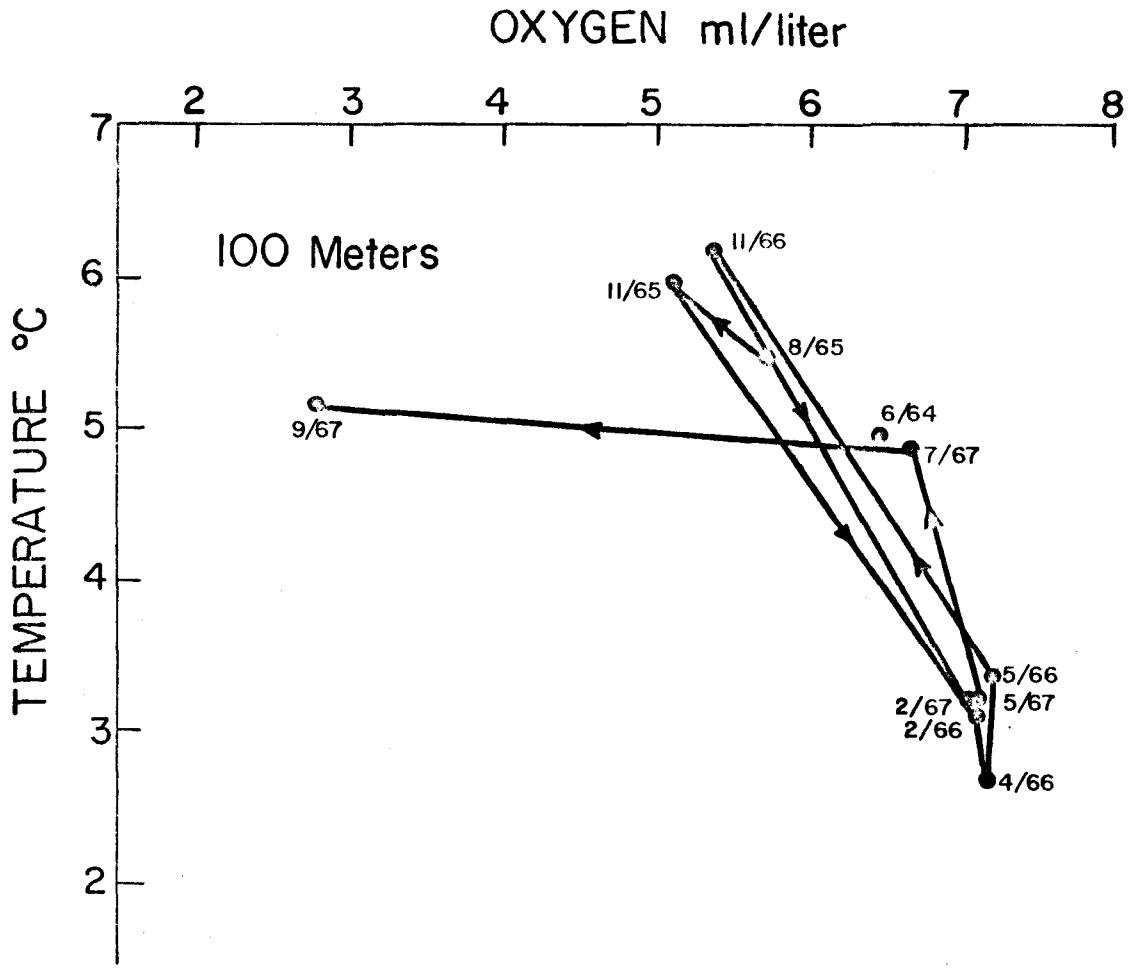

Figure 31. Temperature Versus Dissolved Oxygen Diagram Showing Data Collected at the 100-Meter Level During All Seasons. The data points are connected in chronological order.

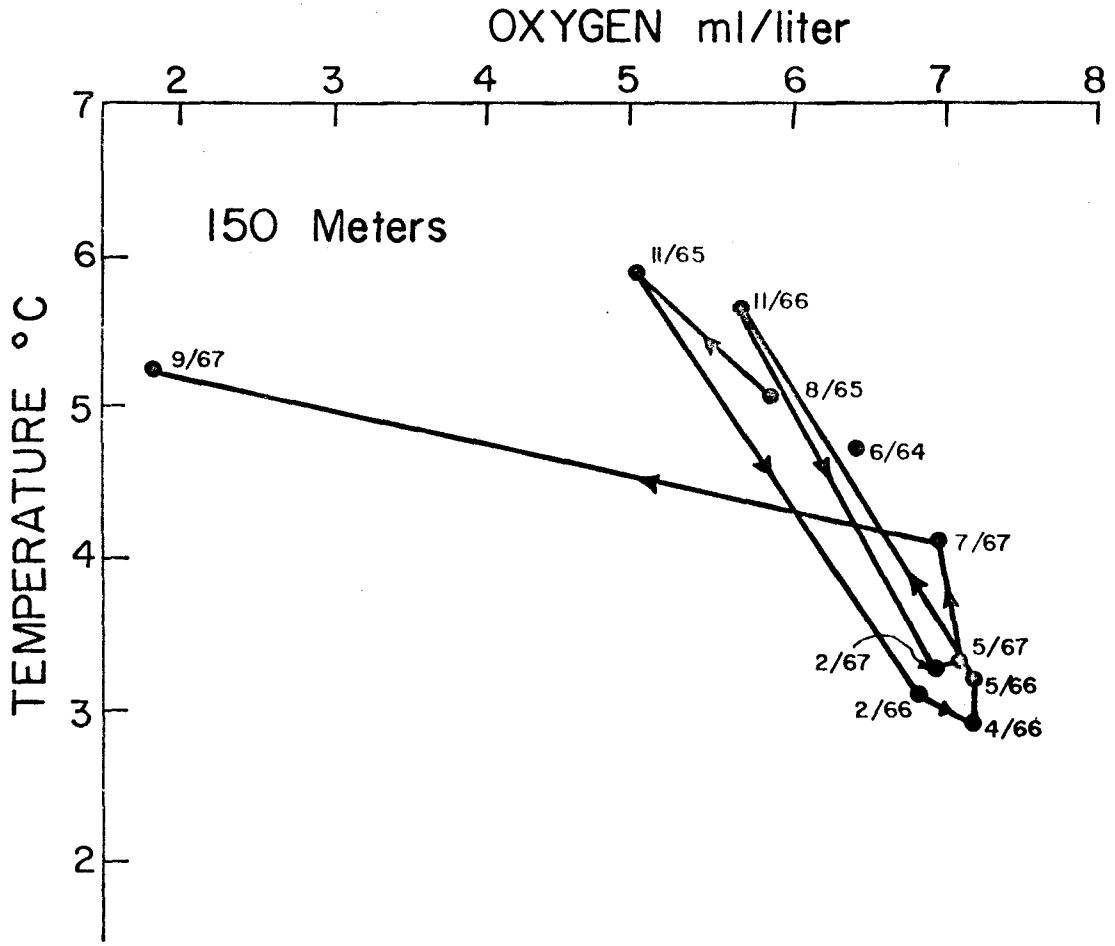

Figure 32. Temperature Versus Dissolved Oxygen Diagram Showing Data Collected at the 150-Meter Level During All Seasons. The data points are connected in chronological order.

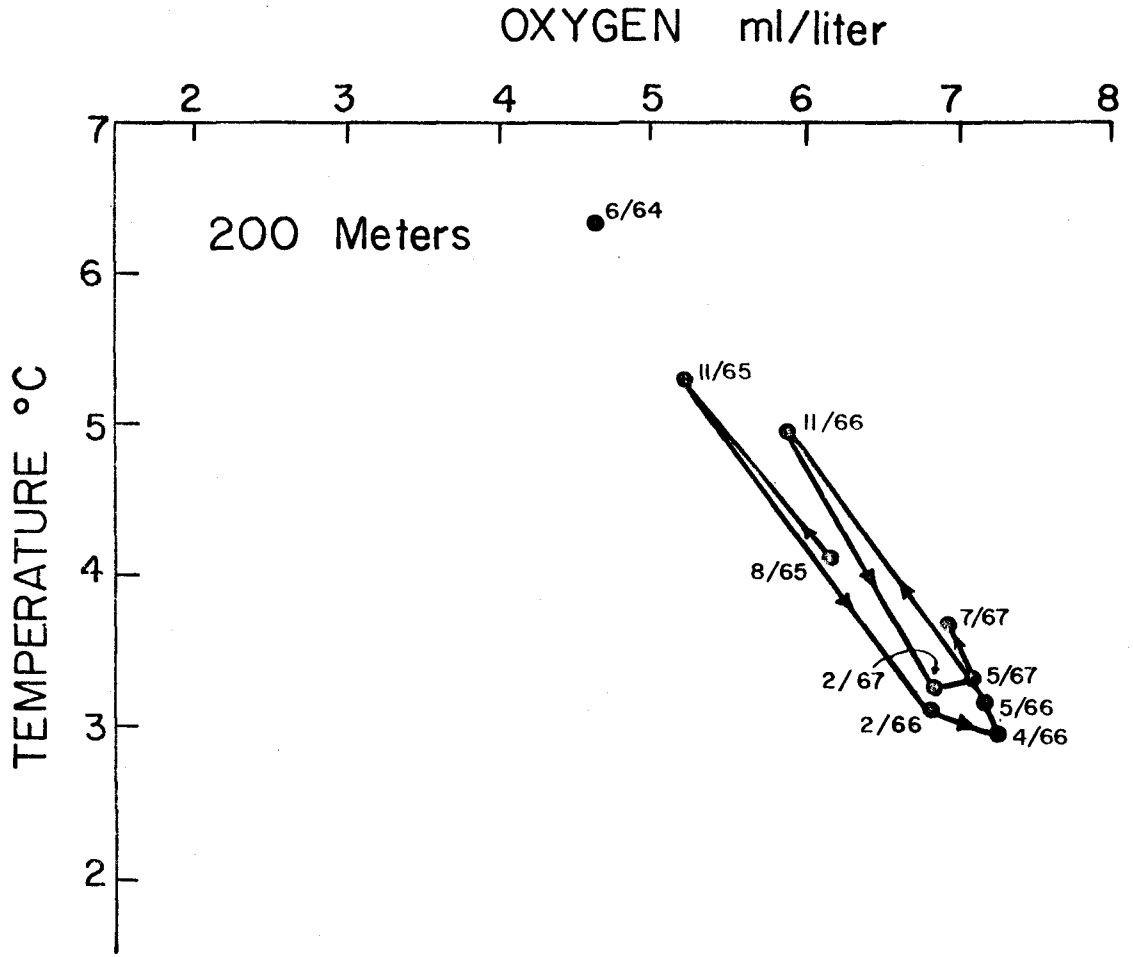

Figure 33. Temperature Versus Dissolved Oxygen Diagram Showing Data Collected at the 200-Meter Level During All Seasons. The data points are connected in chronological order.

dissolved oxygen below the surface layer by controlling the rates of oxygen production, oxygen consumption, and water mass renewal, which are in turn also related to sunshine and salinity. Thus, the temperature-dissolved oxygen correlation may be weak and erratic.

Characteristic Diagrams According to Station

Conventional temperature-salinity and salinity-oxygen diagrams are presented for selected stations and representative months. Each curve represents a particular station. The data points show either the temperature-salinity or the salinity-oxygen characteristics at a specific depth.

Temperature Versus Salinity

The temperature-salinity diagrams show how Pacific Ocean water mass characteristics are modified in Icy Strait and Glacier Bay before reaching Muir Inlet. The months of February 1966 and 1967, April 1966, May 1967, July 1967, and November 1965 and 1966 are represented in Figures 34--40 (pp. 75--81).

For every month sampled, the water at all depths at CRO C and CRO 10 is more saline and warmer than the water at corresponding depths in Icy Strait, Glacier Bay, and Muir Inlet. Flowing into Icy Strait, the Pacific Ocean water

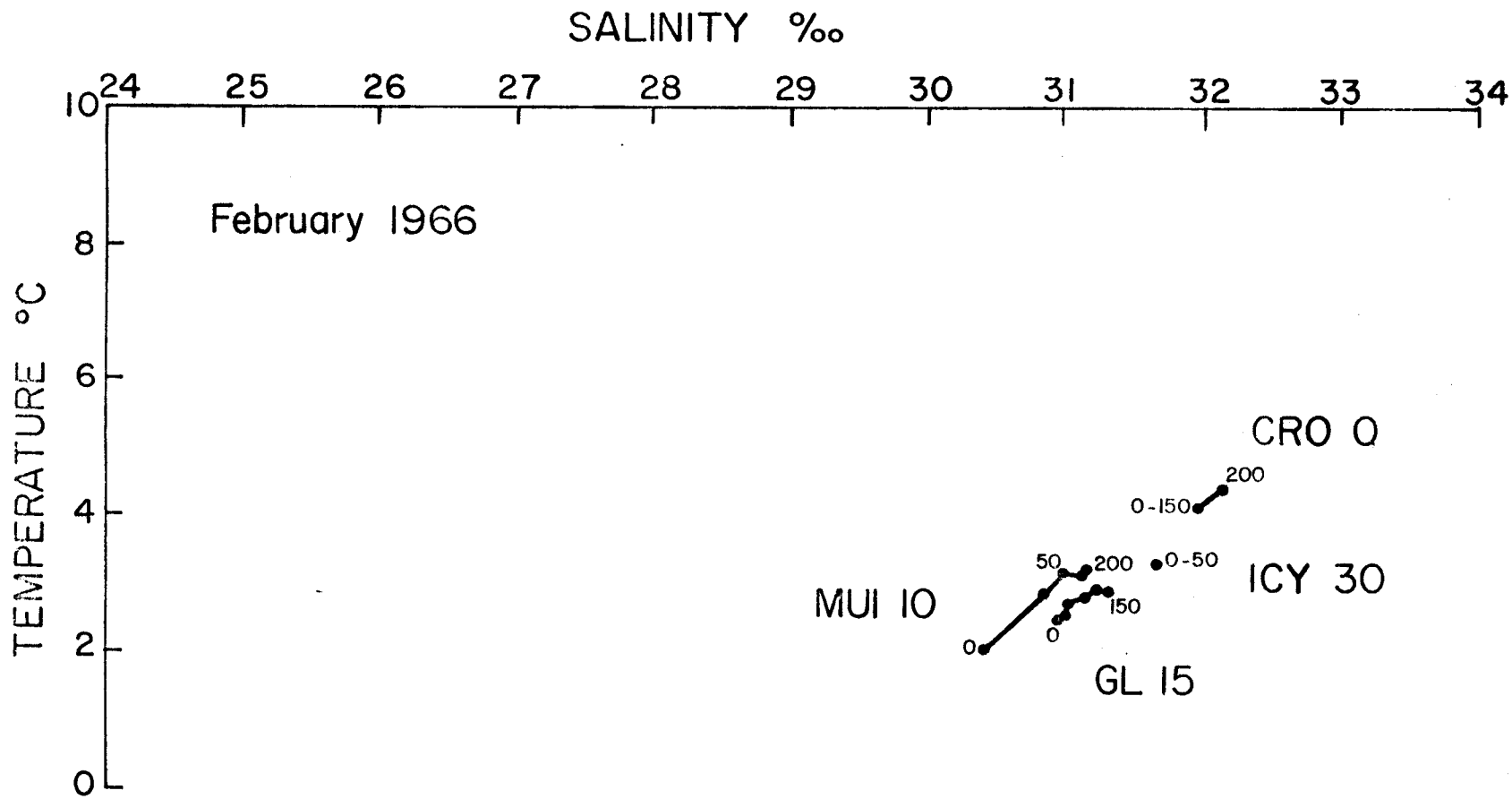

Figure 34. Temperature Versus Salinity Diagram Showing Data from CRO 0, ICY 30, GL 15, and MUI 10 for February 1966

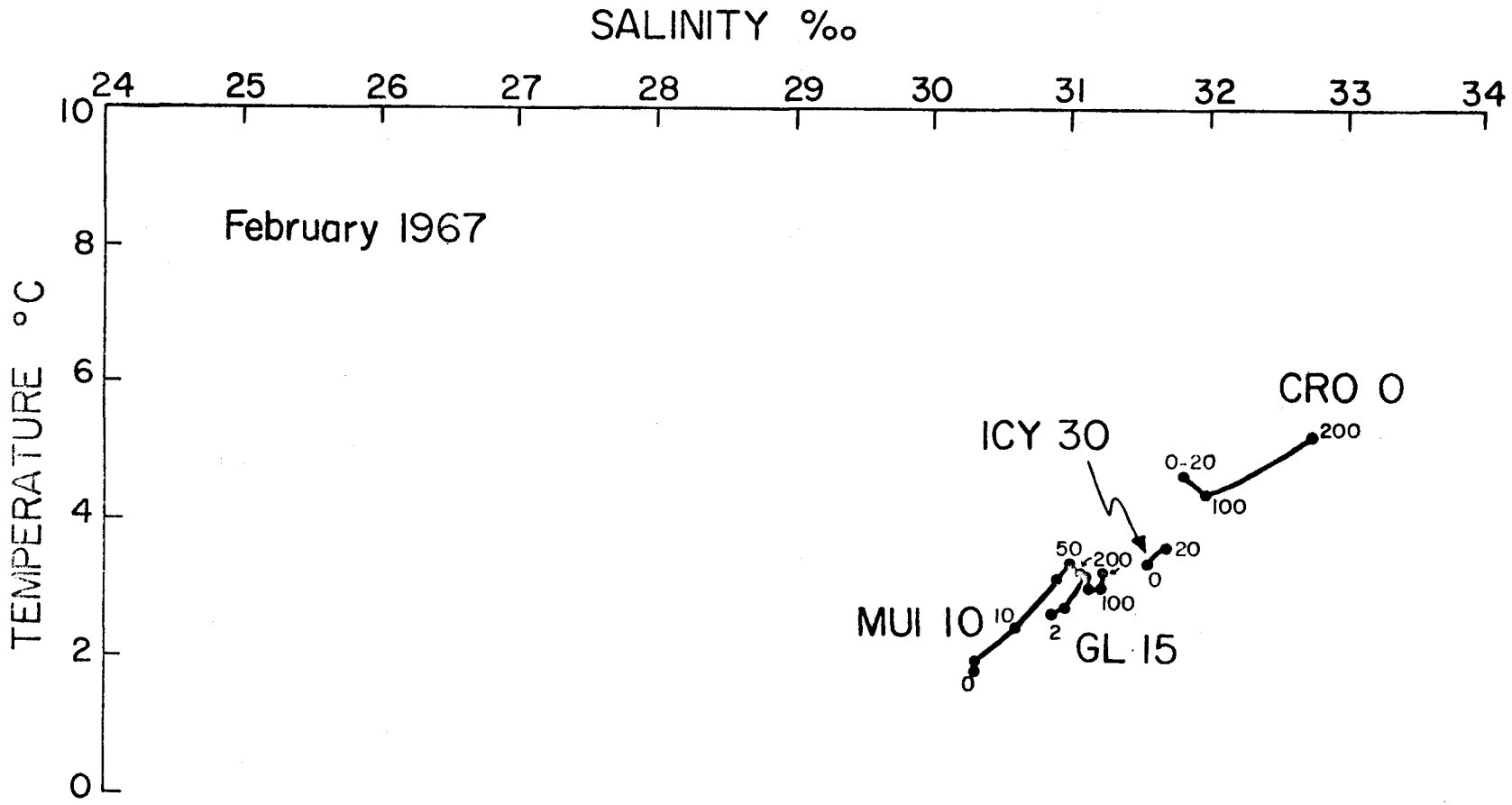

Figure 35. Temperature Versus Salinity Diagram Showing Data from CRO 0, ICY 30, GL 15, and MUI 10 for February 1967

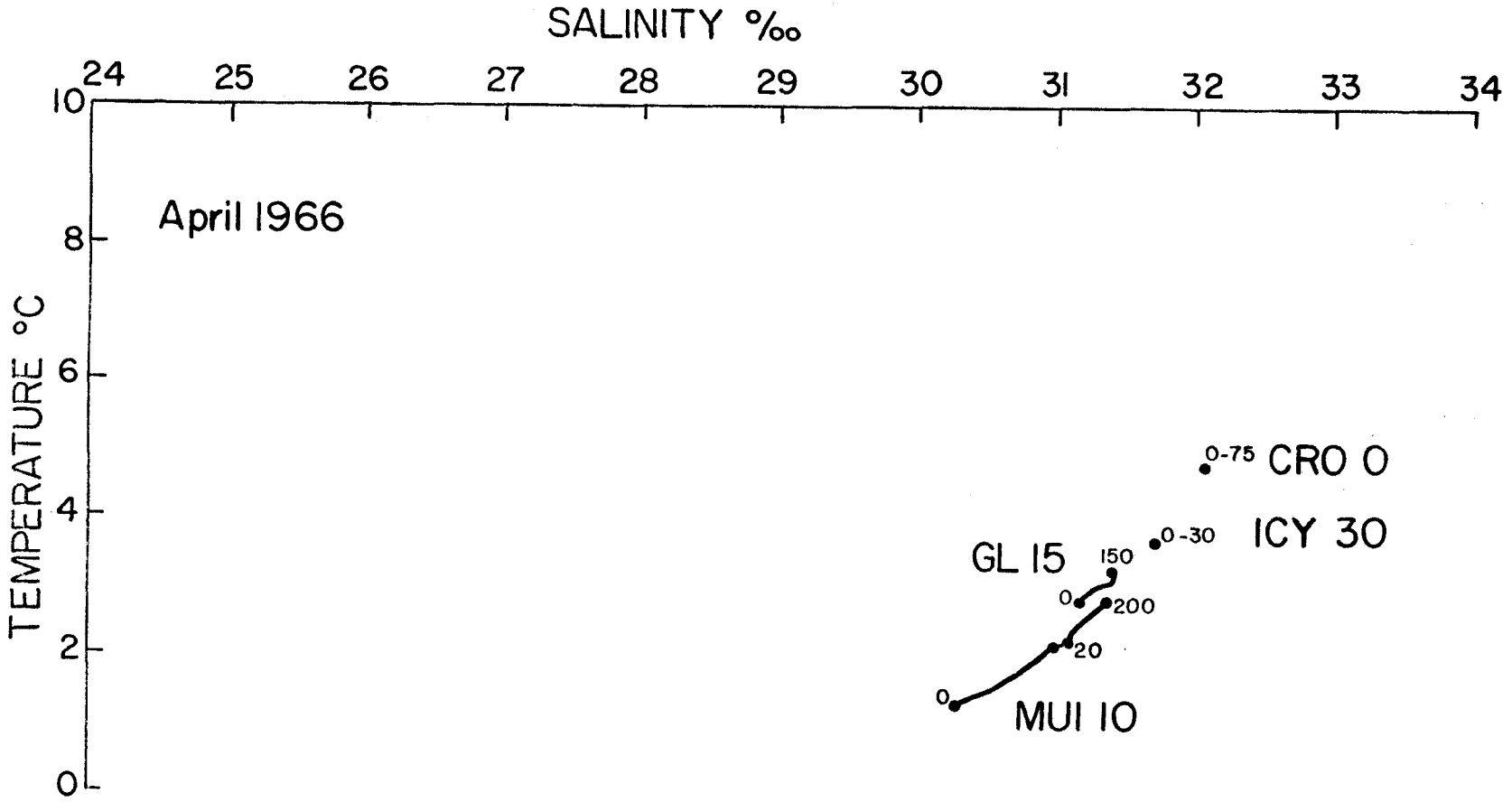

Figure 36. Temperature Versus Salinity Diagram Showing Data from CRO 0, ICY 30, GL 15, and MUI 10 for April 1966

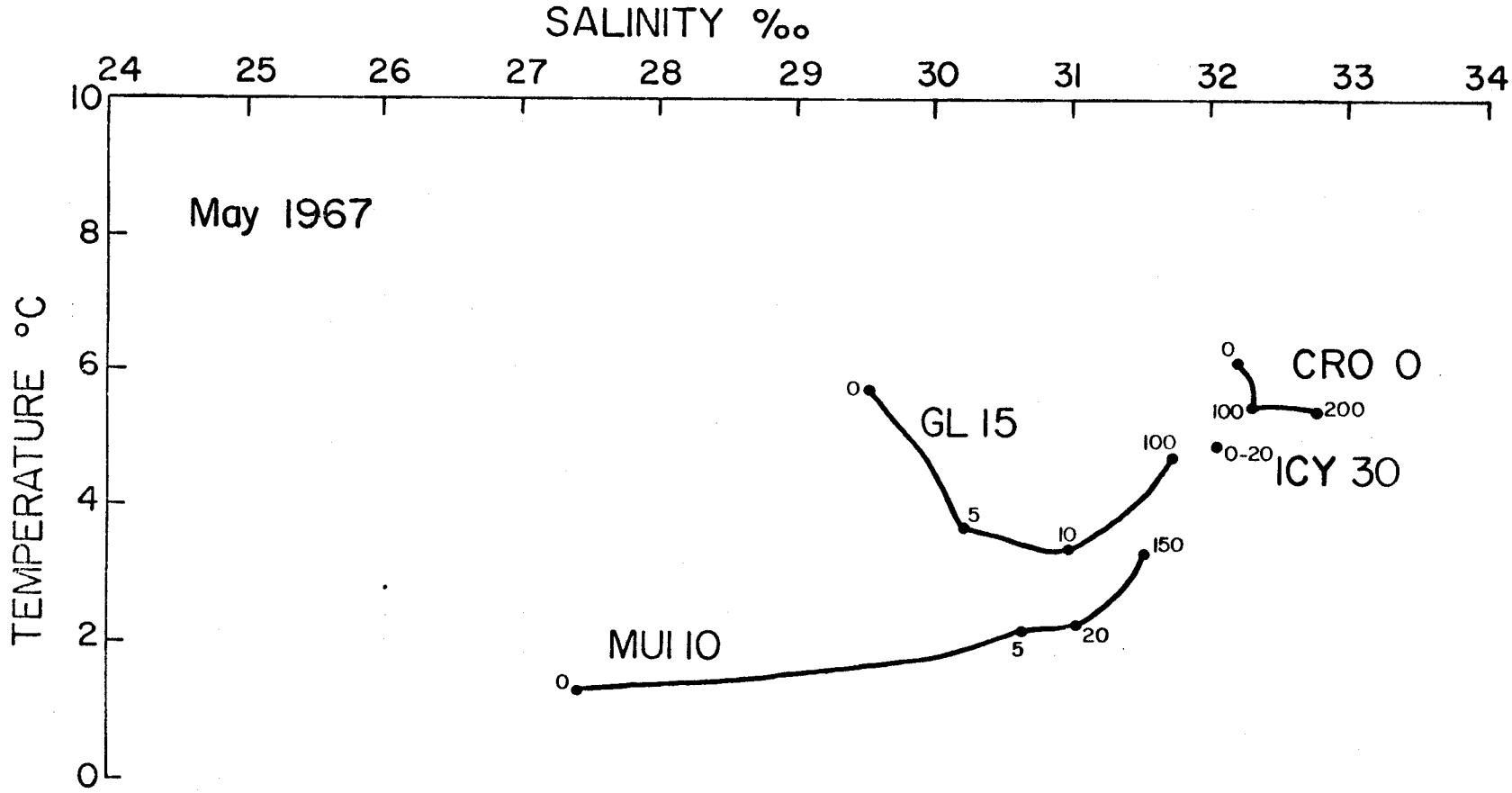

Figure 37. Temperature Versus Salinity Diagram Showing Data from CRO 0, ICY 30, GL 15, and MUI 10 for May 1967

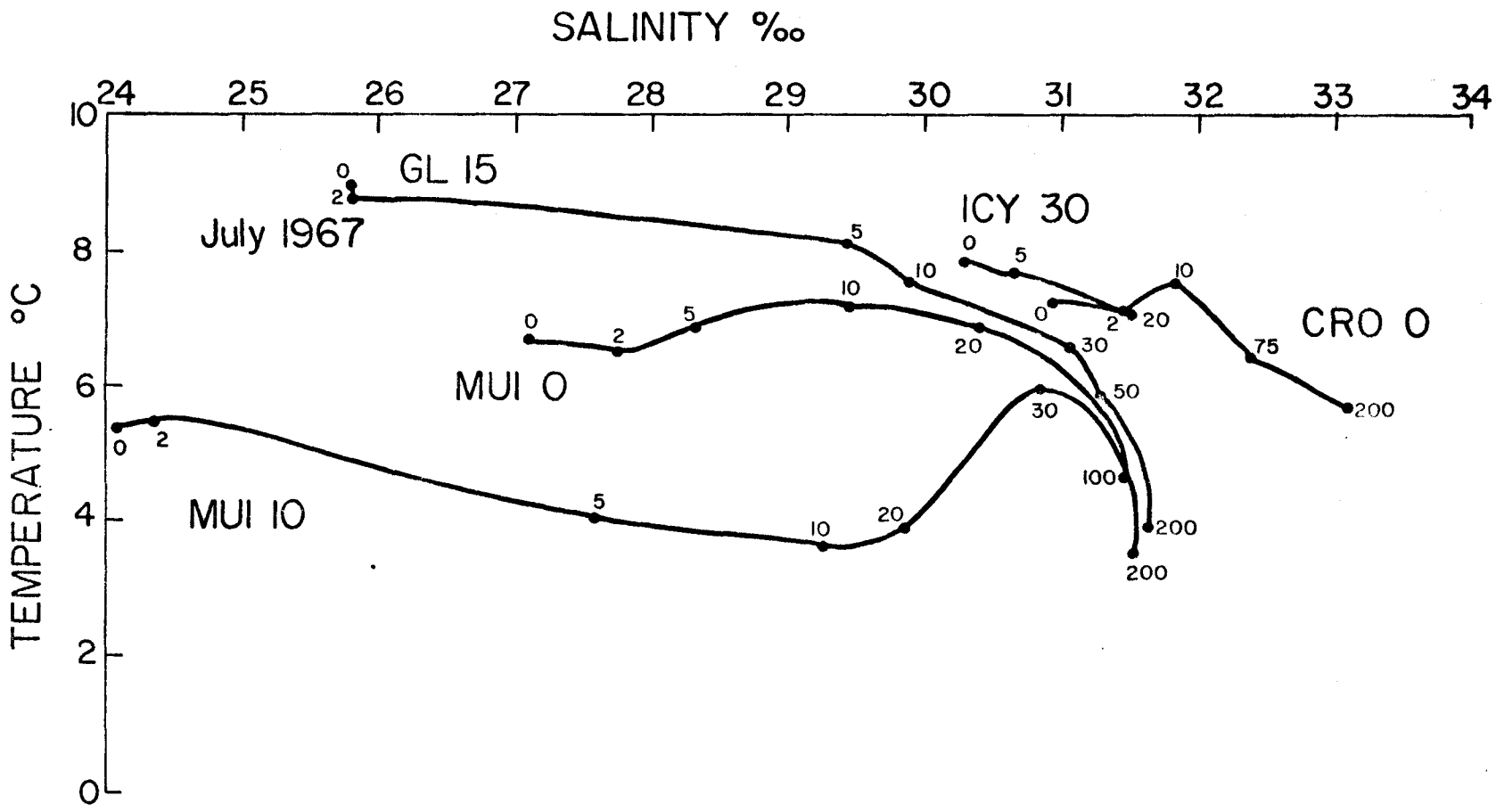

Figure 38. Temperature Versus Salinity Diagram Showing Data from CRO 0, ICY 30, GL 15, MUI 0, and MUI 10 for July 1967

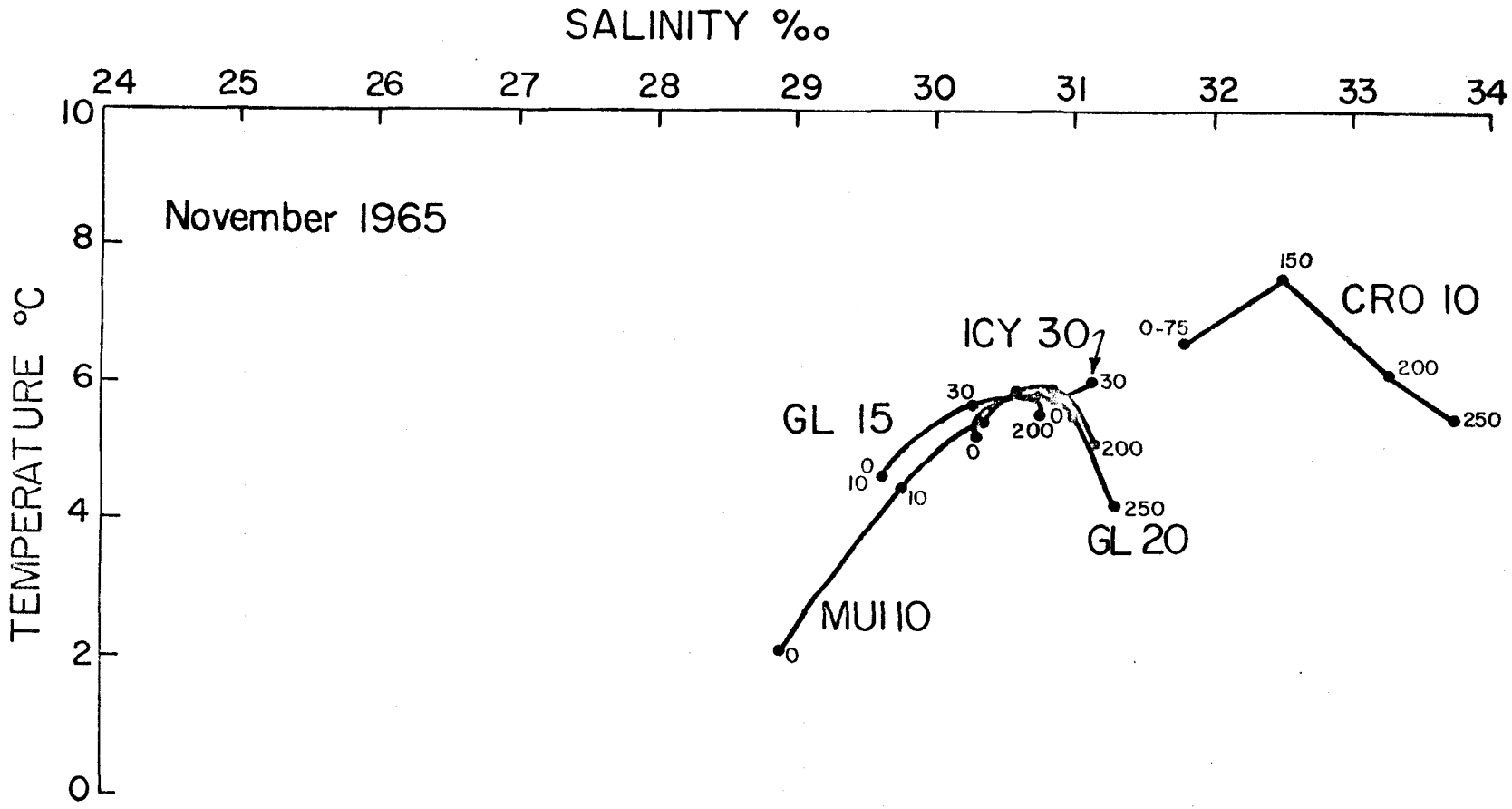

Figure 39. Temperature Versus Salinity Diagram Showing Data from CRO 10, ICY 30, GL 15, GL 20, and MUI 10 for November 1965

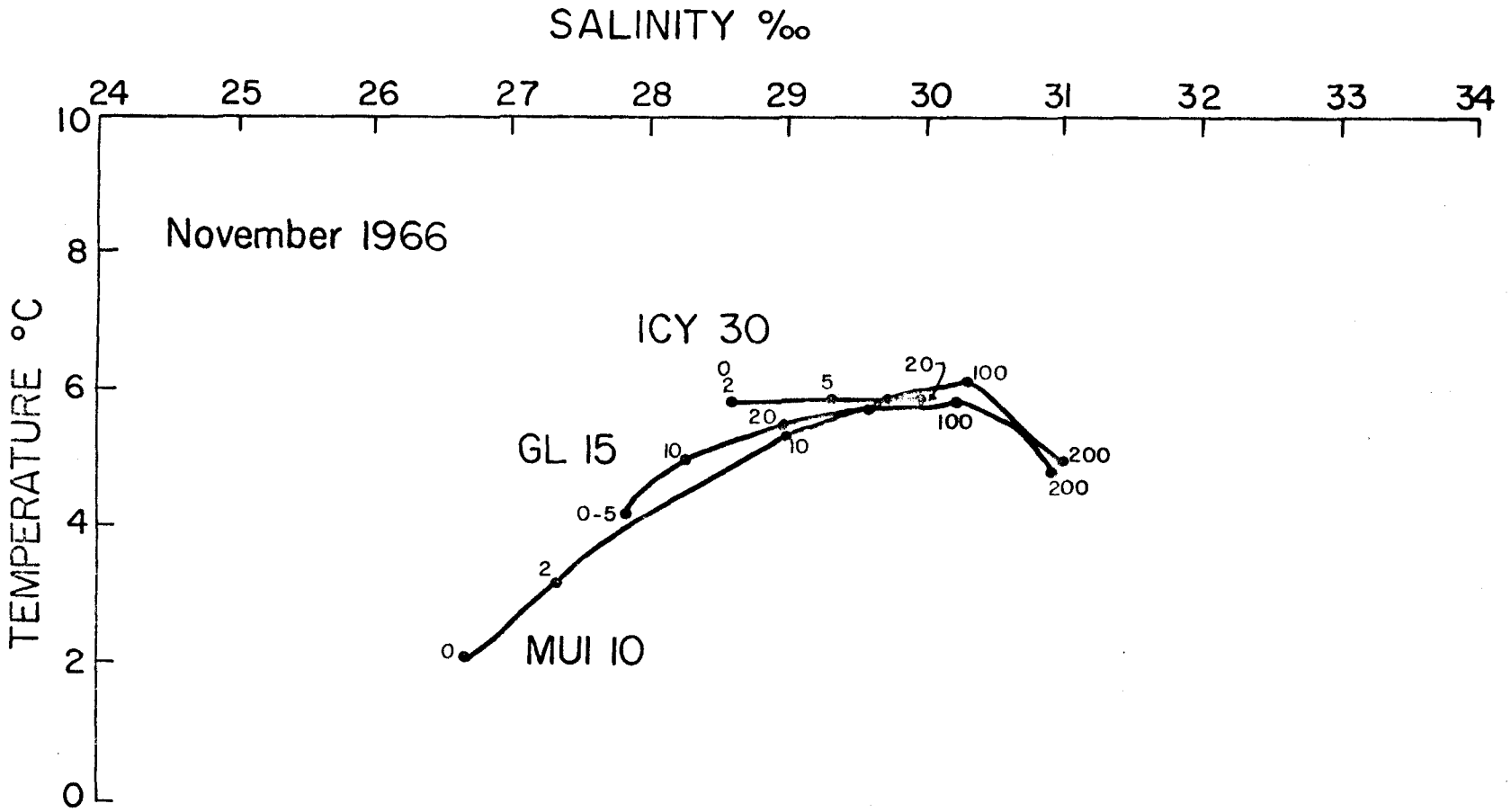

Figure 40. Temperature Versus Salinity Diagram Showing Data from ICY 30, G1 15, and MUI 10 for November 1966

becomes well-mixed with colder, brackish meltwater from the fjords beyond the shoal region, owing to the swift tidal currents and obstructions in the vast shoal regions of Icy Strait and Glacier Bay. As a result, no unmodified Pacific Ocean water is able to penetrate Icy Strait. Consequently, Glacier Bay and especially Muir Inlet water characteristics are more under the control of local climatological features than Pacific Ocean conditions.

For February 1966 and 1967, the temperature-salinity curves for CRO 0, ICY 30, GL 15, and MUI 10 show a progressively greater influence of cold, brackish surface water and mixing processes from the Pacific Ocean toward Glacier Bay and Muir Inlet. The CRO 0 water column becomes more homogeneous from 1966 to 1967; while its characteristics still remain in the same region of the diagram. The other stations show no such change in characteristics between 1966 and 1967.

For April 1966, CRO 0 water is homogeneous at 32.05‰ and 4.7°C. from the surface to the deepest observation at 75 meters. ICY 30 water is also homogeneous, but at 31.70‰ and 3.7°C. Farther inshore at GL 15, the water is beginning to become stratified, with definite evidence of a cold, brackish surface layer overlying fairly homogeneous water, which is less saline and colder than ICY 30 water. At MUI 10, the stratified flow regime is fully developed, and the deep water is similar to that at GL 15.

For May 1967, CRO 0 shows the effects of surface warming down to at least 100 meters. Comparison of this curve with that for CRO 0 in February 1967 shows that no dilution effects from spring meltwater runoff are yet evident in the Pacific Ocean right off the coast. The seasonal changes are even more pronounced at ICY 30 where for both February 1967 and May 1967 the water is homogeneous, but in May the water is about 1.5°C. warmer and 0.40‰ more saline. At GL 15 and at MUI 10, however, a different sequence of seasonal changes occurs. Between February 1967 and May 1967, the water below 10 meters becomes more saline by as much as 0.60‰ and warmer by as much as 1.5°C.; above 10 meters, both surface warming and dilution are well in progress. The dramatic rise in salinity and temperature below 10 meters suggests that an influx of relatively warm and saline water must have occurred between February and May. During a period of low runoff, such as occurs in March, warmer and higher salinity Pacific Ocean water might be able to penetrate up Glacier Bay with a minimal amount of dilution and enter Muir Inlet as a higher density inflow. More data, both oceanographic and climatological, are needed to explain the mechanism accounting for these changes.

By July 1967, the entire water column at each station has experienced some warming and dilution effects. The hump in the curve for MUI 10 is produced by the very cold

meltwater coming from the glaciers at the heads of the fjords. As the meltwater flows downfjord, it becomes warmed by the sun and mixed with entrained saline water.

For November 1965 and 1966, the stations from CRO 10 to MUI 10 exhibit the same spatial variations as found in July 1967. Tidal effects were studied at GL 20 for 12 hours in 1965. All the curves prepared from data obtained over the tidal cycle are identical, suggesting that no tongue of dense saline water penetrates that far into Glacier Bay on the flood tide. Cyclic tidal effects do not produce correspondingly cyclic variations in water mass characteristics near the mouth of Muir Inlet. This is not to discount the effects of tidal mixing processes throughout the whole tidal ebb and flood cycle. The only conclusion is that a pulse of dense, saline water is not introduced near the mouth of Muir Inlet on a flood tide at this time of the year.

Salinity Versus Dissolved Oxygen

MUI 10 data from four months, February 1967, May 1967, July 1967, and November 1966, are shown in Figure 41 (p. 85).

From February to May, the oxygen levels increase at all depths. From May to July, the oxygen levels above 5 meters continue to rise and below 5 meters decrease below February's values. By November, the oxygen content at all depths is further decreased. Then between November and February, the oxygen levels at all depths are increased.

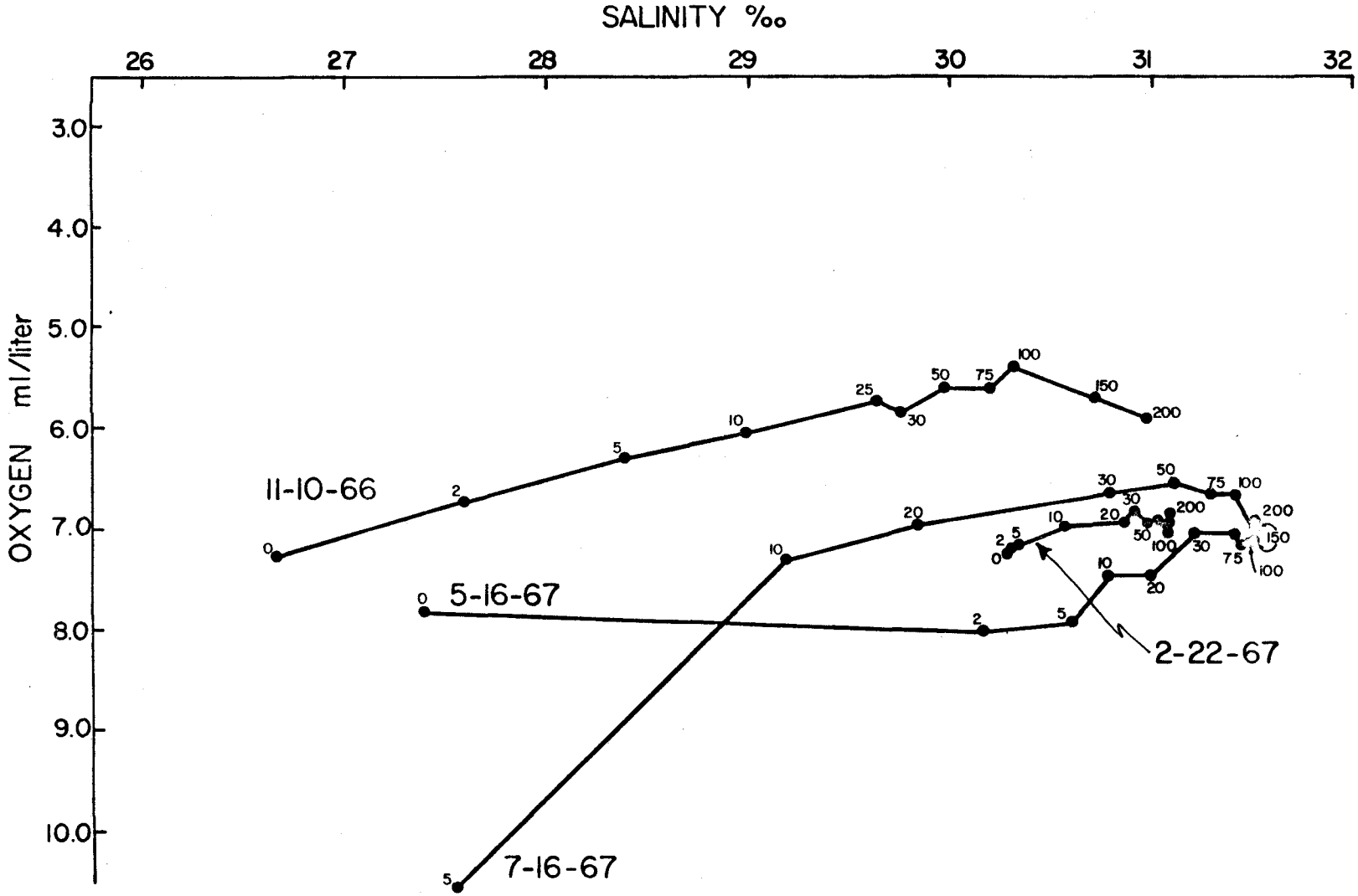

Figure 41. Salinity Versus Dissolved Oxygen Diagram Showing Data Collected at MUI 10 for February 1967, May 1967, July 1967, and November 1966

CHAPTER III

QUANTITATIVE ANALYSIS OF THE SEASONAL DISTRIBUTIONS OF SALINITY AND TEMPERATURE

The seasonal changes in the water mass characteristics of Muir Inlet, a fjord with a moderately shallow sill and tidal glaciers, are quantitatively analyzed in this chapter.

The amounts of water of different types are estimated according to the method developed in a series of papers by Cochrane (1956, 1958), Montgomery (1958), Pollak (1958), Rochford (1962), Sturges (1965), and Miller and Stanley (1966).

The results of this study are presented on quantitative temperature-salinity diagrams, which are shown in Figures 42, 43, 44, and 45 (pp. 87--90). The abscissa represents salinity (‰); the ordinate, temperature (°C.). The volume of water having temperature and salinity characteristics falling within a particular 0.5°C. and 0.1‰ class is expressed in cubic kilometers and written in the appropriate area on the diagram. Classes containing in excess of 1% of the total volume of sampled fjord waters are outlined by heavy lines.

The bivariate distributions shown in the quantitative temperature-salinity diagrams are further analyzed in the form of univariate temperature and univariate salinity diagrams. The univariate temperature and the univariate

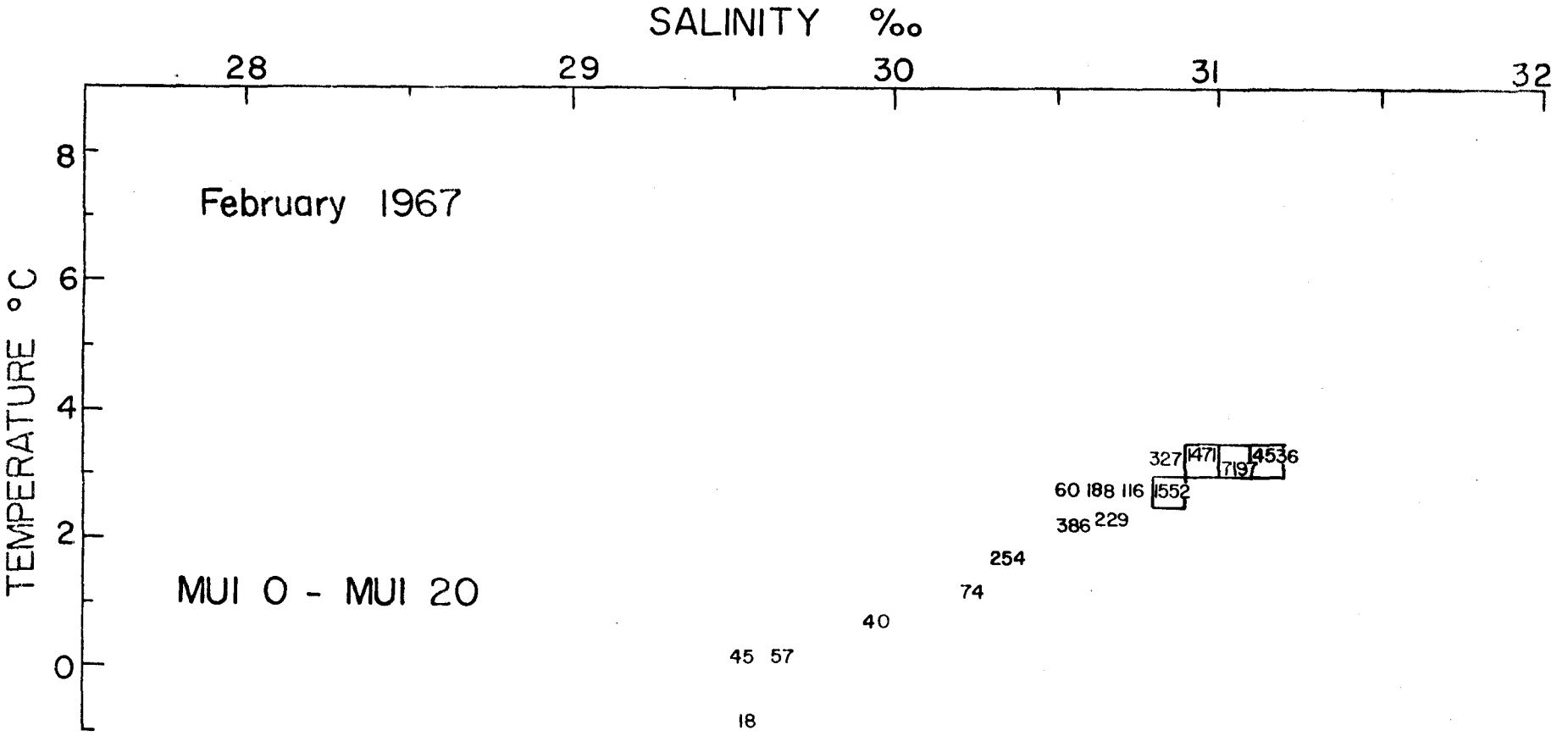

Figure 42. Quantitative Temperature-Salinity Diagram for February 1967. The volume of water having temperature and salinity characteristics falling within a particular 0.5°C. and 0.1 ‰ class is expressed in cubic kilometers multiplied by 10^3 and is written in the appropriate area on the diagram. Classes containing in excess of 6 % of the total volume of sampled fjord waters are outlined by heavy lines.

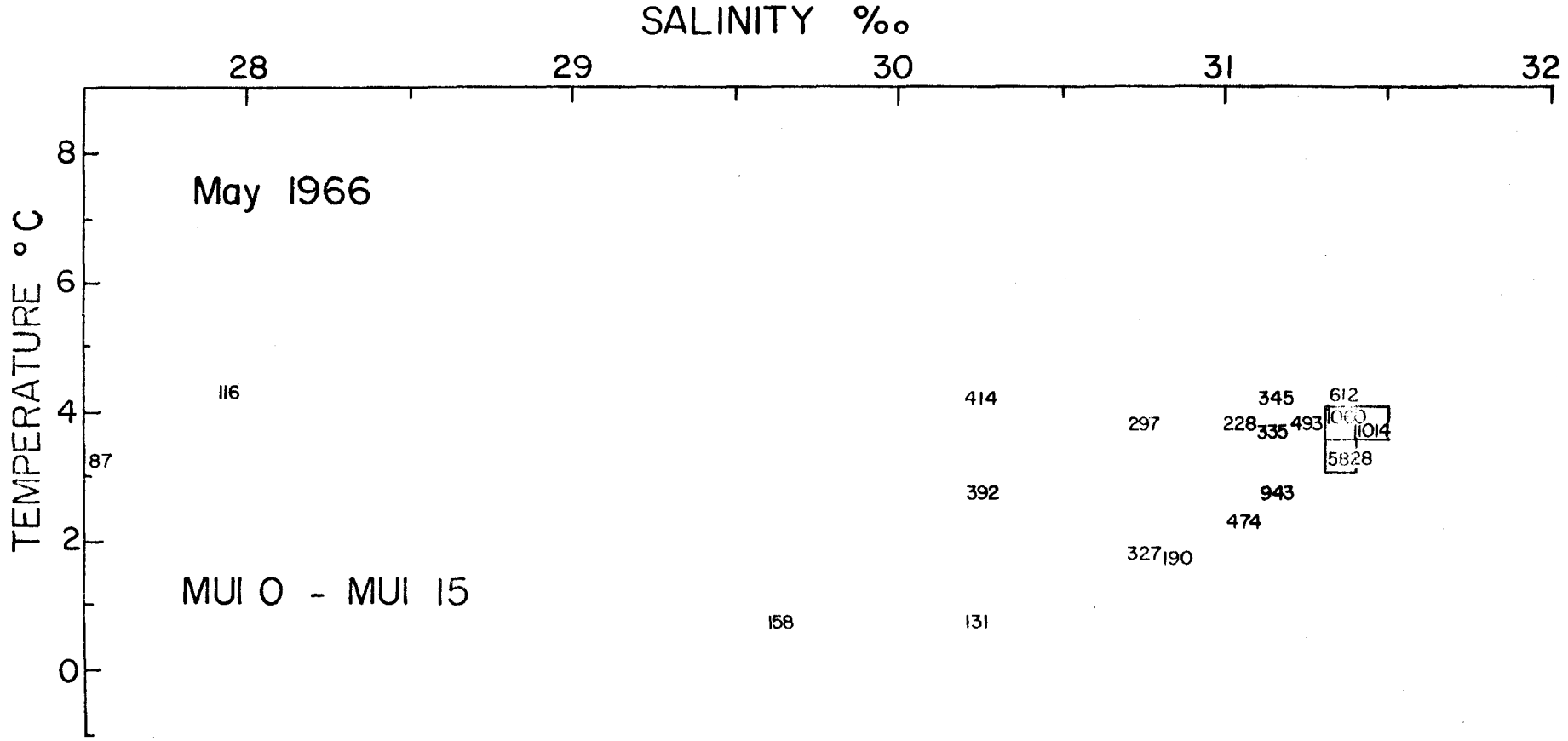

Figure 43. Quantitative Temperature-Salinity Diagram for May 1966. The volume of water having temperature and salinity characteristics falling within a particular 0.5°C. and 0.1 ‰ class is expressed in cubic kilometers multiplied by 10^3 and is written in the appropriate area on the diagram. Classes containing in excess of 6 % of the total volume of sampled fjord waters are outlined by heavy lines.

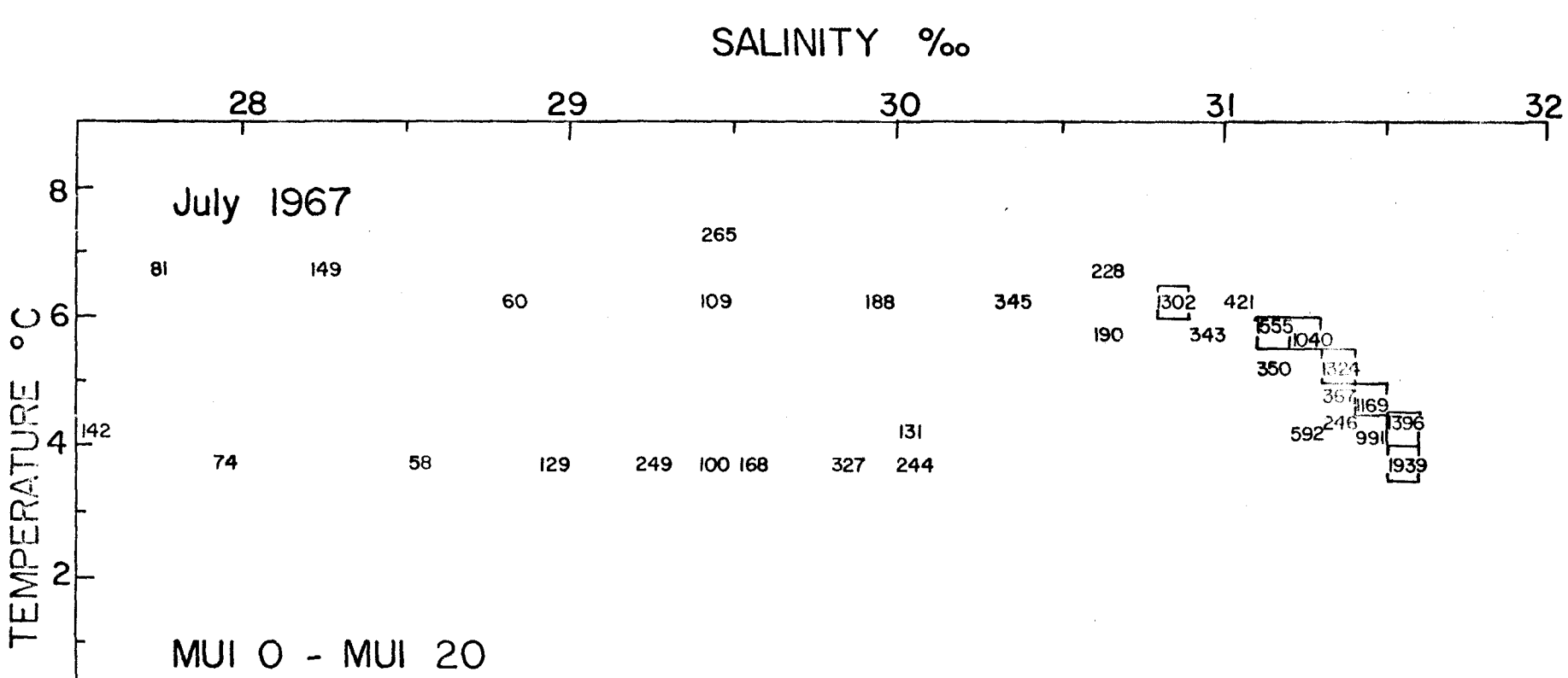

Figure 44. Quantitative Temperature-Salinity Diagram for July 1967. The volume of water having temperature and salinity characteristics falling within a particular 0.5°C. and 0.1 ‰ class is expressed in cubic kilometers multiplied by 10^3 and is written in the appropriate area on the diagram. Classes containing in excess on 6 % of the total volume of sampled fjord waters are outlined by heavy lines.

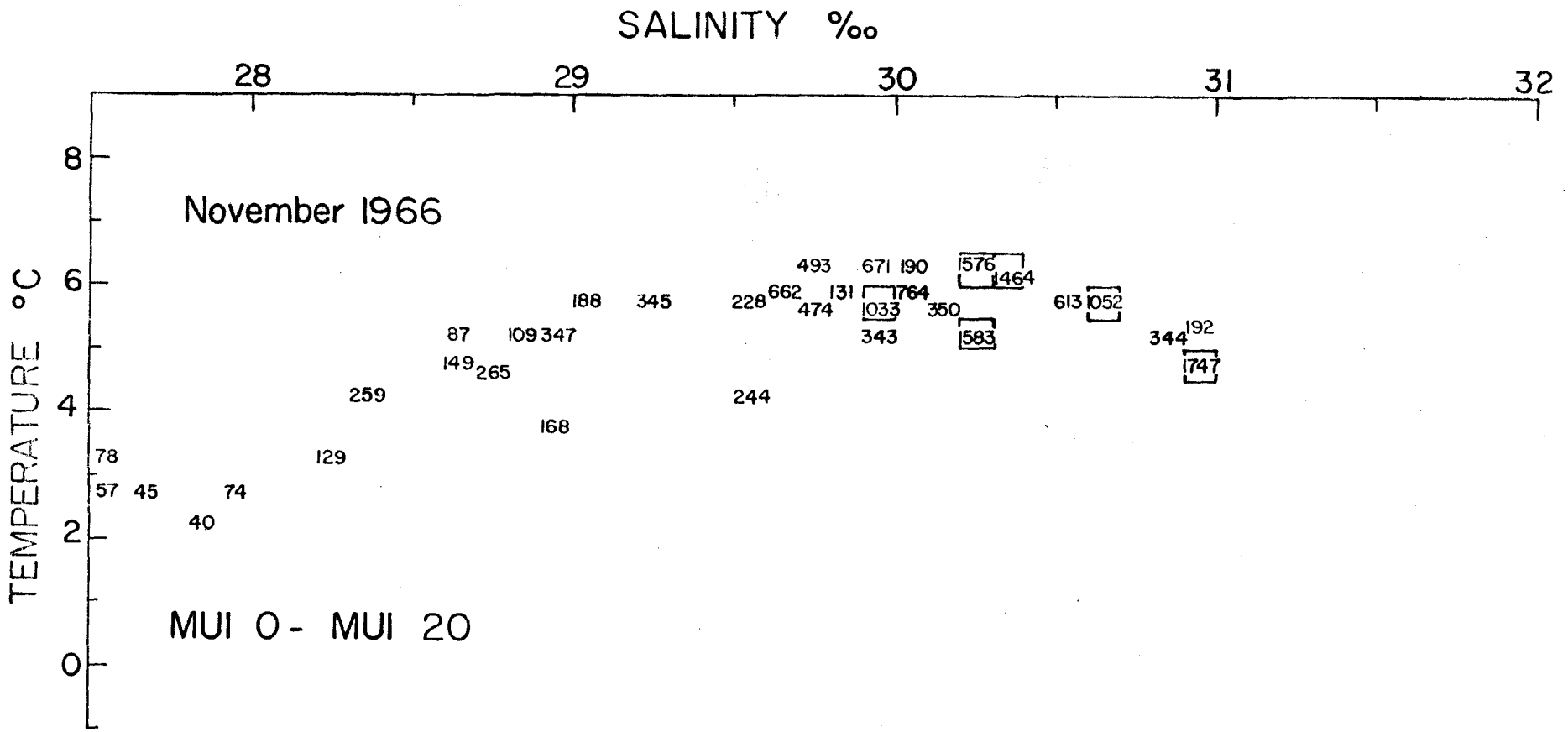

Figure 45. Quantitative Temperature-Salinity Diagram for November 1966. The volume of water having temperature and salinity characteristics falling within a particular 0.5°C. and 0.1 ‰ class is expressed in cubic kilometers multiplied by 10^3 and is written in the appropriate area on the diagram. Classes containing in excess of 6 % of the total volume of sampled fjord waters are outlined by heavy lines.

salinity diagrams are shown in Figures 46, 47, 48, and 49 (pp. 92--95). The abscissa shows either temperature or salinity marked off in the appropriate intervals. The upper half of the figures shows the volume of water found in each interval; the lower half, the percent of the sampled water mass which falls within the specified range.

Quantitative Temperature-Salinity Diagrams

The temperature and salinity data for each of four representative cruises (November 1966, February 1967, May 1966, and July 1967) are plotted on separate temperature-salinity diagrams. The frequency of occurrence of a water type is expressed in cubic kilometers of water and is recorded in the temperature-salinity region for that class.

Method of Analysis

Each of the data pairs is weighted according to the volume of water it is assumed to represent. Each volume is defined vertically by the mid-points between sample depths and the physical boundaries of the fjord; longitudinally by the mid-points between stations, except at the head and at the mouth where arbitrary boundaries are set; and laterally

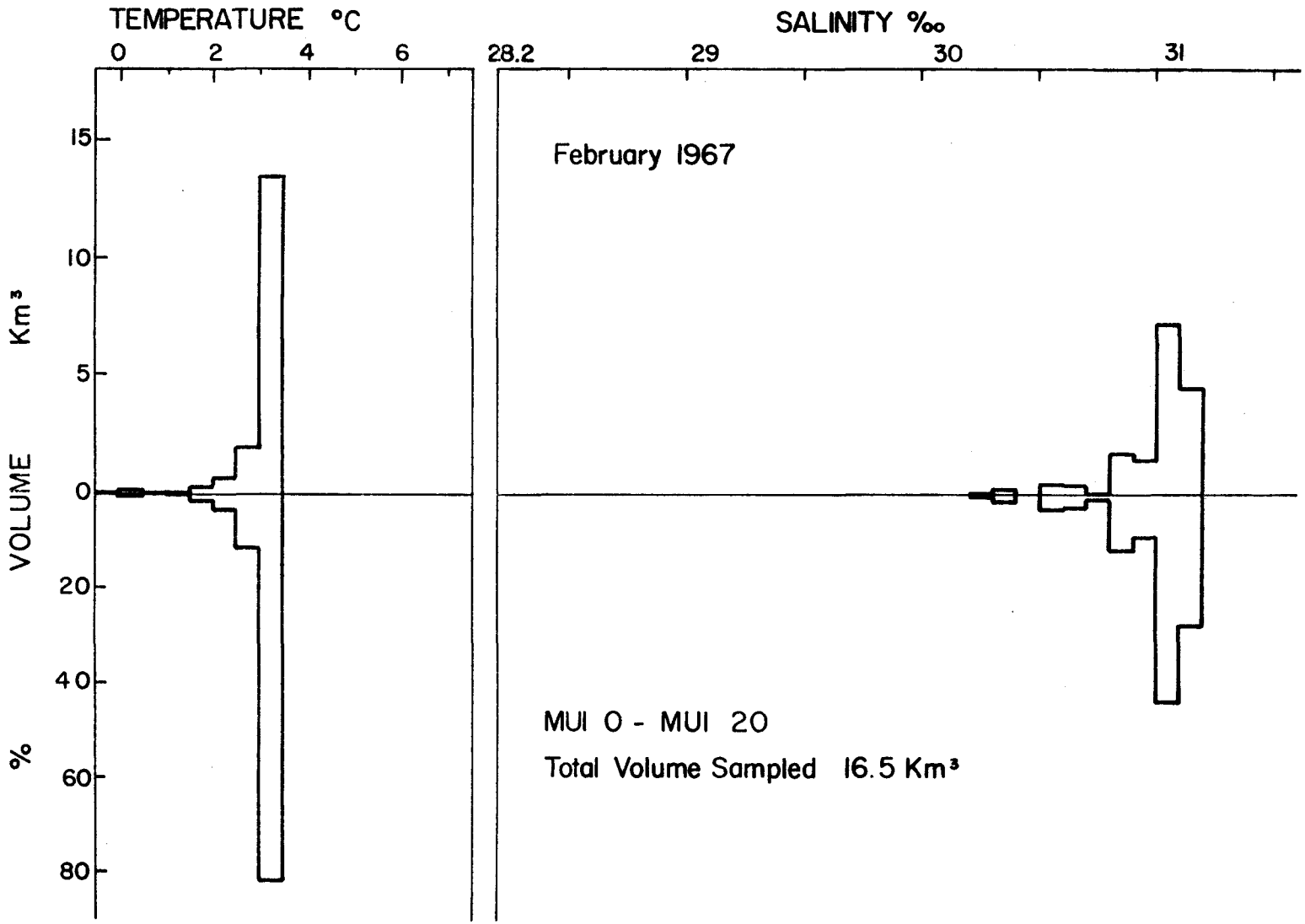

Figure 46. Univariate Temperature and Univariate Salinity Diagrams for February 1967

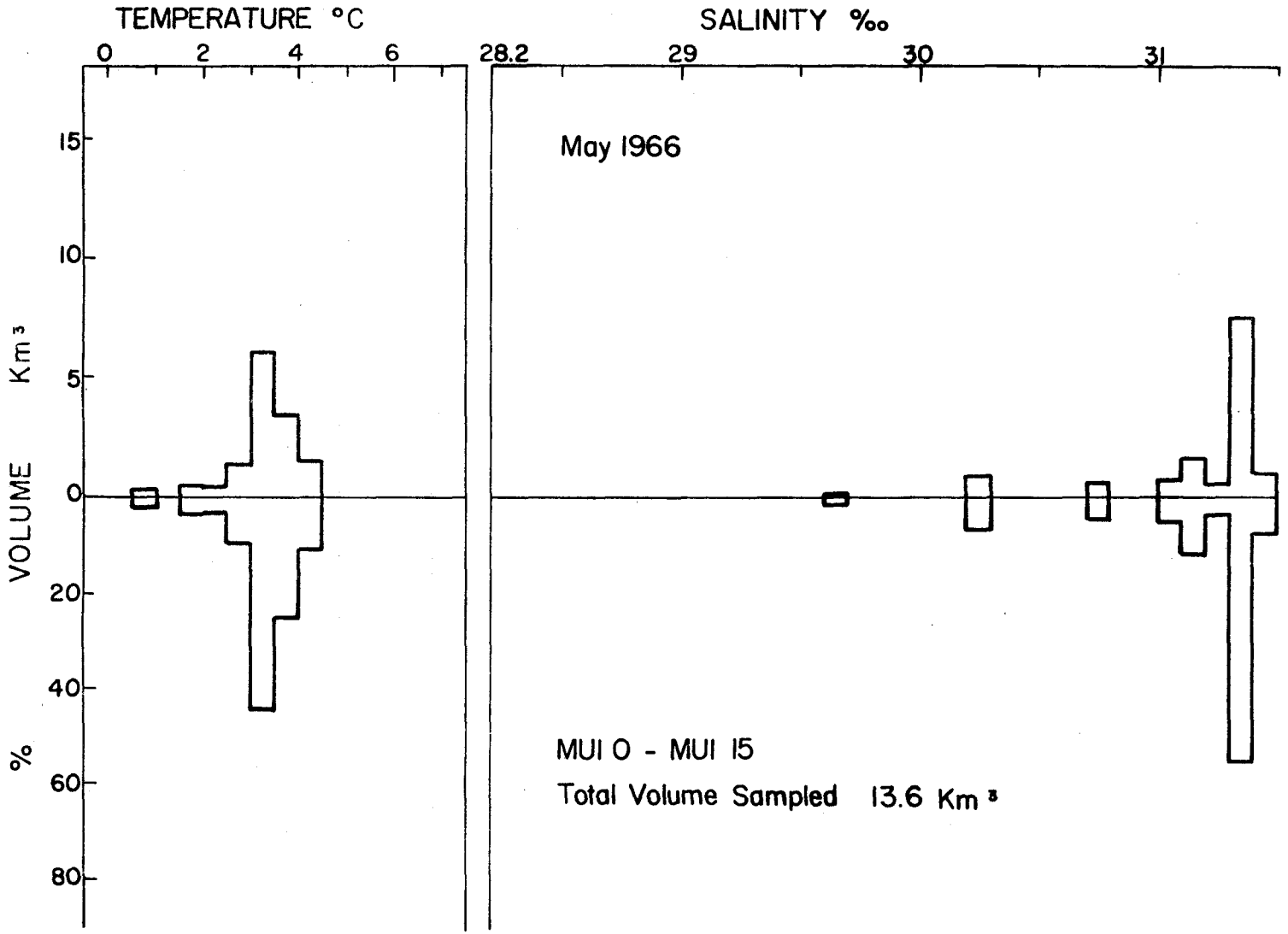

Figure 47. Univariate Temperature and Univariate Salinity Diagrams for May 1966

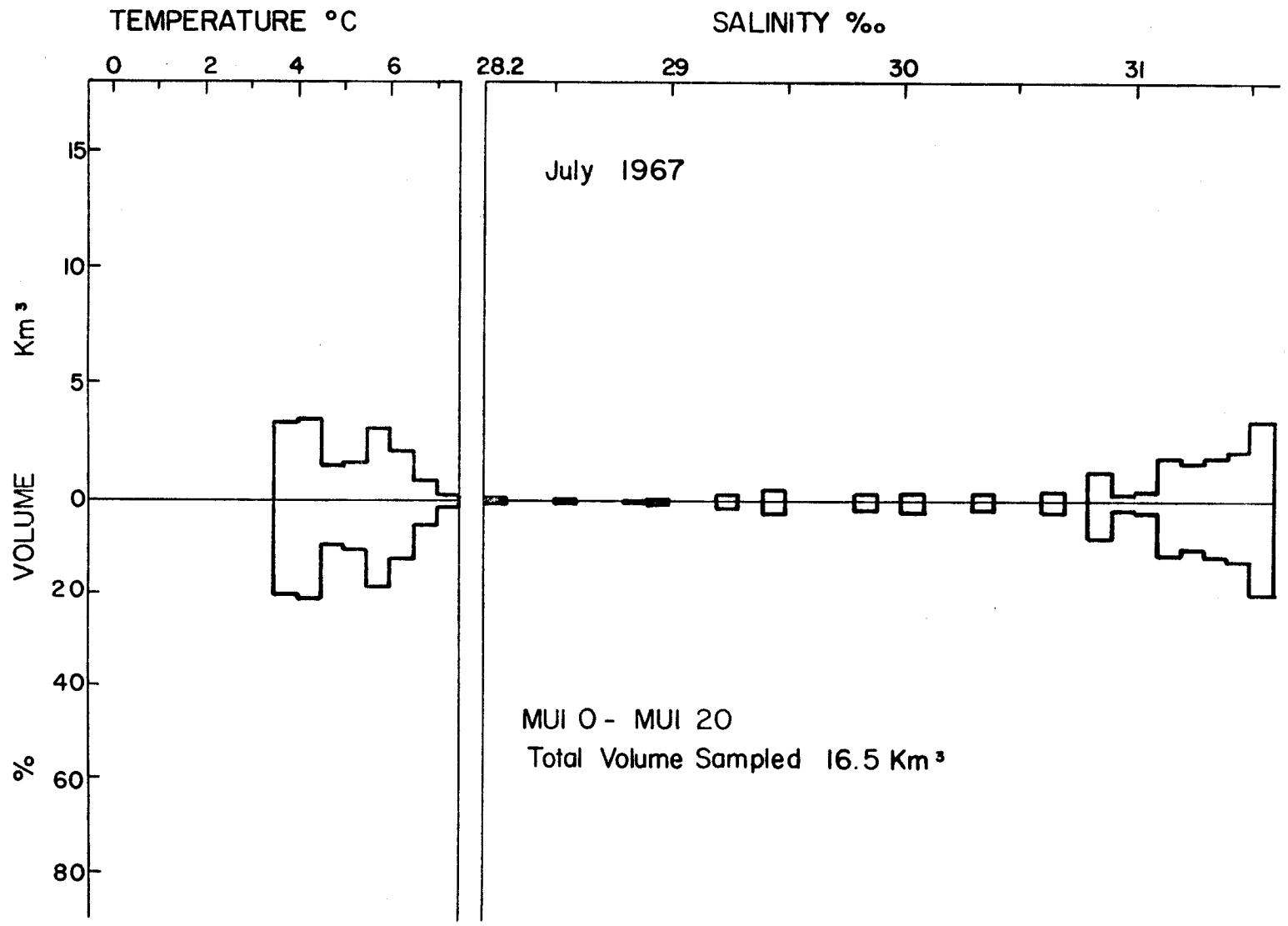

Figure 48. Univariate Temperature and Univariate Salinity Diagrams for July 1967

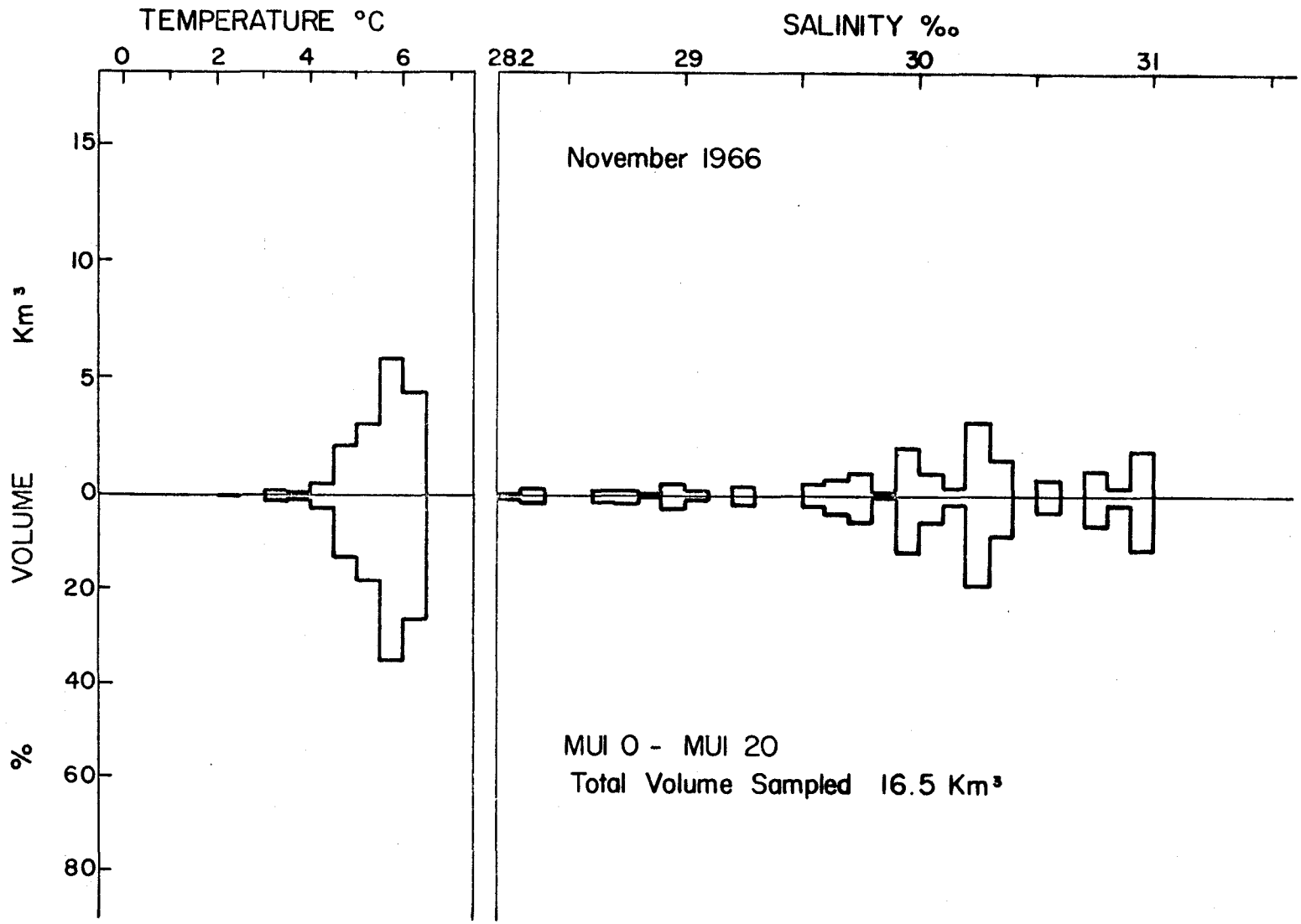

Figure 49. Univariate Temperature and Univariate Salinity Diagrams for November 1966

by the fjord banks and the arbitrary lines drawn across the mouths of Adams and Wachusetts Inlets.

The volumes assigned to each sample depth are listed in Table 9 (p. 97). They range from 0.014 cubic kilometers, for a surface sample, to 1.052 cubic kilometers, for a 150-meter sample; thus, the characteristics of the deeper layers dominate the overall distributions. These volumes are roughly estimated by dividing the fjord into sub-volumes approximating pyramids and frustrums of pyramids, for ease of calculation. The percent error in the volumes is assumed to be large. This error reflects the lack of precise knowledge of the bathymetric detail of the fjord and the approximation of the irregular fjord volume by a summation of regularly shaped sub-volumes.

To facilitate the sorting of the data, the data for each sample are placed on an index card, which shows salinity, temperature, depth, cruise number, date, station name, and volume. The cards are sorted first into 0.1‰ salinity intervals, and then each salinity interval is organized according to increasing temperature. The volume of water in each class is found by summation.

Results

Each quantitative temperature-salinity diagram (Figures [illegible]) shows the data for a particular cruise

TABLE 9. VOLUMES (IN CUBIC KILOMETERS) USED TO ESTIMATE THE FREQUENCY OF OCCURRENCE OF WATER TYPES IN MUIR INLET

Depth	Stations					Total volume
	MUI 0	MUI 5	MUI 10	MUI 15	MUI 20	
0 meters	.036 Km^3	.027 Km^3	.037 Km^3	.014 Km^3	.018 Km^3	.129 Km^3
2	.081	.060	.078	.031	.040	.290
5	.141	.109	.142	.057	.074	.531
10	.265	.188	.249	.100	.129	.931
20	.345	.228	.327	.131	.168	1.199
30	.493	.335	.474	.190	.244	1.736
50	.612	.421	.671	.272	.343	2.319
75	.764	.369	.685	.276	.350	2.444
100	.250	.269	.919	.367	.592	2.397
150		.246	1.052	.344	.383	2.025
200			.900	.192	.482	1.574

TABLE 9 (Continued)

Depth	Stations					Total Volume
	MUI 0	MUI 5	MUI 10	MUI 15	MUI 20	
250 meters			.647 Km^3		.127 Km^3	.774 Km^3
300			.200			.200
Total	2.995	2.252	6.378	1.974	2.950	16.549

typical of a season. The months depicted are November 1966, February 1967, May 1966, and July 1967. These sets of data were chosen because of their relative completeness. Each diagram states which stations are covered and the total amount of water represented by them. Table 10 (p. 100) lists the most prevalent water types by month.

Water samples having salinities less than 27.50‰ fall off the chosen scale. In all instances, these water masses account for only a negligible fraction of the total volume sampled.

The February diagram indicates that very homogeneous conditions exist in the fjord at that time. Most of the water is concentrated in the high salinity, low temperature region of the diagram. Table 10 shows the water types with a frequency greater than 1.000 cubic kilometers. In February, there are four such water types, involving 88.9% of the total volume sampled.

The major changes between February and May are a decrease in homogeneity and an increase in both the temperature and the salinity of the most prevalent water types. Table 10 shows, however, that the frequencies of occurrence of the most prevalent water types is diminished with respect to those for February. In May, there are three classes with a frequency greater than 1.000 cubic kilometers, comprising 58.2% of the total volume sampled.

TABLE 10. MOST PREVALENT WATER TYPES BY MONTH

Month	Prevalence		Salinity (‰)	Temperature (°C.)
	Volume in cubic kilometers	Percent of total volume sampled		
February 1967	7.197	43.4	31.0--31.1	3.0--3.5
	4.536	27.4	31.1--31.2	3.0--3.5
	1.515	9.2	30.8--30.9	2.5--3.0
	1.471	8.9	30.9--31.0	3.0--3.5
May 1966	5.828	42.9	31.3--31.4	3.0--3.5
	1.060	7.8	31.3--31.4	3.5--4.0
	1.014	7.5	31.4--31.5	3.5--4.0
July 1967	1.939	11.7	31.5--31.6	3.5--4.0
	1.555	9.4	31.1--31.2	5.5--6.0
	1.396	8.4	31.5--31.6	4.0--4.5
	1.324	8.0	31.3--31.4	5.0--5.5
	1.302	7.9	30.8--30.9	6.0--6.5
	1.169	6.7	30.4--30.5	4.5--5.0
	1.040	6.3	30.2--30.3	5.5--6.0
November 1966	1.747	10.5	30.9--31.0	4.5--5.0
	1.583	9.6	30.2--30.3	5.0--5.5
	1.576	9.5	30.2--30.3	6.0--6.5
	1.052	6.4	30.6--30.7	5.5--6.0
	1.033	6.2	29.9--30.0	5.5--6.0

By July, a pronounced shift toward warmer temperatures and lower salinities can be seen. The formerly homogeneous high salinity and low temperature winter--spring water masses are spreading out toward higher temperatures and lower salinities as a result of solar heating and downward mixing of brackish water. The lower salinity classes align themselves along two isotherms, about 3.5--4.0°C. and 6.0--7.0°C. Table 10 shows that there no longer is a dominant water type. Instead, there are seven classes with a frequency greater than 1.000 cubic kilometers; the most prevalent water type contains only 11.7% of the total volume sampled. These seven most prevalent water types account for 58.4% of the total volume sampled.

Univariate Temperature and Univariate Salinity Distributions

The univariate temperature and univariate salinity diagrams are shown in Figures 46, 47, 48, and 49 (pp. 92--95).

For February 1967, 84% of the sampled water has a temperature of 3.0--3.5°C.; 44%, a salinity of 31.0--31.1‰; and 28%, a salinity of 31.1--31.2‰. The distributions are unimodal with an abrupt cutoff at the larger-valued side of the peak. No sample has a temperature greater than 3.5°C. or a salinity greater than 31.2‰.

For May 1966, both distributions are unimodal, but sample points fall on both sides of the peaks. The

temperature distribution shows that 44% of the water sampled falls between 3.0--3.5°C.; 25%, between 3.5--4.0°C. The salinity peak is sharper than the temperature peak, with 55% of the water in the 31.3--31.4‰ salinity range.

For July 1967, no solitary peaks appear. The water has been both warmed and diluted from above. The temperature distribution is barely bimodal, with slight peaks at 3.5--4.0°C. and 5.5--6.0°C. These two temperature ranges combined contain 60% of the water sampled. The salinity distribution shows a peak of 20% at 31.5--31.6‰, which trails gradually down to 11% at 31.1--31.2‰. These salinity ranges combined contain about 66% of the volume sampled.

For November 1966, the temperature distribution is unimodal, with 35% of the water having a temperature between 5.5--6.0°C.; 27%, between 6.0--6.5°C. The salinity distribution shows that a very heterogeneous situation exists, with the most dominant salinity range containing only 19% of the volume sampled.

CHAPTER IV

MUIR INLET IN RELATION TO OTHER FJORDS

Many questions may be asked about the significance of the results of this study. Two questions are considered in this chapter: How unique is the physical oceanography of Muir Inlet, a fjord with tidal glaciers, when compared to similar fjords lacking tidal glaciers? What are the dominant factors controlling the characteristics of the water masses of Muir Inlet? To answer these questions, a survey of the results of investigations of the physical oceanography of Muir Inlet, Port Nellie Juan Fjord, Taiya Inlet, and Endicott Arm in Alaska; Bute Inlet in southern British Columbia; Oslofjord, Nordfjord, and Hardangerfjord in Norway; "Brown Zone" fjords in Greenland and West Spitzbergen; and anoxic fjords in British Columbia and Norway is presented and discussed.

Effect of Tidal Glaciers on Muir Inlet Water Masses

To facilitate an evaluation of the effect of the tidal glaciers on the physical oceanography of Muir Inlet, seasonal data from MUI 20 is collected in Table 11 (p. 104), since MUI 20 is the station farthest from marine influences and most dominated by the glacial environment. Table shows the salinity, temperature, dissolved oxygen, and

TABLE 11. DISSOLVED OXYGEN EXPRESSED AS PERCENT SATURATION FOR SOME MUI 20 DATA*

10-XI-66						22-II-67					
Z	S	T	O	Sat* O	% Sat	Z	S	T	O	Sat* O	% Sat
0	26.95	1.26	7.05	8.06	87.5	0	29.56	-0.01	6.82	8.18	83.4
2	27.81	2.48	7.05	7.74	91.1	2	29.91	0.72	6.82	8.00	85.2
5	27.90	2.69	6.46	7.69	84.0	5	30.25	1.43	6.76	7.81	86.5
10	28.27	3.25	6.17	7.56	81.7	10	30.62	2.17	6.76	7.64	88.5
20	28.93	3.98	5.82	7.38	78.9	20	30.82	2.74	6.76	7.53	89.9
30	29.58	4.30	5.88	7.28	80.9	30	30.96	3.11	6.82	7.46	91.4
50	29.91	5.37	5.55	7.08	78.4	50	31.03	3.31	6.93	7.42	93.4
75	30.13	5.94	5.94	6.97	85.2	75	31.04	3.30	6.88	7.42	92.7
100	30.21	5.49	5.48	7.04	77.9	100	31.10	3.26	6.88	7.41	92.7
150						150	31.11	3.25	6.88	7.41	92.7
200						200	31.11	3.26	6.82	7.41	92.1

*Z = depth in meters; S = salinity in ‰ ; T = temperature in °C.; O = dissolved oxygen in milliliters per liter; Sat O = saturation value in milliliters per liter as a function of temperature and salinity; % Sat = percent oxygen saturation.

*Oxygen saturation from Richards and Corwin 1956.

TABLE 11 (Continued)

	16-VII-67					28-IX-67					
Z	S	T	O	Sat* O	% Sat	Z	S	T	O	Sat* O	% Sat
0	13.95	3.76	8.73	8.22	106	0	13.08	1.91	8.05	8.68	92.7
2	25.21	3.57	7.43	7.67	96.9	2	16.73	3.44	7.04	8.15	86.4
5	27.98	3.53	7.06	7.53	93.9	5	23.94	2.97	6.44	7.88	81.8
10	28.96	3.50	7.01	7.49	93.9	10	26.46	4.06	5.94	7.52	79.0
20	29.51	3.56	6.92	7.45	92.9	20	28.57	5.24	5.62	7.18	78.4
30	30.06	3.93	6.86	7.35	93.4	30	29.30	6.59	5.36	6.91	77.6
50	30.98	5.75	6.53	6.97	93.7	50	29.80	6.21	5.58	6.93	80.5
75	31.17	5.44	6.64	6.82	97.3	75	30.12	5.64	5.54	7.03	78.9
100	31.27	4.47	6.64	7.18	92.5	100	30.47	5.16	2.80	7.10	39.4
150	31.47	4.26	6.85	7.20	95.2	150	30.98	5.24	1.82	7.06	25.8
200	31.47	4.04	6.76	7.25	93.2	200		5.08			

percent oxygen saturation data for November 1966, February 1967, July 1967, and September 1967.

The saturation values for dissolved oxygen, as a function of temperature and salinity, are determined from a nomograph prepared by Richards and Corwin (1956). The data upon which this nomograph is based are not the most accurate available (Carpenter 1966). Because of probable errors in the determination of the dissolved oxygen content of the water samples and because of an intent to emphasize merely the seasonal trends in saturation levels, the accuracy of the saturation values obtained from this nomograph are deemed sufficient for this study.

Between November and February, there is a general increase in salinity and a decrease in temperature and stability throughout the entire water column, as the solar and sky radiation, air temperature, and runoff minima are approached and passed. Below 10 meters, the dissolved oxygen content and percent saturation increase during this period, as advective density flows across the sill and thermohaline convection work to replenish the oxygen content of the deep water and produce a homogeneous winter water mass.

Comparison of the February and July data reveals several trends. For both months, the salinities at 50 meters are nearly equal. Below 50 meters, the July

salinities and temperatures are higher than the corresponding February values. To account for these changes, water of higher salinity and temperature must be introduced over the sill during the spring and early summer. A forced tidal, continuity, or gravity flow of denser, modified Pacific Ocean water over the sill during this period can explain the observed changes. The likelihood of such a flow is high, since the runoff minimum occurring around March should allow a period of minimal dilution of intruding warmer and more saline Pacific Ocean water. Furthermore, the existence of both a temperature discontinuity and a leveling off in the vertical salinity gradient between 30--50 meters suggests that the effects of spring and summer climatological changes have penetrated the water column only to 50 meters. In both February and July, the oxygen saturation values below 20 meters are similarly high. From 20 meters to the surface, February's values show a slight decrease in oxygen saturation; July's, an increase, possibly becoming supersaturated near the surface as a result of photosynthesis.

In the two and a half months from the July to the September observations, radical changes occur in the dissolved oxygen levels at MUI 20. The dissolved oxygen content throughout the water column is markedly lower during September. The 100-meter and 150-meter values represent the three-year observed saturation minimum, with values in

one vicinity o[illegible] and 26‰ respectively. There is apparently a sharp discontinuity in saturation levels between 75 and 100 [illegible]. Considered by itself, this [illegible] tendency [illegible] would imply either weak [illegible] conditions within the [illegible] sum[illegible]. On the other hand, the warming [illegible] water between [illegible] renewal of bottom water, [illegible] upward [illegible] surface or over the sill, [illegible]. Mixing schemes, however, should introduce highly undersaturated water resulting from the transport of water [illegible] in contact with air through [illegible] or tidal-induced mixing of air and water or through the release of gas bubbles from melting ice.

The role of [illegible] water in supplying sub-pycnoclinic [illegible] low-salinity water (Pickard 1967) can be [illegible], an examination of Table 11 shows [illegible] development in September of a very cold, nearly [illegible], meltwater-dominated runoff layer overlying [illegible] sills, only [illegible] sufficient water [illegible] 32 meters. The depth of the temperature [illegible] the seaward limit of direct vertical [illegible].

Contrary to Pickard's (1967) speculation on the [illegible] tidal [illegible] and icebergs on the properties

of the deep water, glacial ice seems to serve mainly as a heat sink for water masses below the pycnocline. Figure 18 (p. 50) shows the upfjord decrease in the temperature and depth of the temperature maximum within the tongue of warmer water.

A more probable explanation for the spring--fall deep water changes rests in the circulation regime driven by the outflowing meltwater, producing a density barrier which impedes the downward mixing of cold, brackish, oxygenated surface water while concurrently inducing a net upward transport of deep water through the entrainment mechanism described by Keulegan (1949). Continuity of flow then demands that sub-pycnoclinic water be drawn across the sill and upfjord to replace the entrained deep water (Tully 1958; Bowden 1967).

The water coming over the sill periodically on account of the tide and continually on account of entrainment and continuity will initially be the well-mixed, relatively warmer and less saline, highly oxygenated sill water. In moving upfjord, however, this water becomes cooled as heat flows away from it, along the negative temperature gradient, and is absorbed by the melting ice and cold meltwater. Furthermore, respiration beneath the photosynthetic compensation depth, where oxygen consumption equals oxygen production by biological processes, will

eventually deplete the deep water of oxygen, if there is no direct downward mass transport between the surface layer and the deep water. Moreover, if surface water were transported downward through the pycnocline, an upfjord gradient of decreasing salinity below the pycnocline should be obvious; such is not the case in Muir Inlet.

In summary, investigation of the longitudinal temperature and salinity gradients (Figures 14--19, pp. 46--51), and the seasonal variations at MUI 20 reveals that the primary effect of the tidal glaciers on the characteristics of Muir Inlet water masses appears to be as a heat sink at the head of the fjord. Meltwater from icebergs and tidal glaciers does not directly control the salinity and dissolved oxygen content of the deep water. Instead, meltwater acts indirectly by setting up a circulation regime through which several environmental phenomena interact to control the salinity, temperature, and dissolved oxygen distributions. Some important environmental factors are turbulence generated by tides, winds, and obstructions in the access channel between the Pacific Ocean and Muir Inlet; biological processes, such as photosynthesis and respiration; precipitation and runoff, sunshine, and air temperature; and the location and discharge of streams.

Comparison of Muir Inlet with Other Fjords

An investigation of the characteristics of Muir Inlet with respect to those of other studied fjords may reveal features unique to its class, as well as features common to all fjords.

Port Nellie Juan Fjord

Port Nellie Juan Fjord (60°30'N, 148°20'W) is an Alaskan fjord north and west of Muir Inlet. It has three basins (780, 470, and 455 meters) and three sills (360, 220, and 183 meters), with each basin and each sill progressively shallower upfjord. It is a fjord with a relatively deep outer sill, no tidal glaciers, and comparatively free access to the open ocean.

Spring conditions in this fjord are described by Jones (1964). The surface water has a maximum temperature of 11°C., a salinity range from 9.60--28.45‰, and a maximum concentration of dissolved oxygen of 8.22 milliliters per liter. The deep water has a maximum temperature of 5--6°C., a maximum salinity of 33.03‰, and a minimum dissolved oxygen concentration of 3.09 milliliters per liter.

The very deep access channel between the Pacific Ocean and Port Nellie Juan Fjord and the deep outer sill allow the entry of high salinity, warm, low-oxygen ocean

water into the fjord's deep basin. These characteristics fit well into Pickard's (1967) "non-ice" Alaskan fjord class. Figure 50 (p.113) shows the envelopes of temperature-salinity data defining Pickard's fjord classes.

Taiya Inlet

Lying slightly north and east of Muir Inlet, Taiya Inlet (59°24'N, 135°21'W) has characteristics intermediate to those of Port Nellie Juan Fjord and Muir Inlet. It has a sill depth of 70 meters and a maximum depth of 420 meters. It is a fjord with a moderately shallow sill, no tidal glaciers, and an extremely limited communication with the ocean.

Summer conditions are described by Pickard (1967) and are found to be more saline and colder than those of Muir Inlet during the same period. Figure 50 (p.113) displays the summer ranges of temperature and salinity for Taiya Inlet, labeled "LYN 1-4" on the diagram. An immediate explanation for its water being colder and more saline than Muir Inlet water at the same time, especially when Taiya Inlet is even more isolated from the ocean, is not apparent during the summer.

Fall--winter conditions in Taiya Inlet are discussed by Rosenberg (1966). From October to November, the temperature below 200 meters remains nearly constant at

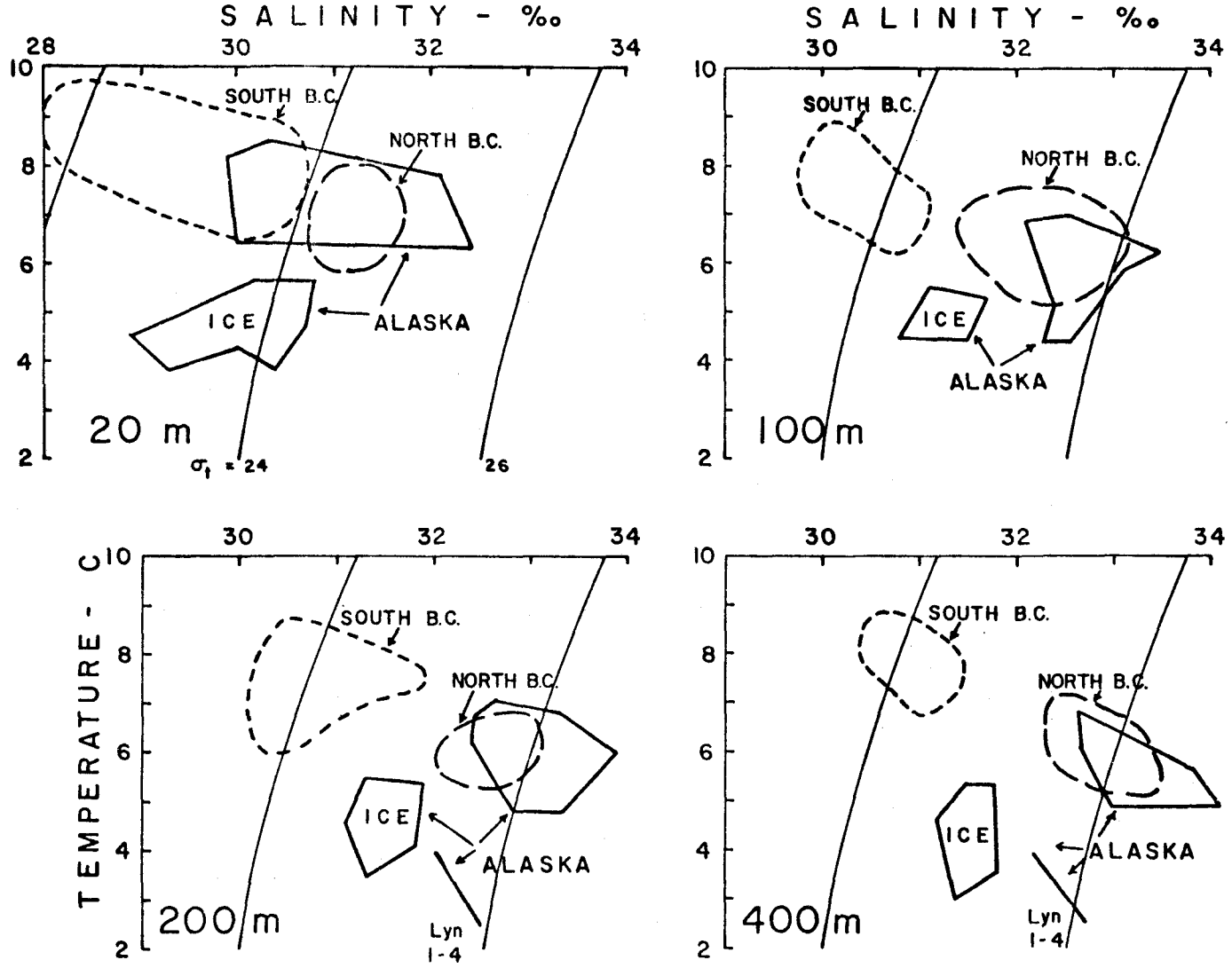

Figure 50. Envelopes of Temperature-Salinity Data Points for Inlets of Southeastern Alaska (Solid Lines) and British Columbia (Broken Lines). "ICE" denotes Southeastern Alaskan inlets with icebergs (after Pickard 1967).

2.5°C.; between 75 and 200 meters, November has the warmer water (4.2°C.), by up to 1.2°C.; above 75 meters, October has the warmer water. A temperature maximum is found at the surface in October; a temperature minimum, in November. By February, temperatures at all levels are at their lowest values, with the lowest recorded value of 1.34°C. at 100 meters.

From October to November, the salinity above 50 meters increases; between 50 and 300 meters, decreases; and below 300 meters, remains constant. From November to February, the salinity above 175 meters increases and below 175 meters decreases. The maximum deep water salinity of about 33.1‰ is found in the fall.

From November to February, the dissolved oxygen levels increase at all depths, ranging from 7.5 milliliters per liter at the surface to 5.0 milliliters per liter at 400 meters.

Rosenberg (1966) interprets the data as suggesting the formation and/or intrusion of new water masses between November and February. Matthews and Rosenberg's (1969) evaluation of the regional meteorological and oceanographic conditions indicates that the new water results from surface freezing and subsequent thermohaline convection of highly oxygenated, high salinity, very cold water from the surface of the fjord to the deep waters.

Matthews and Rosenberg (1969) report that of the Alaskan fjords studied, only Taiya Inlet demonstrates thermohaline convection to be the major source of deep water. This phenomenon may not be unique to Taiya Inlet, however, since some British Columbia fjords also appear to possess similar properties.

In relation to Muir Inlet, Taiya Inlet appears to be even more dependent on local environmental conditions, to the point where its water masses are formed locally under the influence of severe winter temperature and runoff minima.

Endicott Arm

Endicott Arm (57°41'N, 133°24'W) is an Alaskan fjord south and east of Muir Inlet. It has a sill depth of 33 meters and a maximum depth of 330 meters. It is a fjord with a shallow sill, tidal glaciers, and a restricted communication with the Pacific Ocean.

Matthews and Rosenberg (1969) report that below 10 meters two seasonally distinct water masses can be identified in Endicott Arm. The first is the winter--spring water mass, with temperatures less than 4°C. and salinities between 31.2--32.0‰. The other water mass is found in the fall and has temperatures greater than 4°C. and salinities less than 31.4‰. During the summer, Endicott Arm water

characteristics are in transition between these two water masses.

Winter--spring deep water is thought to result from a major inflow over the sill during December or January, with subsequent minor inflows occurring throughout the spring. Fall water properties are attributed to a subsurface inflow of well-mixed Stephens Passage water.

Endicott Arm and Muir Inlet thus appear to be similar both physically and oceanographically.

Bute Inlet

Located in southern British Columbia, Bute Inlet ($50^{o}45'N$, $124^{o}45'W$) has a sill depth of 355 meters and a maximum depth of 660 meters. It is a fjord with a very deep sill, no tidal glaciers, and very limited contact with the Pacific Ocean.

The major deviations between the characteristics of Muir Inlet and those of Bute Inlet are found in the deep water masses. According to Tabata and Pickard (1957), Bute Inlet deep water maintains the same temperature, salinity, and dissolved oxygen structures throughout the year. Below 20 meters, no seasonal salinity variations are seen. Seasonal temperature variations are obvious down to 50 meters. The deep water has a year-around salinity of [illegible] and temperature of 8.0--8.2°C. Even though

the temperature and salinity values seem fixed, the deep water must be continually, but slowly, renewed to maintain the oxygen saturation at 35--50%. If the bottom water were not involved in exchange processes, anoxic conditions would result.

The properties of the surface and intermediate layers are correlated with fluctuations in stream runoff. Two seasonal water masses associated with periods of high and low runoff are identified.

The small runoff period occurs from October to April. Average salinity values of 20‰ at the head and 29‰ at the mouth are common at this time. Typical winter surface temperatures are 5--6°C.

The large runoff period lasts from May through September. Salinities of 1‰ at the head and 15‰ at the mouth are found then. Typical summer surface temperatures range from 10--15°C.

Dissolved oxygen reaches saturation values of 90--130% in the surface layer, dropping at 20 meters to 80% in winter and 70% in summer and leveling off in the deep water at 35--50%.

Temperature fluctuations in the surface and intermediate layers are believed to be controlled directly by the temperature of the freshwater runoff and insolation and indirectly by the climate.

Wind mixing is deemed the dominant mechanism producing the homogeneity of winter surface water.

A tongue-like intrusion of warm water is found all year between 100 and 300 meters.

No cyclic changes in the salinity and temperature structure are noted in response to the tidal cycle.

Coriolis deflection of lateral isohalines is observed.

During March, the spring transition toward higher temperatures and lower salinities in the surface layer begins. During September, the fall transition toward lower temperatures and higher salinities in the surface layer is encountered.

In relation to Muir Inlet, the higher temperatures and lower salinities of Bute Inlet may be attributed to its more southern climate and extensive mixing of Pacific Ocean water and freshwater in the Strait of Georgia. Wind and coriolis effects have not been investigated in Muir Inlet. Both spring and fall temperature and salinity inversions occur one to two months earlier in Bute Inlet than in Muir Inlet. The constancy of Bute Inlet water characteristics results from its moderate climate.

Oslofjord

Situated at a latitude comparable to that of Muir Inlet, the Oslofjord (59°30'N, 10°35'E) has an outer sill depth of 120 meters. Within the outer sill are four more basins and three more sills. The first two basins, having maximum depths of 360 and 200 meters and separated by a 100-meter sill, are referred to as the outer Oslofjord. The inner two basins, both having maximum depths of 150 meters and separated by a 50-meter sill, are called the inner Oslofjord. The inner and outer fjords are in partial contact through a constricted channel with a 19.5-meter sill.

Hjort and Gran (1900) (as reported in Gade 1963) describe a two-layered system, in which the characteristics of the upper layer differ from those of the open ocean and in which the characteristics of the deep water remain constant for long periods. Surface characteristics depend on river inflow and the prevailing winds. River inflow approaches its minimum in January and its maximum in May. During winter, the winds blow downfjord, resulting in higher surface salinities in the fjord than outside. Wind and surface conditions reverse during the summer.

Gade (1963) reports the hydrographic conditions in the Oslofjord during 1959. Investigation of the salinity characteristics of the outer 200-meter basin reveals that in January very high salinities occur, ranging from 33‰

at the surface to 35‰ at 100 meters. From January to July, the salinities at all depths decrease, reaching minimum values in July of 21.3‰ at the surface and 34.39‰ at 100 meters. From July through mid-December, the salinities below 75 meters remain constant and above 75 meters fluctuate, achieving mid-December values of 24.1‰ at the surface and 29.2‰ at 50 meters.

Temperatures in the 200-meter basin in January range from 4°C. at the surface to 8°C. at 75 meters. In February, an annual minimum surface temperature of 0.95°C. is measured. By April, spring warming effects are significant. Surface temperatures of 12°C. are recorded in May. Surface temperatures continue to rise through July, reaching 20°C. at the surface and 15°C. at 15 meters. From August through winter, the surface temperatures decrease. In September, an influx of 9--10°C. (and 32--33.5‰) water is detected between 40--60 meters. In December, the deep water is 5°C. colder.

In the inner Oslofjord, annual temperature and salinity variations are less extreme, while the dissolved oxygen distribution shows lower values. Around the beginning of the year, both surface and deep water dissolved oxygen values vary from 5.4 milliliters per liter at the surface to 5.7 milliliters per liter at 80 meters, with a minimum of 2.9 milliliters per liter sandwiched between at 20--30

meters. In the following months, the oxygen levels at all depths below 10 meters decrease and above 10 meters increase. By the end of the year, the oxygen content of the deep water falls to 2.0 milliliters per liter.

Oxygen maxima and minima at intermediate depths are attributed to inflows, which must be infrequent and weak since the dissolved oxygen levels are very low and the passage to the inner basin is very narrow and shallow.

The main differences between Muir Inlet characteristics and those of the Oslofjord relate to differences in physiography, climate, and the basic salinity of the contiguous open ocean. The outer Oslofjord has a freer access to the open ocean; the inner Oslofjord is more isolated because of the small cross sectional area over its 19.5-meter sill. All other factors being equal, greater stability and less likelihood of overturning is expected in the Oslofjord, since its deep basin water has as its source North Atlantic water which is more saline and denser than that found at similar latitudes and depths in the North Pacific. Thus, there is a greater probability that an effective density barrier to deep water renewal will be found in a Norwegian fjord and that as a result anoxic bottom water will be more commonly found in Norwegian fjords. Again wind is an important factor influencing surface salinities.

Central Western Norwegian Fjords

Saelen (1967) discusses the hydrography of a fjord located in central western Norway (59--63°N, 5--6°E).

In general, winter convection penetrates only to 20--30 meters. Thermohaline convection penetrating to the bottom is found much farther north. The severe winter climatic conditions in the fjord system Tromsø (70°N) do produce thermohaline convective processes strong enough to erode the vertical stratification (Saelen 1950).

In central western Norway, the runoff minimum occurs in February and March; a primary maximum, resulting from meltwater is found in June and July; a secondary maximum, reflecting the precipitation maximum, comes in October. This pattern is similar to that found in Alaska and British Columbia. However, in Norway, the surface brackish layer is always thin, and the salinity below 20 meters is always greater than 30‰.

Hardangerfjord is a typical central western Norwegian fjord. It has a 150-meter sill, no tidal glaciers, and free communication with the open ocean. In August, there is a strong vertical stratification. The surface salinity ranges from 2.15‰ at the head to 31.31‰ at the mouth. The deep water is uniform around 35‰. In February, the fjord is less stratified but still vertically stable. The

surface salinities vary from 33.92‰ at the head to 33.79‰ at the mouth, an unusual decrease in salinity downfjord. The deep water salinity still is constant at 35‰.

Data from the Nordfjord is also considered representative of typical conditions in central western Norway. The Nordfjord has two basins, with an effective outer sill depth of 100 meters and an inner sill depth of 125 meters. During the summer, an annual intrusion of outside water occurs in the outer basin. The inner basin, however, experiences renewal of its deep water only every 7--8 years. This infrequent event is dramatically demonstrated by the changes in the dissolved oxygen distribution at the 400-meter level. First, a jump to 90% saturation is observed, and then the levels slowly decrease over the next 7--8 years to about 43%; whereupon another abrupt rise to 90% happens. This pattern is supported by temperature and salinity changes too.

Even in Norwegian fjords with shallow sills, the deep basin waters have salinities greater than the highest salinities found in Alaskan fjords. The higher deep water salinities found in Norwegian fjords reflect the basically higher salinity values typical of North Atlantic water compared to North Pacific water. It naturally follows that Norwegian fjords must also have greater vertical stabilities, since the density difference between the

surface brackish layers and the deep water can attain much higher values in Norwegian fjords. The greater the vertical stability, the greater the resistance to vertical turbulence and mixing and hence the smaller the probability of renewal of bottom water by any mechanism other than the infrequent density flow over the sill. Thus, the major differences between central western Norwegian fjords and Muir Inlet result from the different salt contents of their sources of saline water, in the amount of dilution occurring in the access channels between ocean and fjord, and in sill depths.

"Brown Zone" Fjords

Very little is known about the characteristics of the water masses and the details of the circulatory processes near the termini of tidal glaciers in fjords, mainly because of the danger of calving and floating icebergs. Some oceanographic data are available from measurements of hydrographic conditions within and outside the perimeter of upwellings at the termini of tidal glaciers in the Icefjord (78°40'N, 16°30'E), West Spitzbergen (Stott 1936) and at the head of Ata Sound (69°45'N, 50°20'W), Disco Bay, West Greenland (Hartley and Dunbar 1937--1938).

According to Hartley and Dunbar (1937--1938), an upwelling of saline bottom water is associated with the termini of two tidal glaciers in Ata Sound. The water is

very muddy, hence the name "Brown Zone," and rises at the face of the glaciers, turning into a surface current of about 0.5 knot away from the glacier. On reaching the perimeter of the Brown Zone, the current plunges under the brash ice. The Brown Zones have a radius on the order of 250 meters.

Within the Brown Zones, the bottom water at 50 meters has a salinity between 33.2--33.6‰ which decreases steadily to 29.2--32.2‰ at the surface. Just outside the Brown Zone, surface salinities of 22.1--27.4‰ are measured. The muddy water is found only to a depth of 10 meters.

Stott (1936), describing a similar phenomenom in the Icefjord in West Spitzbergen, observes that the higher the air temperature, the greater the amount of meltwater produced by the glacier and the larger the tongue of brown water extending out into the inlet. The tongue contains cold, dilute seawater running out from the glacier above slightly warmer and more saline seawater. The hotter the weather, the lower the salinity of the tongue; thus, the salinity of the Brown Zone is correlated with air temperature.

The data from these studies are inadequate to identify the driving forces for these localized upwellings, but they do raise intriguing questions about the dynamics of circulation at the face of the glaciers.

Anoxic Fjords

Several fjords are peculiar in that their basin waters are oxygen deficient. Some fjords known to develop anoxic conditions are Lake Nitinat (Pickard 1963) and Saanich Inlet (Herlinveaux 1962) in British Columbia and the Dramsfjord (Richards and Benson 1961), an arm of the Oslofjord.

According to Richards (1965), anoxic conditions arise when circulatory processes are insufficient to replenish oxygen levels faster than the oxygen is utilized in respiratory processes. Usually, dissolved oxygen deficiencies occur in basins where horizontal circulation is restricted by a shallow sill; and vertical circulation, by a strong pycnocline. Particularly prone to develop anoxic conditions are fjords in which the pycnocline lies at or below sill depth, since both advective and convective exchange mechanisms are then impeded.

Muir Inlet has never been observed to develop anoxic conditions. Its temperature and salinity data suggest that its bottom water is frequently, if not continually, renewed.

CHAPTER V

CONCLUSIONS

Among fjords, the water mass characteristics of each fjord are unique, being locally determined by topography, climate, and salt source. Among estuarine systems, fjords exhibit characteristic seasonal and spatial responses in parameter structures and circulation patterns.

Seasonal Variations in Muir Inlet Water Types

The cyclic variations in water mass properties reflect annual variations in climatological parameters, which are in turn influenced by local and marine environmental features.

During the winter, sub-freezing air temperatures, low intensities and short durations of sun and sky radiation, and small runoff can work together to produce a renewal and densification of the entire fjord water mass, first by allowing local thermohaline convection and second by allowing high density inflows. Uniformly high dissolved oxygen levels are restored at this time, as the effective rates of oxygen transfer are increased owing to the destruction of density barriers, turbulent mixing, and density flows.

As spring approaches, the surface input of heat increases. The snow and ice melt; the air warms; and the

surface layers become less dense. Soon a stratified flow system develops, and the water mass characteristics begin their summer migration toward the heterogeneous, lower density water masses.

At its peak development during the summer, the stratified flow system is composed of a surface layer of lighter, brackish water, an intermediate zone of strong temperature, salinity, and density gradients, and a deep water mass of relatively uniform properties. The surface layer responds most immediately to local climatological fluctuations. The strong vertical density gradient dampens out short-term and local surface changes related temperature, sunshine, runoff, and precipitation fluctuations. The general summertime trends toward warming and dilution, however, do penetrate the pycnocline. Their progress down through the water column proceeds at a measureable rate, with temperature changes transmitted more directly and more rapidly than salinity changes. By mid-summer, all the winter--spring water down to 200 meters is eradicated.

Also correlated with the solar and sky radiation cycle is the dissolved oxygen content of the surface layer. Generally, near the surface during spring and summer, photosynthesis is the dominant biological process, and an excess of oxygen is produced and released to the water column. Supersaturated levels of dissolved oxygen are

frequently encountered near the surface during this period. In the deep waters, respiration, involving oxygen consumption, is the dominant biological process. Decomposition of organic detritus utilizes dissolved oxygen, resulting in an oxygen deficiency in the deep water, since renewal of deep water oxygen is hindered by the density barrier of the pycnocline and the physical barrier of the sill.

As fall approaches and advances toward winter, the surface input of heat and freshwater diminishes. Surface densities increase until thermohaline convection is initiated, and the pycnocline is eroded. High density water may flow over the sill into the basin. The fall tendency throughout the initially heterogeneous fall water masses is to achieve a homogeneous winter water mass of increased salinity and decreased temperature. Dissolved oxygen levels are restored at all depths to winter's nearly saturated levels, as the surface oxygen-saturated water is convectively mixed, or advected, to all depths. Thus one annual cycle is completed.

Spatial Variations in Muir Inlet Water Types

Several consistent spatial patterns are observed among the fjords. These patterns develop in response to the topographic and hydrographic peculiarities of the fjord and the channels through which it is in contact with the

open ocean. Some important topographic and hydrographic features to consider are the presence or absence of flow obstructions such as shoals, sills, islands, bends, and channel constrictions, localized runoff sources such as streams, tidal glaciers, and icebergs, localized heat sinks such as tidal glaciers and icebergs, and salt sources such as open ocean water.

Flow obstructions work to modify and isolate water masses by disturbing smooth flow patterns producing turbulence and mixing and by physically separating water masses of different densities. For example, the deep basin water owes its existence and properties to the presence and depth of the sill, or sills, confining it. Its properties depend on its density structure in relation to that of contiguous water masses, to the relationship between sill depth and the thickness of the layer of outflowing brackish water, and to the ease of transmittance of seasonal changes in water properties through the pycnocline.

Localized runoff sources produce local intensifications of vertical and horizontal temperature, salinity, and density gradients, which in turn alter the water mass characteristics and circulation regime of the whole fjord. A sufficient outflow of freshwater will set up the three-layered flow structure typical of stratified estuaries: outflowing

lighter surface layer, intermediate zone of net upward transport of saline water and turbulent mixing of saline and freshwater, and the denser deep water with a net upfjord transport compensating for the loss of entrained deep water.

The location and characteristics of heat sinks and salt sources control the density, stability, and renewal rates of the contiguous fjord water masses. The extent of their ability to control the characteristics and circulation of fjord water masses is intimately related to the topographic features of the access channel connecting ocean and fjord. For example, shoals and sills limit the influence of Pacific Ocean water on Muir Inlet water by the intense mixing and resulting modifications of its properties on flowing up Icy Strait; in contrast, the relatively deep access channels of the Nordfjord allow the very high salinity, dense Atlantic Ocean water to fill its basins, producing a very strong positive stability in its deep water which hinders the annual renewal of bottom water and leads to oxygen-deficient deep water.

Assessment of the State of Knowledge of the Physical Oceanography of Fjords

This thesis summarizes the state of knowledge of the physical oceanography of Muir Inlet, Glacier Bay, Alaska, stating what is known, pointing out areas

requiring further observational detail, offering interpretations of the data, and comparing Muir Inlet with other fjords.

Much field work yet remains to be done and must be performed in order to understand the fundamental nature of the local contributions from and interactions among the oceanographic, topographic, bathymetric, glaciological, hydrological, and meteorological features peculiar to Glacier Bay National Monument and Icy Strait before one can achieve predictive knowledge of the seasonal and spatial variations in the water mass characteristics of this unique fjord system.

REFERENCES

REFERENCES

Anonymous

1965. British Columbia and Alaska Inlet Cruises, 1964. Data Rept. 24, Institute of Oceanography, the University of British Columbia, 34 pp.

1966. British Columbia and Alaska Inlet Cruises, 1965. Data Rept. 25, Institute of Oceanography, The University of British Columbia, 39 pp.

Bohn, David

1967. Glacier Bay: The Land and the Silence, Sierra Club, San Francisco, 165 pp.

Bowden, K. F.

1967. Circulation and Diffusion. In: The Estuaries, G. F. Lauff (Ed.), AAAS, Washington, 757 pp.

Carpenter, J. H.

1966. New Measurements of Oxygen Solubility in Pure and Natural Water. Limnol. Oceanogr., 11: 264--277.

Cochrane, J. D.

1956. The Frequency Distribution of Surface-Water Characteristics in the Pacific Ocean. Deep-Sea Res., 4: 45--53.

1958. The Frequency Distribution of Water Characteristics in the Pacific Ocean. Deep-Sea Res., 5: 111--127.

Cooper, W. S.

1937. The Problem of Glacier Bay, Alaska. A Study of Glacier Variations. Geogr. Rev., 27: 37--62.

1956. A Contribution to the History of the Glacier Bay National Monument. Dept. of Botany, University of Minnesota, 36 pp.

Gade, H. G.

1963. Some Hydrographic Observations of the Inner Oslofjord during 1959. Hvalrådets Skrifter, 46: 1--62.

Gilmartin, M.

1962. Annual Cyclic Changes in the Physical Oceanography of a British Columbia Fjord. J. Fish. Res. Bd. Canada, 19: 921--974.

Goldthwait, R. P., Loewe, F., Ugolini, F. C., and others

1966. Soil Development and Ecological Succession in a Deglaciated Area of Muir Inlet, Southeast Alaska. Institute of Polar Studies 20, Ohio State University, 167 pp.

Hartley, C. H., and Dunbar, M. J.
1937--1938 On the Hydrographic Mechanism of the So-Called Brown Zones Associated with Tidal Glaciers. J. Mar. Res., 1: 305--311.

Herlinveaux, R. H.
1962. J. Fish. Res. Bd. Canada, 19: 1.

Hjort, J., and Gran, H. H.
1900. Hydrographic-Biological Investigations of Skager-Rack and the Christiania Fjord. Rep. Norweg. Fish. Inves. 1: 1--56.

Jones, R. B.
1964. Oceanographic Investigation of Port Nellie Juan Fiord, Alaska. U. S. Dept. of Commerce, Environmental Science Services Administration, Coast and Geodetic Survey, 46 pp.

Keulegan, G. H.
1949. Interfacial Instability and Mixing in Stratified Flows. J. Res. Natl. Bur. Std., 43: 487--500.

Matthews, J. B., and Rosenberg, D. H.
1968. Progress Rept. to ONR, Contract No. NONR 3010 (05), Vol. 2, Ann. Rept., Institute of Marine Science, University of Alaska, 73 pp.
1969. Progress Rept. to ONR, Contract No. NONR 3010 (05), Rept. No. 69-4, Institute of Marine Science, University of Alaska, 77 pp.

McKenzie, G. D.
1968. Glacial History of Adams Inlet, Southeastern Alaska. Institute of Polar Studies, Ohio State University.

McLain, D. R.
1968. Oceanographic Surveys of Traitors Cove, Revillagigedo Island, Alaska. U. S. Fish and Wildlife Service, Special Scientific Rept.--Fisheries No. 576, Washington, D. C., 15 pp.

Miller, A. R., and Stanley, R. J.
1966. Volumetric T-S Diagrams for the Mediterranean Sea. Contrib. 1627, Woods Hole Oceanographic Institution, 5 pp.

Montgomery, R. B.
1955. Characteristics of Surface Water at Weather Ship J. Deep-Sea Res., 3, Suppl., Papers in Marine Biology and Oceanography Dedicated to Henry Bryant Bigelow: 331--334.

Montgomery, R. B.
1958. Water Characteristics of the Atlantic Ocean and of the World Ocean. Deep-Sea Res., 5: 134--148.

Peacock, M. A.
1935. Fiord-Land of British Columbia. Bull. Geol. Soc. Am., 46: 633--696.

Pickard, G. L.
1961. Oceanographic Features of Inlets in the British Columbia Mainland Coast. J. Fish. Res. Bd. Canada, 18: 907--999.
1963. J. Fish. Res. Bd. Canada, 20: 1109.
1967. Some Oceanographic Characteristics of the Larger Inlets of Southeast Alaska. J. Fish. Res. Bd. Canada, 24: 1475--1505.

Pollak, M. J.
1958. Frequency Distribution of Potential Temperatures and Salinities in the Indian Ocean. Deep-Sea Res., 5: 128--133.

Powers, C. F.
1962. Some Aspects of the Oceanography of Little Port Walter Estuary, Baranof Island, Alaska. Fishery Bulletin, 63: 143--163.

Price, R. J.
1964. Land Forms Produced by the Wastage of the Casement Glacier, Southeast Alaska. Ohio State University Research Foundation, Institute of Polar Studies, Rept. No. 9, 24 pp.

Richards, F. A.
1965. Anoxic Basins and Fjords. In: J. P. Riley and G. Skirrow (Eds.), Chemical Oceanography, Vol. 1, Academic Press, New York, 712 pp.

Richards, F. A., and Benson, B. B.
1961. Deep-Sea Res., 7: 254.

Richards, F. A., and Corwin, N.
1956. Some Oceanographic Applications of Recent Determinations of the Solubility of Oxygen in Seawater. Limnol. Oceanogr., 1: 263--267.

Rochford, D. J.
1963. Mixing Trajectories of Intermediate Water of the South-East Indian Ocean as Determined by a Salinity Frequency Method. Australian J. of Marine and Freshwater Res., 14: 1--23.

Rosenberg, D. H.
1966. Progress Rept. to ONR, Contract No. NONR 3010 (05), Annual Rept., Institute of Marine Science, University of Alaska, 31 pp.

Saelen, O. H.
1950. The Hydrography of Some Fjords in Northern Norway. Tromsø Museume Årshefter, Nat. Hist. Avd. No. 38, Vol. 70.
1967. Some Features of the Hydrography of Norwegian Fjords. In: The Estuaries, G. Lauff (Ed.), AAAS, Washington, 757 pp.

Stott, F. C.
1936. The Marine Foods of Birds in an Inland Fjord Region in West Spitzbergen. J. Animal Ecology, 5: 356--369.

Sturges, W.
1965. Water Characteristics of the Caribbean Sea. J. Mar. Res., 23: 147--162.

Tabata, S., and Pickard, G. L.
1957. The Physical Oceanography of Bute Inlet, British Columbia. J. Fish. Res. Bd. Canada, 14: 487--520.

Taylor, L. D.
1962. Ice Structures, Burroughs Glacier, Southeast Alaska. Institute of Polar Studies, Rept. 3, Ohio State University, 110 pp.

Tide Tables
1967. West Coast North and South America, U. S. Coast and Geodetic Survey.

Tully, J. P.
1949. Oceanography and Prediction of Pulp Mill Pollution in Alberni Inlet. Bull. Fish. Res. Bd. Canada, 83: 1--169.
1958. On the Structure, Entrainment, and Transport in Estuarine Embayments. J. Mar. Res., 17: 523--535.

U. S. Coastal Pilot 8
1962. Pacific Coast, Alaska, Dixon Entrance to Cape Spencer, Eleventh Edition, U. S. Dept. of Commerce, Coast and Geodetic Survey, U. S. Government Printing Office, Washington, 246 pp.

Waldichuk, M.
1957. Physical Oceanography of the Strait of Georgia. J. Fish. Res. Bd. Canada, 14: 321--486.

Wallen, D. D., and Hood, D. W.
1968. Progress Rept. to ONR, Contract No. NONR 3010 (05), Annual Rept., Institute of Marine Science, University of Alaska, 114 pp.

APPENDIX

TABLE 12. STATION POSITIONS (Anon. 1965; Rosenberg 1966; Wallen and Hood 1968)

Location	Station name	Position		Depth
		Latitude	Longitude	
Cross Sound	CRO 0	58°11.6°N	136°32.2°W	280 meters
	CRO 10	58 03.3	136 43.3	280
Glacier Bay	GL 0	58 22.4	135 58.8	76
	GLA 10*	58 24.6	135 58.7	57
	GL 5	58 26.8	136 01.8	57
	GL 10	58 31.6	136 04.2	100
	GL 15	58 37.1	136 05.3	246
	GLA 8*	58 40.3	136 10.3	322
	GL 18A	58 40.4	136 12.0	336
	GL 18C	58 41.4	136 06.4	95
	GL 18E	58 42.6	136 01.1	130
	GL 20	58 42.1	136 14.0	330
Icy Strait	ICY 30	58 20.0	135 59.3	40
	ICY 1*	58 17.1	136 13.6	205
	ICY 40	58 18.0	136 17.7	240
Muir Inlet	MUI 0	58 44.6	136 07.4	120
	MUI 5	58 50.0	136 05.8	165
	MUI 3*	58 51.5	136 05.0	298
	MUI 10	58 55.0	136 05.5	295
	MUI 2*	58 56.5	136 06.5	294
	MUI 15	58 58.0	136 08.4	230
	MUI 20	59 03.0	136 09.0	210

*These are University of British Columbia, Institute of Oceanography station designations. All the other station names represent University of Alaska Institute of Marine Science stations.

TABLE 13. METEOROLOGICAL STATION POSITIONS

Station name	Position		Elevation
	Latitude	Longitude	
Adams Inlet	58°52'N	135°55'W	
Annette	55 02	131 33	
Cape Spencer	58 12	136 39	0 meters A.S.L.*
Casement Glacier			300
Delta	58 54	136 03	4
Gustavus	58 25	135 25	
Haines	59 14	135 20	0
Juneau	58 18	134 34	22
Little Port Walter	56 53	134 39	
Nunatak Cove	58 59	136 06	
Terminus			
Wachusetts Inlet	58 56	136 15	30
Yakutat	59 33	139	

*This is to be read as follows: zero meters above sea level.

TABLE 14. HYDROGRAPHIC CRUISES, R/V ACONA, INSTITUTE OF MARINE SCIENCE, THE UNIVERSITY OF ALASKA

Cruise number	Station name	Station number	Date	Data*
014	CRO 0	0199		
	GL 5	0200	6-X-65	T S σ_t
	GL 10	0201	"	T S σ_t
	GL 15	0202	"	T S σ_t
	GL 20	0203	"	T S σ_t
	ICY 30	0191	5-X-65	T S σ_t
	MUI 0	0210	8-X-65	T S σ_t
	MUI 5	0208	"	T S σ_t
	MUI 10	0207	"	T S σ_t
	MUI 15	0207	"	T S σ_t
017	CRO 0	0251		
	CRO 10	0243	15-XI-65	T S O σ_t
	GL 0	0252	16-XI-65	T S O σ_t
	GL 5	0253	"	T S O σ_t
	GL 10	0254	"	T S O σ_t
	GL 15	0255	"	T S O σ_t
	GL 20	0256	"	T S O σ_t
	ICY 30	0241	14-XI-65	T S O σ_t
	ICY 40	0242	"	T S O σ_t
	MUI 0	0264	18-XI-65	T S O σ_t
	MUI 5	0263	"	T S O σ_t
	MUI 10	0262	17-XI-65	T S O σ_t
019	CRO 0	0313	7-II-66	T S O σ_t
	CRO 10	0312	"	T S O σ_t
	GL 0	0328	9-II-66	T S O σ_t
	GL 5	0315	7-II-66	T S O σ_t
	GL 10	0316	"	T S O σ_t
	GL 15	0317	"	T S O σ_t
	GL 20	0318	"	T S O σ_t
	ICY 30	0334	12-II-66	T S O σ_t
	ICY 40	0314	7-II-66	T S O σ_t
	MUI 0	0327	9-II-66	T S O σ_t
	MUI 5	0326	"	T S O σ_t
	MUI 10	0325	"	T S O σ_t
	MUI 15	0324	"	T S O σ_t

*This table is to be read as follows: S = salinity; T = temperature; O = oxygen; σ_t = "Sigma-t" (density).

TABLE 14 (Continued)

Cruise number	Station name	Station number	Date	Data*
021	CRO 0	0404	9-IV-66	T S O σ_t
	CRO 10	0403	"	T S O σ_t
	GL 0	0415	11-IV-66	T S O σ_t
	GL 5	0416	"	T S O σ_t
	GL 10	0417	"	T S O σ_t
	GL 15	0418	"	T S O σ_t
	GL 18A	0429	14-IV-66	T S O σ_t
	GL 18C	0430	"	T S O σ_t
	GL 18E	0431	"	T S O σ_t
	GL 20	0419	11-IV-66	T S O σ_t
	ICY 30	0414	"	T S O σ_t
	ICY 40	0405	9-IV-66	T S O σ_t
	MUI 0	0428	13-IV-66	T S O σ_t
	MUI 5	0427	"	T S O σ_t
	MUI 10	0426	"	T S O σ_t
	MUI 15	0425	"	T S O σ_t
023	GL 0	0496	22-V-66	T S O σ_t
	GL 5	0479	19-V-66	T S O σ_t
	GL 10	0480	"	T S O σ_t
	GL 15	0481	"	T S O σ_t
	GL 18A	0494	22-V-66	T S O σ_t
	GL 18E	0495	"	T S O σ_t
	GL 20	0482	19-V-66	T S O σ_t
	MUI 0	0493	20-V-66	T S O σ_t
	MUI 5	0492	"	T S O σ_t
	MUI 10	0491	"	T S O σ_t
	MUI 15	0490	"	T S O σ_t
030	GL 0	0857	10-XI-66	T S O
	GL 5	0858	"	T S O
	GL 10	0859	"	T S O
	GL 15	0847	9-XI-66	T S O
	GL 18A	0854	10-XI-66	T S O
	GL 18C	0855	"	T S O
	GL 18E	0856	"	T S O
	GL 20	0853	"	T S O
	ICY 30	0846	9-XI-66	T S O
	MUI 0	0860	10-XI-66	T S O
	MUI 5	0861	"	T S O
	MUI 10	0862	"	T S O
	MUI 15	0863	"	T S O
	MUI 20	0864	"	T S O

TABLE 14 (Continued)

Cruise number	Station name	Station number	Date	Data*
032	CRO 0	0959	21-II-67	T S O
	GL 0	0979	23-II-67	T S O
	GL 5	0978	23-II-67	T S O
	GL 10	0977	"	T S O
	GL 15	0976	"	T S O
	GL 20	0970	22-II-67	T S O
	ICY 30	0958	21-II-67	T S O
	ICY 40	0960	"	T S O
	MUI 0	0975	22-II-67	T S O
	MUI 5	0974	"	T S O
	MUI 10	0973	"	T S O
	MUI 15	0972	"	T S O
	MUI 20	0971	"	T S O
034	GL 5	1030	19-III-67	T S
	GL 18C	1029	18-III-67	T S
	MUI 10	1028	"	T S
040	CRO 0	1192	15-VII-67	T S O
	CRO 10	1193	"	T S O
	GL 0	1209	16-VII-67	T S O
	GL 5	1208	"	T S O
	GL 10	1207	"	T S O
	GL 15	1206	"	T S O
	GL 18A	1203	"	T S O
	GL 18C	1204	"	T S O
	GL 18E	1205	"	T S O
	GL 20	1199	"	T S O
	ICY 30	1190	15-VII-67	T S O
	ICY 40	1191	"	T S O
	MUI 0	1202	16-VII-67	T S O
	MUI 15	1515	"	T S O
	MUI 20	1514	"	T S O
053	MUI 20	1854	28-IX-67	T S O

TABLE 15. HYDROGRAPHIC CRUISES, INSTITUTE OF OCEANOGRAPHY, THE UNIVERSITY OF BRITISH COLUMBIA

Cruise number	Station name	Station number	Date	Data*
64/21	GLA 8		10-VI-64	T S O σ_t
	GLA 10		11-VI-64	T S O σ_t
	ICY 1		"	T S O σ_t
	MUI 2		10-VI-64	T S O σ_t
	MUI 3		"	T S O σ_t
65/21	GLA 8		9-VIII-65	T S O σ_t
	GLA 10		8-VIII-65	T S O σ_t
	ICY 1		12-VIII-65	T S O σ_t
	MUI 3		8-VIII-65	T S O σ_t

*This table is to be read as follows: S = salinity; T = temperature; O = oxygen; σ_t = "Sigma-t" (density).